ELSEVIER

8. Iron 1993

Ebbe Nordlander, Anne M. Whalen and Fabio Prestopino

CONTENTS

INTRODUCTION

This review covers the coordination chemistry of iron for 1993. The following journals have been covered by a combination of searching in *Chemical Abstracts* and independent searches in the following journals: *Acta Chemica Scandinavica; Acta Crystallographica, Sect. C; Angewandte Chemie International Edition in English; Chemische Berichte; Chemistry Reviews; Coordination Chemistry Reviews; Gazzetta Chimica Italiana; Helvetica Chimica Acta; Inorganic Chemistry; Inorganica Chimica Acta; Journal of the American Chemical Society; Journal of the Chemical Society, Chemical Communications; Journal of the Chemical Society, Dalton Transactions; Journal of Coordination Chemistry; Mendeleev Communications; New Journal of Chemistry; Polyhedron; Recueil des Travaux Chimiques de Pays-Bas; Transition Metal Chemistry (London); Zeitschrift für Anorganische und Allgemeine Chemie; Zeitschrift für Naturforschung.*

Although carbonyl compounds have been included in previous iron reviews in this journal, they have - for the purpose of this review - been classified as organometallic compounds and are not included. Most iron-heterometal complexes have been excluded. All reported magnetic exchange values have been normalized to fit the following exchange Hamiltonian: $H = -2J\ S_1 \cdot S_2$. This review does not aim to be fully comprehensive; omissions or errors are entirely the fault of the authors.

8.1   COMPLEXES WITH HYDROGEN OR HYDRIDE LIGANDS

The trihydride complex $[FeH_3(dmpe)_2]^+$ may be described as $[FeH(H_2)(dmpe)_2]^+$. Relaxation time (T_1) measurements demonstrate the presence of a dihydrogen complex; the H-H separation was calculated to be 0.81 Å. The presence of hydride and dihydrogen ligands could not be resolved in the X-ray structure of the cation. The dihydrogen ligand is readily displaced by dinitrogen to form $[FeH(N_2)(dmpe)_2]^+$. It may also be replaced by CO, MeCN, MeNC and C_2H_4. The reaction of the former complex with $(Mo(N_2)_2(dppe)_2]$ leads to H_2/N_2 exchange to form $[FeH(N_2)(dmpe)_2]^+$ and $[MoH_4(dppe)_2]$. Deprotonation of $[FeH(N_2)(dmpe)_2]^+$ yields a complex formulated as $[Fe(N_2)(dmpe)_2]$ [1].

### 8.2   COMPLEXES WITH HALIDE LIGANDS

Acetamidinium hexafluoroiron(II) $[CH_3C(NH_2)_2]_3[FeF_6]$ (1) has been prepared and its crystal structure has been determined. It consists of tetrahedral $[FeF_6]^-$ anions which are linked *via* the acetamidinum ions through an N-H-F hydrogen-bonding network. Thermal decomposition of

(2)
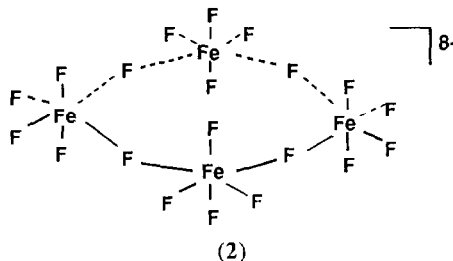
(1) leads to the formation of FeF_2 and FeF_3 [2]. Lead iron fluoride, $Pb_3Fe_2F_{12}$, has been prepared by hydrothermal synthesis and its crystal structure has been determined. The solid state structure contains isolated tetrameric $[Fe_4F_{20}]^{8-}$ groups (2) in which four Fe-F octahedra share apices so that an eight-membered Fe-F ring is formed [3].

The kinetics of formation of the $FeCl_2^{2+}$ complex as a function of pressure have been studied. The complex formation occurs predominantly *via* the conjugate acid/conjugate base pathway according to a dissociative activation mechanism:

$$Fe(OH)^{2+} + HClO_2 \rightarrow FeClO_2^{2+} + H_2O$$
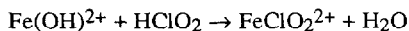
where $k'_1 = (3.0 \pm 0.2) \times 10^3 \ M^{-1}s^{-1}$ and $\Delta V^{\ddagger} = +6.9 \pm 2.3 \ cm^3 \ mol^{-1}$ [4]. Iron(III)chloride and polyaniline in the presence of oxygen catalyzes the dehydrogenation of cinnamyl alcohol into cinnamaldehyde. It is suggested that an iron-polyaniline coordination complex is the active catalyst [5].

The reaction of ferric chloride with *tris*(2,4,6-trimethoxyphenyl)phosphine (tmpp) in benzene leads to the formation of the phosphonium salt of $[Fe_2Cl_6]^{2-}$, the first homoleptic dinuclear iron(II) chloride species whose structure has been unambiguously proven by X-ray crystallography. The Fe-Fe separation is approximately 3.35 Å; the average Fe-Cl bond length for the terminal chloro ligands is approximately 2.23 Å while the corresponding distance for the bridging chloro ligands is approximately 2.40 Å. The anion $[Fe_2Cl_6]^{2-}$ reacts with oxygen to form the phosphine oxide adduct (Otmpp)·FeCl_3 in high yield [6].

8.3   COMPLEXES WITH CYANIDE AND OTHER PSEUDO-HALIDE LIGANDS

Single crystals of anhydrous thallium hexacyanoferrate have been prepared. In the solid state, the $[Fe(CN)_6]^{4-}$ octahedra are linked to the thallium cations to form a three-dimensional network in which the thallium ions have four different coordination spheres [7].

Kinetic and spectroscopic studies of ligand substitution reactions of pentacyanoferrate(II) complexes with three series of *N*-heterocyclic dicationic ligands in aqueous solution have been carried out. The parent *N*-heterocycles (R), pyrazine, aminopyrazine, methylpyrazine, bipyridine, and *trans*-1,2-bis(4-pyridyl)ethylene, were reacted with α,ω-dibromo alkane, α,α'-dibromo-*o*-xylene, or α,α'-dibromo-*p*-xylene to yield the bromide salts of the dications $[R(CH_2)_nR]^{2+}$, $[R(o$-xyl)R]^{2+}$ and $[R(p$-xyl)R]^{2+}$. These ligands react with $[Fe(CN)_5OH_2]^{3-}$ to form the monomeric $[Fe(CN)_5L]^-$ and the bridged dimeric $[(NC)_5Fe(\mu$-L)Fe(CN)_5]^{4-}$ complexes. The rates and activation parameters for the ligand dissociation reactions were found to be consistent with dissociative mechanisms. The dependence of the rate constants on the polymethylene chain length, n, for the formation of $[Fe(CN)_5(R(CH_2)_nR)]^-$ decreases in the order R = pyz > bpy > bpe, as the donor nitrogen atom is further removed from the site of positive charges [8].

The pentacyanoferrate(II) centre $[Fe(CN)_5]^{3-}$, was employed as a kinetic and spectroscopic probe of the inclusion processes of neutral and cationic aromatic *N*-heterocyclic ligands in α- and ß- cyclodextrin (3, 4). The *N*-adamantan-1'-ylpyrazinium cation (ADpyz$^+$) (5) and *N*-adamantan-1'- ylpyrazinium pentaferrate(II) ion (Fe(CN)_5(ADpyz)$^{2-}$) from 1:1 inclusion complexes with α- and ß- cyclodextrins in aqueous media. The stability constants for the ferrate inclusion complexes were

determined to be $(1.6\pm0.2) \times 10^3$ M^{-1} [9]. A kinetic study on the effects of the α- and ß-cyclodextrin inclusions of a series of neutral N-heterocyclic ligands on their ligand substitution reaction with [Fe(CN)$_5$OH$_2$]$^{3-}$ ion in solution has also been completed. The stability constants for the inclusion of [Fe(CN)$_5$L]$^{3-}$ complexes where L = substituted pyridines and symmetrical bipyridyls have been established. The rate constants for the formation of [Fe(CN)$_5$L]$^{3-}$ complexes for the reaction of [Fe(CN)$_5$OH$_2$]$^{3-}$ with L decrease upon cyclodextrin inclusion of the entering N-heterocyclic ligand. Likewise, the rate constants for the dissociation of L from [Fe(CN)$_5$L]$^{3-}$ complexes also decrease upon inclusion of the coordinated H-heterocyclic ligand in ß- cyclodextrin [10].
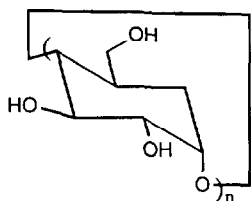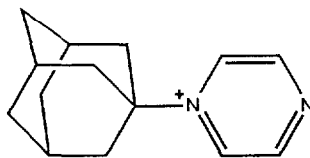
(3) (n = 6), (4) (n = 7)　　　　　　　　　　　(5)

The oxidation of thiosulfate by [Fe$_2$(CN)$_{10}$]$^{4-}$ has been investigated by stopped-flow and conventional spectrophotometry. The overall reaction occurs in two distinct processes. The initial process is the reduction of [Fe$_2$(CN)$_{10}$]$^{4-}$ to [Fe$_2$(CN)$_{10}$]$^{5-}$. It appears to be a biphasic process with the formation of a transient intermediate. It is postulated that this transient intermediate is [Fe$_2$(CN)$_9$(CNS$_2$O$_3$)]$^{6-}$ which is decomposed to [Fe$_2$(CN)$_{10}$]$^{5-}$ in two parallel pathways with the formation of S$_2$O$_3$·$^-$ and S$_4$O$_6$·$^-$. The second, slower part of the reaction leads to the formation of [Fe(CN)$_5$(S$_2$O$_3$)]$^{4-}$ and [Fe(CN)$_5$(S$_2$O$_3$)]$^{5-}$. This is postulated to occur *via* the formation of the complex [(NC)$_5$Fe(III)-CN-Fe(II)(CN)$_4$(S$_2$O$_3$)]^4 [11].

The solvation structure of the iron(III) ion in N,N-dimethylacetamide (DMA) has been determined by EXAFS; the octahedral [Fe(DMA)$_6$]$^{3+}$ complex is formed. The complex formation of iron(III) with thiocyanate ions has been studied calorimetrically and spectrophotometrically in DMA; the whole series of [Fe(SCN)$_n$]$^{3-n+}$ (n = 1-6) could be detected [12].

8.4　　COMPLEXES WITH N-DONOR LIGANDS

8.4.1　　Complexes with N-heterocyclic ligands

8.4.1.1　　Complexes with pyridine and polypyridine ligands

The kinetics of the substitution of [Fe(phen)$_2$]$^{2+}$, [Fe(bpy)$_3$]$^{2+}$ and [Fe(Me$_2$bipy)$_3$]$^{2+}$ (Me$_2$bipy =4,4'-dimethyl-2,2'-bipyridine) by cyanide in aqueous solution have been studied. The rates are significantly decreased by the application of high pressure. The volumes of activation are relatively insensitive to ligand or to attacking nucleophile and an associative mechanism is invoked to explain these results [13].

The crystal structure of *bis*[2,6-*bis*(aminomethyl)pyridine] iron dichloride (**6**) hydrate has been determined. The unit cell contains molecules with approximate as well as crystallographically imposed C_2 symmetry [14].

(**6**)
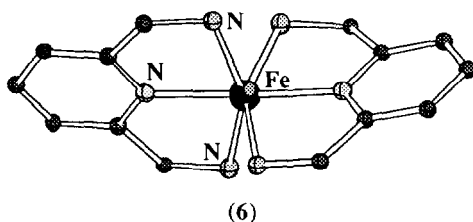
Reaction of 4-octadecylaminopyridine with pentacyanoammine ferrate (II) results in the formation of pentacyano(4-octadecylaminopyridine)ferrate(III), $Na_2[(CN)_5Fe(odapy)] \cdot 5\ H_2O$. Exchange of the sodium cations with hexadecyltrimethylammonium cations yields an amphiphilic species. This allows the solvatochromism (LMCT transition) of the pentacyano(pyridyl)ferrate complex to be transferred to nonpolar solvents such as chloroform. Molecular orbital calculations indicate that the ligand-to-metal charge transfer is from the HOMO of the 4-aminopyridine ligand (which is largely based on the nitrogen of the amino group) to the d_{xz} metal orbital [15].

The complexes *trans*-[Fe(III)(**7**)X$_2$]$^{+/-}$ (X = py (**8**), N_3^- (**9**), $MeCO_2^-$ (**10**), CN^- (**11**)) and *trans*-[Fe(III)(**12**)X$_2$]$^{+/-}$ (X = py (**13**), Cl^- (**14**), $MeCO_2^-$ (**15**)) have been synthesized and characterized. Variable-temperature magnetic and Mössbauer measurements show that (**8**), (**11**) and (**13**) are low spin while (**9**), (**10**), (**14**) and (**15**) are high spin both in solution and in the solid state. All complexes display LMCT transitions in the visible region. The average Fe-N(py) bond distance in (**15**) is relatively large when compared to related complexes; this is attributed to the strain exerted by the ligand. Electrochemical reduction of the low-spin complexes is facile while the Fe(III)/Fe(II) couple is electrochemically irreversible for the high-spin complexes [16].

(**7**) R=H
(**12**) R=Cl
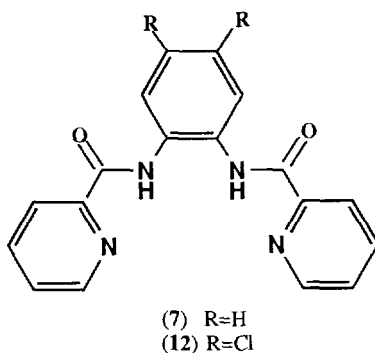
The complex [Fe(**16**)]$^{2+}$ shows two relaxation processes following ^{1}MLCT $\Leftarrow$ ^{1}A$_1$ excitation. This is in contrast to all other previously studied Fe(II) complexes which exhibit only one relaxation process. The observation of two relaxation processes is only seen in CH_3OH, whereas when dmf or CH_3CN is the solvent, a single relaxation profile is seen. It is suggested that

[Fe(16)]$^{2+}$ undergoes a solvent-induced conformational change of the cyclohexyl ring giving rise to two different high spin forms having different spin-state interconversion dynamics [17]. The intramolecular spin crossover of the low spin polypyridyl ferrous compounds [Fe(17)](ClO$_4$)$_2$ and [Fe(18)](ClO$_4$)$_2$ have been studied. Spectroscopic data supports that a $^5T_2$ excited state is formed following photoexcitation of the low spin Fe(II) complexes. The $^5T_2$ state is formed in ≤ 700 fs following ^{1}MLCT $\Leftarrow$ $^1A_1$ excitation and the mechanism of $^5T_2$ formation proceeds via "direct" ^{1}MLCT $\Rightarrow$ $^5T_2$ conversion at or near the Franck-Condon configuration for the ^{1}MLCT $\Leftarrow$ $^1A_1$ excitation [18].

(16): R=

(17): R= (CH$_2$)$_2$

(18): R= (CH$_2$)$_2$
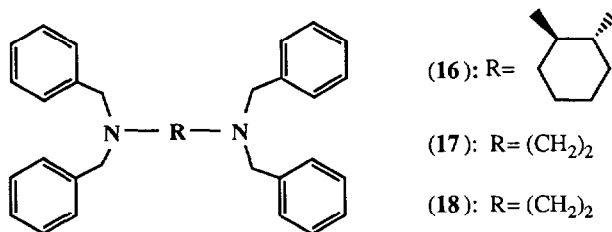
The kinetics and thermodynamics of the solvolysis of tris-(2,2' bipyridine)iron(II) perchlorate [Fe(bpy)$_3$](ClO$_4$)$_2$ has been studied by UV-VIS spectrophotometry. First order kinetics were followed, with activation parameters of $\Delta H^\ddagger = 26.69 \pm 0.39$ kcal mol^{-1} and $\Delta S^\ddagger = 17.1 \pm 1.3$ cal K^{-1} mol^{-1}. The neutral dissociation rate constant is approximately 75% of that in the presence of acid. This is probably due to protonation of a terminal bpy ligand. The [Fe(bpy)$_2$(dmso)$_2$]$^{2+}$ complex is suggested to have a greater thermodynamic stability in dmso than in H$_2$O. The mechanism depicted in Scheme 1 is suggested [19].
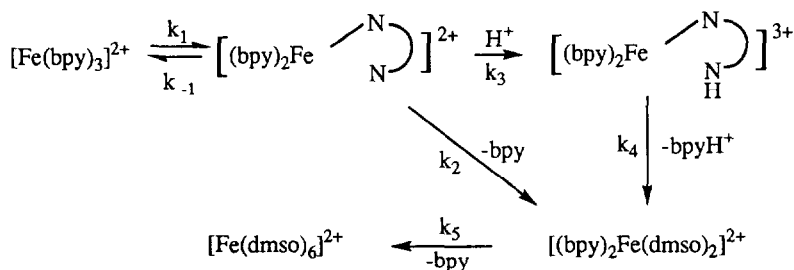
Scheme 1

Complex (19), [Fe(20)(OBz)]ClO$_4$ (20 = *tris*[(6-methyl-2-pyridyl)methyl]amine), has a coordination environment similar to that proposed for native soybean lipoxygenase. Treatment with alkyl hydroperoxide (t-butyl hydroperoxide or cumyl hydroperoxide) of this ferrous complex affords a transient intermediate species. Spectroscopic data suggest that this intermediate is a high spin alkylperoxo complex [20].
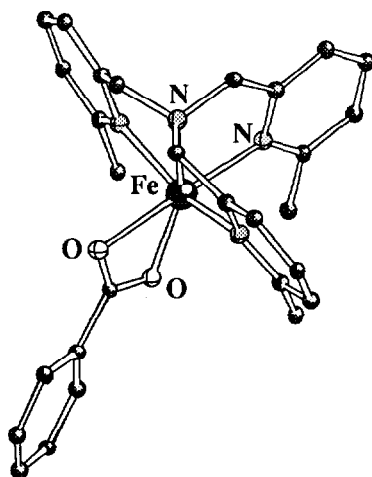
(19)

8.4.1.1   Complexes with other N-heterocyclic ligands

The kinetics of the dissociation of the *tris*(1,10-phenanthroline)iron(II) complex ion in aqueous acid solutions have been studied. It is proposed that the dissociation is a complex reaction involving two parallel processes, leading either to $Fe(phen)_3^{2+}$ or Fe_3^+ and phen H^+ [21].

Single crystal X-ray diffraction investigations at variable pressures and temperature have been carried out on two isostructural iron(II) spin transition complexes, $Fe(phen)_2(NCS)_2$ (from II) and $Fe(Btz)_2(NCS)_2$. Both complexes remain in the space group Pbcn over the whole pressure range of 1000 HPa to 1.3 GPa and over the temperature range of 130 to 300 K. The only noticeable difference in the evolution of the structural properties of these two compounds as a function of pressure is that $Fe(Phen)_2$ exhibits a strong lattice anisotropy compared to $Fe(Btz)_2$ [22].

The ionic liquid-mediated synthesis and X-ray structure of *trans*-difluorotetrakis(1-methylimidazole)iron(III) (**21**) has been reported. The iron(III) centre exists in a *pseudo*- octahedral environment with two axial fluoride ligands and four equatorial 1-MeIm ligands. There are two crystallographically independent 1-MeIm molecules with Fe-N bond distances of 2.102(3) and 2.136(3) Å. EPR spectroscopy of a solid sample of (**21**) in MgO matrix suggests it is high spin iron [23].

The unusual lattice properties of $Fe[B(3\text{-isopropylpyrazol-1-yl})_4]_2$ (**22**) have been studied by Mössbauer spectroscopy. The Mössbauer spectra exhibit a non-symmetric doublet with large quadrupole splitting which has been fit with two quadrupole doublets of equal area. Isomer shifts of the doublets is characteristic of those expected for iron(II) in a tetrahedral environment. The most unusual aspect of the Mössbauer spectra of (**22**) is the temperature dependence of the spectral absorption area. The spectrum follows the Debye model for lattice vibrations for temperatures below 160 K. Above 160 K, the spectral absorption area deviates indicating that the iron nuclide is undergoing additional displacement. It is believed that this additional displacement may be due to the strong ligand-ligand steric interactions in the coordination sphere of the iron (II) ion [24].

(22)
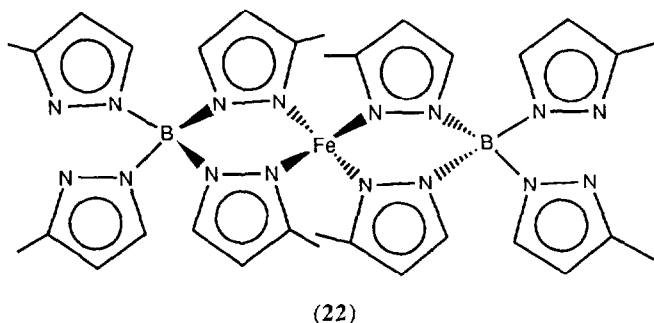
The magnetic susceptibility of solid [Fe(tpm)$_2$](ClO$_4$)$_2$ (tpm = *tris*(1-pyrazolyl)methane) has been recorded from 4.5 to 295 K. In this temperature range, the magnetic moment increases from 1.40 to 1.58 µB indicating a slight population of a paramagnetic state at room temperature. When a solution of the complex is irradiated with a laser pulse within the ligand field absorption band of the singlet isomer, ground state depletion occurs within the pulse duration followed by fast recovery to the original absorbance level. Perturbation of the spin equilibrium is brought about solely *via* ligand field excitation; excitation through the metal-ligand charge transfer transitions are ineffective in promoting perturbation [25].

Gas phase He I and He II photoelectron spectra of the *bis*[tetrakis(pyrazol-1-yl)borato]iron(II) complex have been reported. The spectral pattern of the d^{-1} final ion states is almost identical to that produced upon ionization from the $^5T_2$ ground state of the thermally activated high spin *bis*[*tris*kis(pyrazol-1-yl)borato]iron(II) parent complex. The multiplet onset structure in the photoelectron spectrum suggests the occurrence of the $^5T_2$ ground state and of spin crossover phenomena [26].

Complexation of the ligands (23)-(26) to Fe(II) give intensely coloured *pseudo*-octahedral low spin [Fe(L)$_2$]$^{2+}$ (n = 2-5) complexes in MeCN solution. Spectroscopic results and Extended Hückel calculations performed on 4-(X-phenyl)pyridine fragments of the ligands indicate that the substituent strongly influences the π and π* energy levels of the group and that this influences the strong MLCT bands in the UV-VIS spectra of the complexes [27].
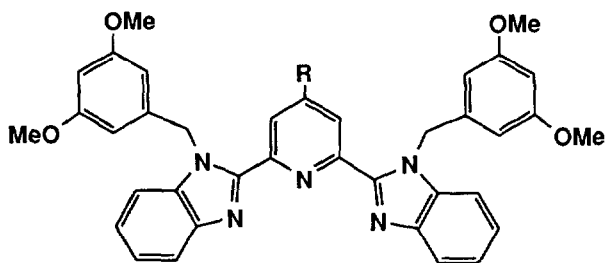
(23) (R = H), (24) (R = C$_6$H$_5$), (25) (R = *p*-NO$_2$C$_6$H$_4$), (26) (R = *p*-NEt$_2$C$_6$H$_4$)

Variable-temperature magnetic measurements on the hexacoordinate complexes [Fe(27)$_2$](ClO$_4$)$_2$·H$_2$O, [Fe(28)$_2$](ClO$_4$)$_2$·2H$_2$O and [Fe(29)$_2$](ClO$_4$)$_2$·2H$_2$O have been made. The complex of (29) follows Curie-Weiss behaviour down to 8K with a Curie constant in good agreement with an S=2 ground state while [Fe(27)$_2$](ClO$_4$)$_2$·H$_2$O exhibits anomalous magnetic properties indicative of a thermally driven singlet ($^1A_1$, ls) to quintet ($^5T_2$, hs) spin-state transition. The ΔH and ΔS parameters for the transition are estimated to be 13 kJ mol^{-1} and 56 J K^{-1} mol^{-1}, respectively. Mössbauer spectroscopy confirms the existence of two spin states in [Fe(27)$_2$](ClO$_4$)$_2$ · H$_2$O; at 300K, the $^5T_2$ state is clearly predominant while at 80K, only the $^1A_1$ state can be detected [28].
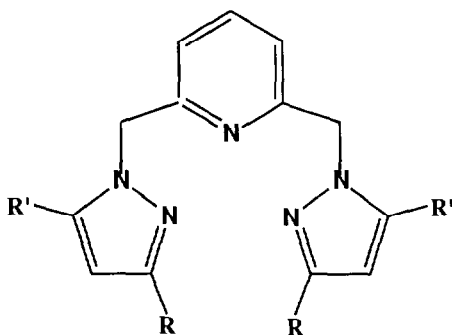
(27) (R = R' = H), (28) (R = H, R' = Me), (29) (R = R' = Me)

The dinuclear complexes [Fe$_2$(H$_2$O)$_8$(bipym)](SO$_4$)$_2$·H$_2$O (30) and [Fe$_2$(H$_2$O)$_6$(bipym)(SO$_4$)$_2$] (31) (bipym = 2,2'-bipyrimidine) have been synthesized and structurally characterized by X-ray crystallography. The structure of (30) consists of discrete dinuclear cations with uncoordinated sulfate anions and crystallization water molecules while that of (31) consists of neutral dinuclear units which are polymerized through hydrogen-bonding interactions between coordinated water and sulfate anions of adjacent dimers. Both configurations contain distorted octahedral coordination geometries around the iron atoms, the Fe-N$_{ave}$ distance being ca. 0.1 Å longer than the Fe-O$_{ave}$ distance. The intramolecular Fe-Fe separations are approximately 5.9 Å. The magnetic properties of (30) and (31) are similar and indicative of antiferromagnetic coupling between two high-spin ferrous ions; J = -1.7 and -1.55 cm^{-1} for (30) and (31), respectively [29].

Iron complexes of the ligand (32) that mimics the metal-binding portion of the anti-tumour drug bleomycin have been isolated and characterized. The anion of (32) ligates to the iron centre through five nitrogens located in the primary and secondary amines, pyrimidine and imidazole rings and amide moiety. The sixth coordination site on the iron complexes is occupied by a solvent molecule. The complex [Fe(II)PMA)]Cl·MeOH (33) binds CO and NO, the former in a reversible manner. Upon exposure to dioxygen, a low spin iron(III) hydroperoxy species, [(PMA)Fe(III)O-O-H] (34), is generated. The reaction of [Fe(PMA)(III)](NO$_3$)$_2$·dmso with H$_2$O$_2$ also affords the hydroperoxy species (34). The two model complexes promote rapid oxo transfer to olefinic substrates. The mono-oxygenase activity of these complexes is unique since they are the first two examples of mononuclear non-heme iron complexes capable of O$_2$ activation [30].

(32)

(35)
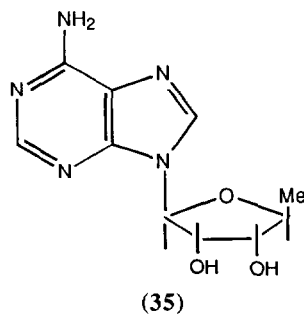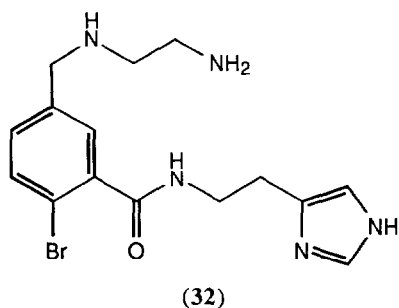
Reaction of $Fe(ClO_4)_3 \cdot x\ H_2O$ with 5'-Deoxyadenosine forms a complex which is suggested to be $[(EtOH)FeL_2(\mu\text{-}ClO_4\text{-}O,O)FeL(EtOH)(ClO_4)_2]$ (LH = 5'-deoxyadenosine, 35) on the basis of elemental analysis, magnetic susceptibility, and IR spectroscopy. It is suggested that the purine coordinates *via* the N_6 and N_7 atoms [31].

The complex $[Fe(Htrz)_3](ClO_4)_2$ (Htrz = 1,2,4-1H-triazole), was synthesized in order to observe a complex which undergoes spin transition with a thermal hysteresis at room temperature. The complex, when dry, exhibits a smooth spin transition around 265 K with a weak thermal hysteresis at approximately 5 K. When a drop of water is added to the system, the transition becomes very abrupt with $T_c\uparrow$ = 313 K and $T_c\downarrow$ = 296 K. The hysteresis is just above room temperature and can be shifted to lower temperatures by replacing Htrz by $4\text{-}NH_2\text{-}Htr$ [32].

8.4.2   Complexes with imines and oximes

The ferric complex of the new Schiff base ligand (36) has been synthesized by reflux of $FeCl_3$ and the ligand in acetone. Elemental analysis suggests the empirical formula $[Fe(36)(H_2O)_2(OH)Cl]$. The magnetic moment of 3.6 μ_B - intermediate between high spin and low spin values - may be due to spin cross-over [33].

(36)
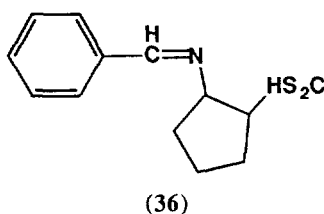
The tetranuclear complex $[L_2Fe(\mu_3\text{-}O)_2(\mu_2\text{-}OAc)_3(37)_2Fe_2]X$ (X = ClO_4^- (38), PF_6^- (39); L = Me_3TACN; Sao = salicylaldoxime) has been synthesized. The preparation of complexes (38) or (39) is very dependent on the ratio of the starting materials salicylaldoxime and $Fe(OAc)_2$, the optimal ratio being 1:1. The use of an excess of ligand (37) and filtration in air yields the dinuclear complex $[LFe(III)(Sao)_3Fe(III)]$ (40). X-ray crystallography reveals that the molecular structure of (40) consists of an $[Fe_4(\mu_3\text{-}O)_2]^{8+}$ butterfly core in which each Fe(III) ion is in a distorted

octahedral environment. Magnetic susceptibility measurements indicate that the ground state is diamagnetic with antiferromagnetic exchange interactions. While the exchange interaction between the two central irons could not be determined due to spin frustration, the peripheral coupling between the "wing-tip" and "body" irons of the butterfly was estimated to be $\approx$46 cm^{-1} [34].

(37)   (40)
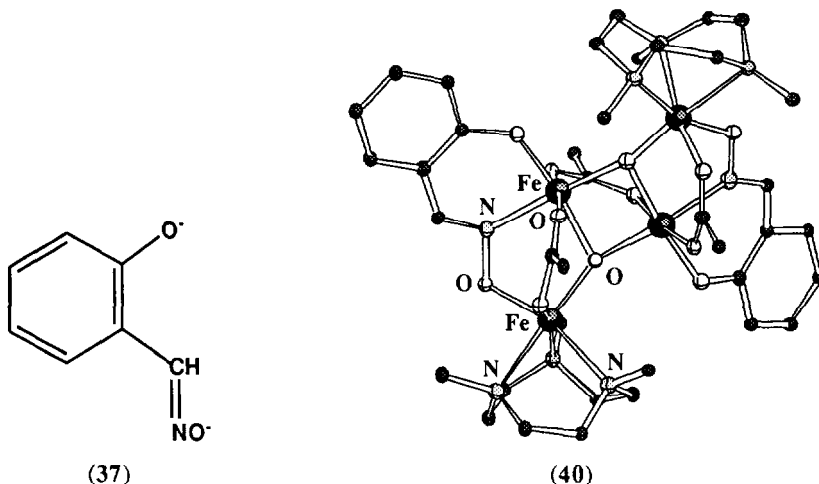
A series of iron clathrochelate complexes based on oxime-hydroazone ligands have been capped with ferrocenylboronic acid to produce the dimetallic species, [Fe(**41**)$_3$(CH$_2$)$_3${B(Cp)$_2$Fe]PF$_6$ (**42**), [Fe(**43**)$_3$(CH$_2$)$_3${B(Cp)$_2$Fe]PF$_6$ (**44**), [Fe(**45**)$_3$(CH$_2$)$_3${B(Cp)$_2$Fe]PF$_6$ (**46**). The ligand 1,1'-ferrocenediyldiboronic acid is also used as a bridging agent between two clathrochelate complexes to produce a trimetallic species, [{Fe(**41**)(CH$_2$)$_3$}$_2${B$_2$(Cp)$_2$Fe}](PF$_6$)$_2$ (**47**). The redox chemistry of these multiple metal complexes was studied by cyclic voltammetry and controlled-potential electrolysis. The reduction potentials of the encapsulated iron of the dimetallic complexes are not effected by the oxidation state of the ferrocenyl iron; there appears to be no interaction between the two iron centres. Similar results were observed in the studies of the trimetallic species [35].

The three iron complexes [Fe(**43**)$_3$(BC$_6$H$_5$)(CH$_2$)$_3$]PF$_6$·H$_2$O, [{Fe(**43**)$_3$(CH$_2$)$_3$}$_2$-(B$_2$C$_6$H$_4$)]PF$_6$ · 2 H$_2$O (**48**) and [Fe(**45**)$_3$(BC$_6$H$_5$)(CH$_2$)$_3$]PF$_6$, have been synthesized and characterized by elemental analysis and NMR spectroscopy. Cyclic voltammetry studies indicate that the oxidation of the iron to the +3 state does not produce a stable complex. Electrochemical studies of the dinuclear complexes indicate that the two iron centres are non-interactive [36].

The reaction of the *tris*(arylazo oximato)iron(II), Fe(RL)$_3^-$ anion (R = Me (**49**), Ph (**50**), *p*-MeC$_6$H$_4$ (**51**)) with Cu(MeCN)$_4^+$ in dichloromethane affords the trinuclear complex Cu(II)Fe$_2$(II)(RL)$_6$. In the presence of PPh$_3$, the dinuclear Cu(I)Fe(II)(RL)$_3$ is formed. The X-ray structures of Cu(I)Fe(II)(**50**)$_3$(PPh$_3$) (**52**) and Cu(II)Fe$_2$(II)(**49**)$_6$ (**53**) have been reported. In both complexes, the Fe(RL)$_3^-$ fragment acts as a facially disposed tridentate oximato-O$_3$ ligand. The Fe(RL)$_3^-$ chelate is chiral and can occur in Δ and Λ configurations. The centrosymmetry of **53** implies that within each molecule the Fe(**50**)$_3^-$ units together constitute a racemic Δ -Λ pair [37].
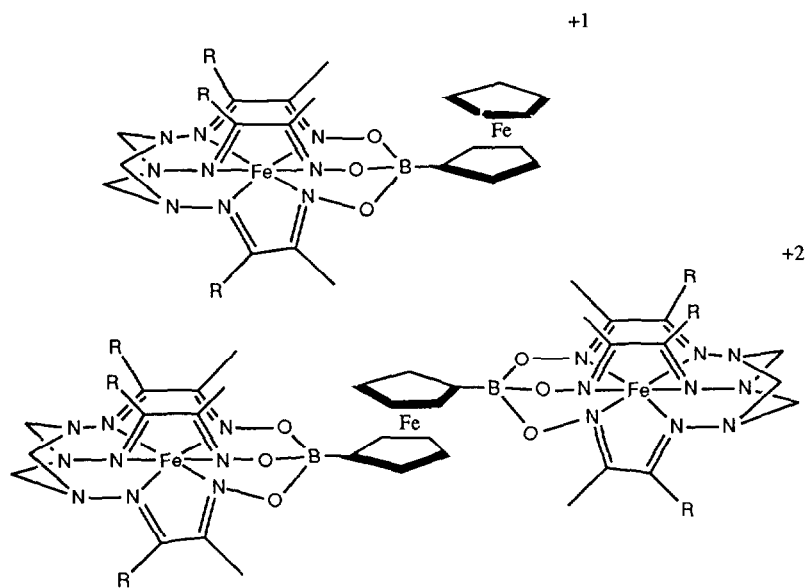
(42), (44), (46) (top) (47) (bottom); R = Me (41), Ph (43), H (45)

(48)

(49)-(50)   (52)
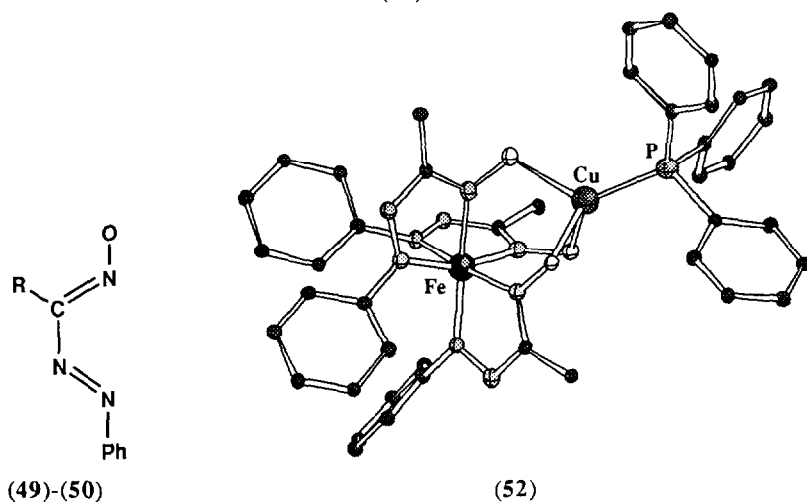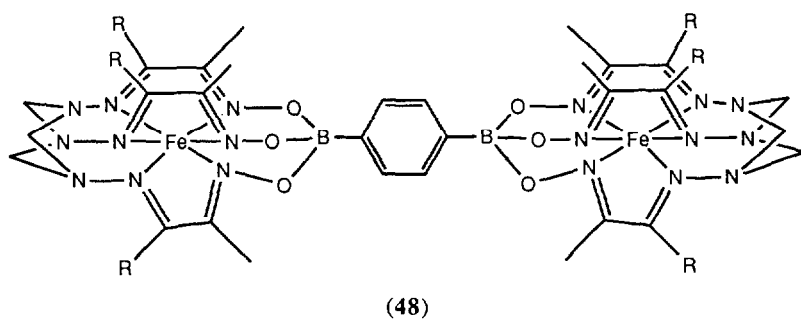
Three phenylglyoximate molecules have been cross-linked with two phenylboric acid molecules on an iron template in the presence of BF_3. The structure of the resultant complex (54) was determined by X-ray crystallography. The trigonal prismatic coordination poly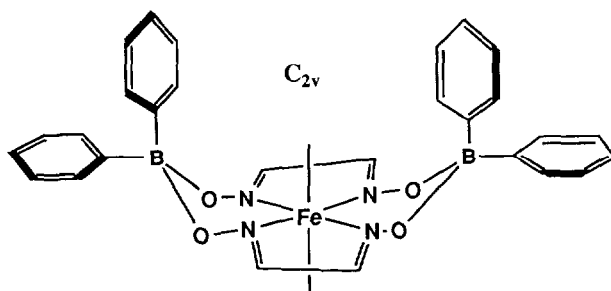hedron formed by 6 N atoms of the macrobicyclic ligand has a distortion angle of 21.8° towards octahedral configuration [38].
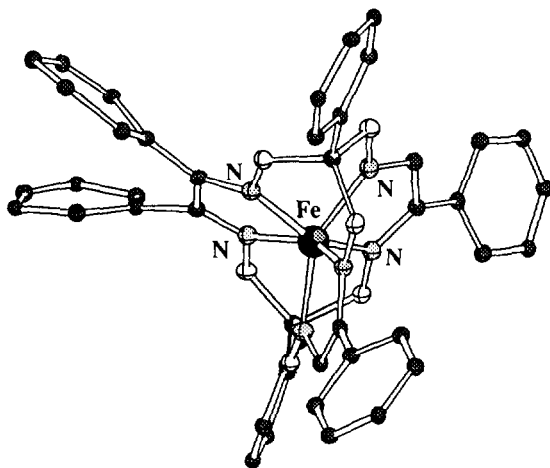
(54)

(55)

A kinetic study has reported evidence that ligand access to non-porphyrinic metal complexes can be mediated by boron-linked groups positioned in close proximity to axial binding sites. The (dimethylglyoximato)diphenylborate (55) complex (56) has two conformational isomers. *Bis*-ligated complexes adopt the C_{2h} conformation while when axial ligands differ, the C_{2v} conformation is adopted directing both axial phenyl moieties towards the smaller ligand. Rates of CO binding to $Fe(Py)_2$ are 500 times faster in the Fe(55) system when compared to the fluoro analogue (dimethylglyoximato)difluoroborate (57). Pyridine loss is faster in the (55) system due to repulsive ground-state interactions with the phenyl groups [39]. Tetracyanoethylene (TCNE) and a variety of other nitriles have been shown to bind to $Fe(57)_2$ *via* the nitrile nitrogen as rather weak σ-donor ligands. The binding of TCNE to (56) is exceptionally strong as a result of charge transfer

interactions with the peripheral phenyl groups. Evidence of a TCNE-phenyl interaction is seen in the electronic spectra with a band at 500 nm. Comparing data for the other nitriles, the charge transfer stabilization drops off in the expected order TCNE > 4-nitrophthalonitrile > phthalonitrile > CH_3CN [40].

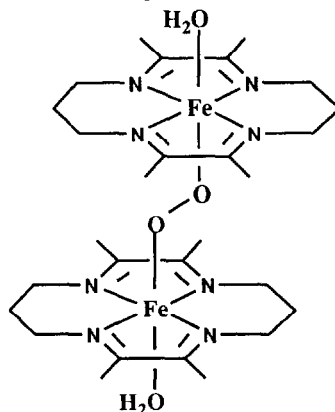### 8.4.3   Complexes with macrocyclic ligands

The reaction of $FeCl_2$ or $FeCl_3$ with cyclam (1,4,8,11-tetraazacyclotetradecane) leads to the formation of dark orange-red plates of $[H_4(cyclam)][FeCl_5(OH_2)](Cl)_2$ (58). The solid state structure of (58) consists of a hydrogen-bonded network of the cyclam, $[FeCl_5(OH_2)]$ and chloride ions [41].

Aeration of the complex $[Fe(II)(59)(H_2O)_2]^{2+}$ leads to the formation of a new species formulated as the peroxo-bridged complex $[Fe_2(III)(59)_2(H_2O)_2O_2]^{4+}$ (60). Electrochemical reduction of the dimer leads to rapid dissociation and re-formation of the reduced monomer species. The dimerization can be monitored by Mössbauer spectroscopy. The Mössbauer spectrum of the dimer indicates that there are two different conformations of this complex in the solid state [42].
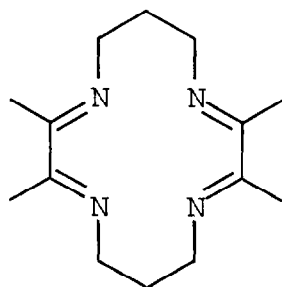
(59)   (60)

The stability constants of iron and iron/sulfate complexes of one cryptand and two macrocyclic ligands have been studied by potentiometric titrations. The predominating species are the dinuclear hydroxo-bridged complexes (61), (62) and (63). There are also mono- and dinuclear Fe(II)/sulfate adducts of the macrocycles [complexes (64)-(67)] [43].
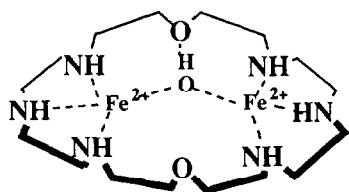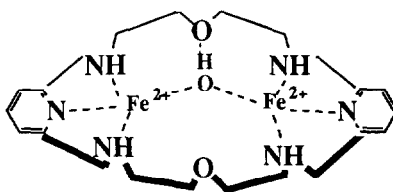
(61)   (62)
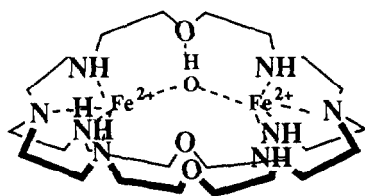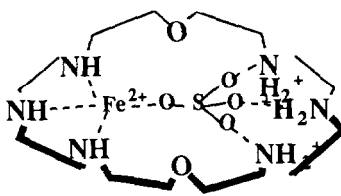
(63)   (64)
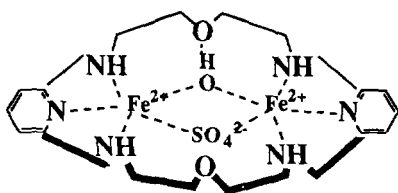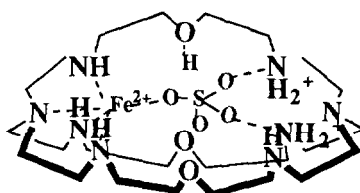
(65)   (66)
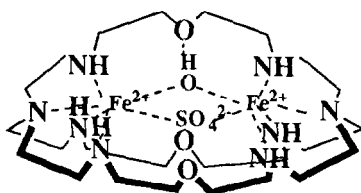
(67)

The reaction of a suspension of (Me₃TACN)FeCl₃ in tetrahydrofuran with Li[AlH₄] under anaerobic conditions produces a deep red solution from which [(Me₃TACN)₂Fe₂(μ-H)₃]BPh₄ (68) precipitates upon addition of NaBPh₄ and cooling. The Mössbauer spectrum of (68) at 77 K displays a symmetric doublet with isomer shift $\delta = 0.38$ mm^{-1} and quadrupole splitting $\Delta E_Q = 0.85$ mm^{-1}, values typical for octahedral low spin Fe(II). The ^{1}H NMR of [L₂Fe₂(μ-H)₃]BPh₄ displays one singlet at $\delta = -23.7$ which is assigned to the three magnetically equivalent bridging hydride ligands [44].
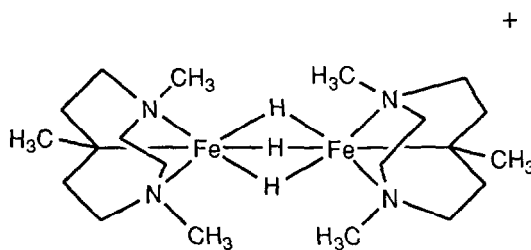
(68)

Two oxidation states of the macrocyclic tetraamide coordination complex [FeCl(η^4-69)] have been studied by Mössbauer and EPR spectroscopy. In the ferric state, the complex has an electronic ground state with intermediate spin S = 3/2. Upon oxidation, the complex becomes high-spin iron(IV), S = 2, a spin state previously not reported for isolated iron(IV) complexes. Analysis of the high field Mössbauer spectra for both [FeCl(η^4-69)]$^{2-}$ (70) and [FeCl(η^4-69)]$^-$ reveals magnetic hyperfine interactions substantially smaller than expected for an ionic complex. The X-ray structure of (69) is also reported [45].

(69)   (70)
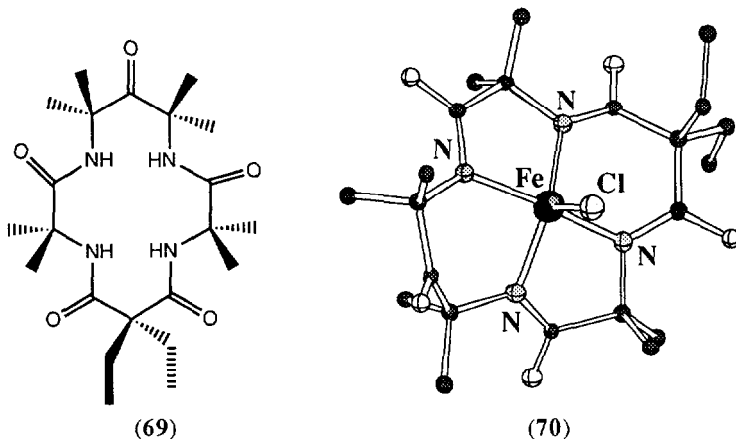
The tetraaza-macrocyclic amino acid (71H$_2$) forms low spin compounds with Fe(III), as the hexadentate deprotonated ligand, [71]$^{2-}$, with *trans* coordination of the carboxylato groups or as the neutral tetradentate planar tetraazamacrocyclic (71H$_2$) for the *trans*-dichloro and dithiocyanato cations. Structures for *trans*-[Fe(71)](ClO$_4$) and *trans*-[Fe(71H$_2$)Cl$_2$][71H$_6$]Cl$_2$(ClO$_4$)$_4\cdot$4H$_2$O are reported [46].

(71H$_2$)
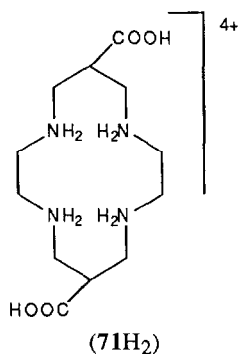
8.4.4   Miscellaneous N-donor complexes

Ab initio calculations on diamidoiron(III) hydroperoxide have been used to model the hydroperoxide intermediate in hemoproteins. Diamidoiron(III) hydroperoxide is a bridged structure with the proximal Fe-O bond only slightly shorter than that of the coordinated distal metal-oxygen

bond. The protonated complex is not bridged and has a negative barrier for oxygen donation to NH_3. This suggests that in certain cases oxygen atom transfer from iron hemoproteins could precede the formation of the ferryl complex [47].

Ion-molecule reactions of excited- and ground-state Fe^+ with NO have been studied. The ground state ^6D ($4s^13d^6$) Fe^+ ions do not react with NO. Conversely, the metastable electronic states react with NO to form charge-transfer product ions (NO^+) and radiative association adducts $[Fe^+(NO)]$. The ^6S ($4s^23d^5$) Fe^+ ion is also unreactive towards NO [48].

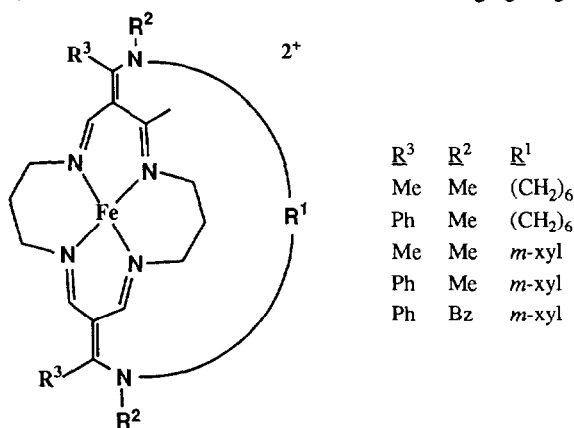The autoxidation of a series of iron(II) cyclidenes of the general formula $[Fe(R,R^2,m$-xyl72)Cl]$^+$ (R = Me, Ph; R^2 = Me, Bz) has been reported. The deduced rate constant k' for the electron-transfer process decreases in the sequence MeMe> MeBz> PhMe> PhBz, which is the order of increasing electron withdrawing power and/or steric bulk of the substituents. A peroxoiron(III) species was identified as one of the products of the autoxidation and can be observed at ambient temperatures. Its EPR signal at g = 2 with low anisotropy suggests a low-spin iron species which is similar to those of natural system analogues but in contrast to the first reported model systems [49]. Similarly, the rates of autoxidation of the iron(II) cyclidenes $Fe(R,R^2,(CH_2)_n72)Cl]^+$ have been studied as functions of dioxygen pressure and with variations in the size of the cavity within the O_2 molecules must reside in order to bind to the iron atom. The complexes studied were $[Fe(II)(Me, Me,(CH_2)_3)]$, $[Fe(II)(Ph, Me, (CH_2)_4)]$, $[Fe(II)(Ph, Me, (CH_2)_5)]$ and $[Fe(II)(Ph, Me, (CH_2)_6)]$. As the size of the dioxygen binding cavity increases, the dioxygen dependencies of the autoxidation rates of the iron cyclidene complexes change, obeying a variety of rate laws including that observed for hemoglobin and myoglobin. Analysis of the rate constants indicates that the molecule of O_2 that oxidizes the iron(II) is not bound suggesting that an electron-transfer mechanism occurs in the autoxidation process and this same mechanism may apply to the hemoglobin and myoglobin [50]. The vibrational spectra of a number of iron(II) cyclidene species of general structure (72) have been studied. The larger the electron-withdrawing power of substituents R^2 and R^3, the higher the v_{O-O} values for the corresponding dioxygen complexes. There appears to be no correlation between v_{O-O} and the oxygen affinity of the complexes, while the stretching frequency alternates with the number of atoms in the bridging R^1 group [51].

$\underline{R}^3$	$\underline{R}^2$	$\underline{R}^1$
Me	Me	$(CH_2)_6$
Ph	Me	$(CH_2)_6$
Me	Me	*m*-xyl
Ph	Me	*m*-xyl
Ph	Bz	*m*-xyl

(72)

8.5   COMPLEXES WITH TETRAPYRROLE MACROCYCLES

8.5.1   Complexes with phthalocyanines

The kinetics and equilibria for the reaction between cyanide and Fe(II)pc in dmso have been studied. The complex $[Fe(pc)(CN)_2]^{2-}$ is formed by two consecutive replacements of axially coordinated dmso ligands. The rate constants for the binding of the first and second cyanide ligands are 17.5 ± 0.8 dm^3 mol^{-1} s^{-1} [52].

Iron(II) phthalocyanine, Fe(Pc), has been found to be superior to metalloporphyrins and Schiff base complexes as a heterogeneous O-activating catalyst in certain systems. The aerobic oxidation of hydroquinone to 1,4-benzoquinone has been used to test the catalytic activity of various forms of Fe(Pc). It was found that the active species is a μ-oxo-Fe(pc) dimer [53].

8.5.2   Complexes with porphyrins

8.5.2.1   Axially ligated porphyrin complexes

Water soluble $[Fe(III)(H_2O)(73)]^{3-}$ and ferrihemoproteins (methemoglobin, metmyoglobin, oxidized cytochrome c and catalase) associate with NO to yield nitric oxide adducts. The equilibrium constants for association of ferrihemoproteins and NO are one order of magnitude larger than that of the $[Fe(III)(H_2O)(73)]^{3-}$ [54].

(73)
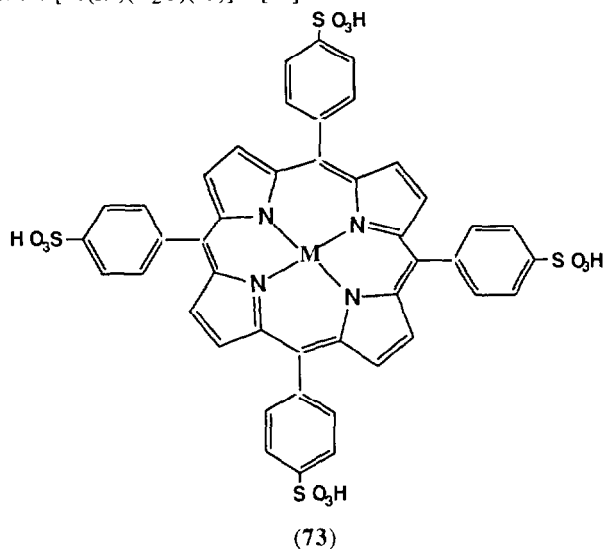
Catalytic systems containing Fe(III)(TPP) or Fe(III)(2,6-Cl$_2$(TPP), axial ligands (imidazole, 1-methylimidazole, 2-methylimidazole or 4-^{t}Bu-pyridine) and tert-Bu-hydroperoxide have been used for the oxidation of primary aromatic amines, $RC_6H_4NH_2$ (R = H, 4-Me, 4-Br, 4-NO$_2$, 4-MeO, 3-Me, 4-Cl, 4-F), to the corresponding nitro derivatives. There is no significant variation in activity within the imidazole series of axial ligands but 4-^{t}Bu-pyridine gave lower yields [55].

In a study of the effects of electron donating and withdrawing substituents on the electronic properties of the pyrrole-substituted porphyrins **74-9**, the Fe(III) complexes were prepared and investigated in both the five-coordinate chloro iron(III) high spin and six- coordinate *bis(N*-methylimidazole) iron(III) low spin states. In both states, ^{1}H NMR spectra showed that the bulky diethyl carbamoyl groups are not in the plane of the porphyrin ring [56].
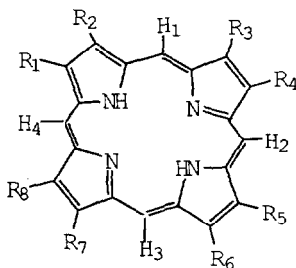
(**74**): R_1, R_2, R_5, R_6 = C(O)NEt$_2$; $R_1, R_2 R_5, R_6$ = Et   (**75**):R_1-R_8 = Et

(**76**): R_1-R_8 = C(O)NEt$_2$ (**77**): R_1, R_2 = C(O)NEt$_2$; R_3-R_8 = Et

(**78**): R_1-R_4 = C(O)NEt$_2$; R_5-R_8 = Et   (**79**): R_1-R_6 = C(O)NEt$_2$; R_7, R_8 = Et

The electronic absorption, magnetic circular dichroism, IR and EPR spectral properties of both the five-coordinate iron(II)complexes and the six-coordinate iron(II)(R) nitrosyl (R = *N*-MeIm; Py; 2, 4, 6-Me$_3$py) complexes of the ligands mono-, bis-, tris- trifluoromethylporphyrin and etioporphyrin have been studied. As the electron deficiency of the porphyrin increases, the g values of the six-coordinate complexes decrease and the g$_{iso}$ value approaches the free spin value. This decrease is attributed to electron donation from the axial ligand to the *trans* to the NO group and resultant destabilization of the d$_{z2}$ orbital [57].
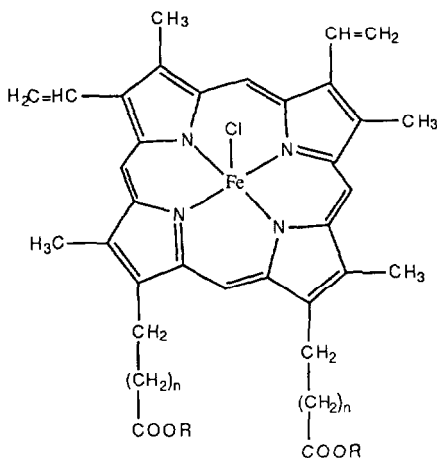
(**80**); n = 2, R = H   (**81**); n = 2, R = Me   (**82**); n = 3, R = H   (**83**); n = 2, R = Me

The reaction of Fe(por)Cl (por = **80-83**) with MeIm to give Fe(por)(MeIm)Cl, which undergoes chloride ionization, is accelerated in the presence of potential hydrogen-bonding moieties. Iron porphyrins having butyric acid side-groups showed an increased chloride ionization rate compared to those containing propionic side chains [58].

Unlike the corresponding alkyl and aryl derivatives, iron(III) acetylide-ligated porphyrins were found to be high spin (S = 5/2) and have characteristics of a more ionic Fe-C bond. Addition of thf or pyridine results in the conversion to low spin (S = 1/2) six-coordinate species. The iron(III) acetylide complexes are not reactive towards dioxygen and are difficult to purify [59].

8.5.2.2   Complexes with oxygen, peroxides and superoxides

Time resolved high resolution resonance Raman spectroscopy indicates that the $Fe_{a3}(II)-O_2$ complex of cytochrome c oxidase is of an end-on type on the basis of observed data for the $^{16}O^{18}O$ derivatives. The $Fe_{a3}(III)-O-OH$ species with a marker band at 785 cm^{-1} is generated as an intermediate following the dioxy complex and is converted to the Fe(IV)=O species. The main pathway for dioxygen reduction by cytochrome c oxidase is Fe(II)-O_2 -> Fe(III)-O-O-H -> Fe(IV)=O -> Fe(III)-OH [60].

The iron porphyrin complex (**84**) cleaves the O-O bond of peroxy acids heterolytically even in highly hydrophobic solvents; the active intermediate can efficiently hydroxylate aliphatic hydrocarbons. The reaction profiles of the oxidation of 2,4,6-tri-*tert*(butylphenol) by peroxyphenylacetic acid catalyzed by hemes were compared using (**84**), an imidazole ligated iron porphyrin, and Fe(TPP)Cl. The more strongly electron-donating axial ligand enhanced heterolytic O-O bond cleavage and its rate [61].

R= -NHC(=O)C(CH$_3$)$_3$ L=S-CH$_2$-(*o*-phenylene)-OCH$_2$

(**84**)
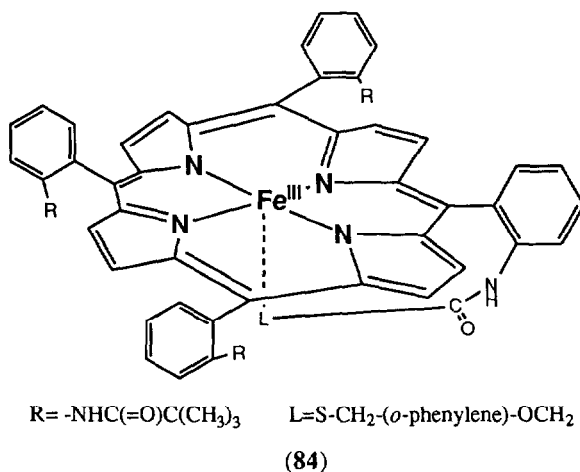
Oxidation of [Fe(TPP)]SbF$_6$ using peroxylauric acid or t-butylhydroperoxide at 0° C leads to new species formulated as the oxo-bridged species [{Fe(IV)(TPP)}$_2$O](SbF$_6$)$_2$ (**85**) and [Fe(IV)(TPP)-O-Fe(III)(TPP)(O$_2$But)]SbF$_6$ (**86**), respectively. The reaction of (**85**) with peroxylauric acid at more elevated temperature (refluxing benzene) leads to the formation of a third

species which is proposed to be the mixed-valence oxo-dimer [Fe(IV)(TPP)-O-Fe(III)(TPP)]SbF$_6$ [62].

The Fe(II) and Fe(III)Br porphyrin complexes (87) and (88) have been prepared. Absorption spectroscopy indicates that the ferrous complexes bind O$_2$ and CO reversibly in toluene. The half-life of the dioxygen adducts with respect to irreversible oxidation to Fe(III) was greater than two days in toluene at 25°C. The complexes may be embedded in phospholipid unilamellar vesicles and are then able to transport dioxygen in an aqueous medium [63].
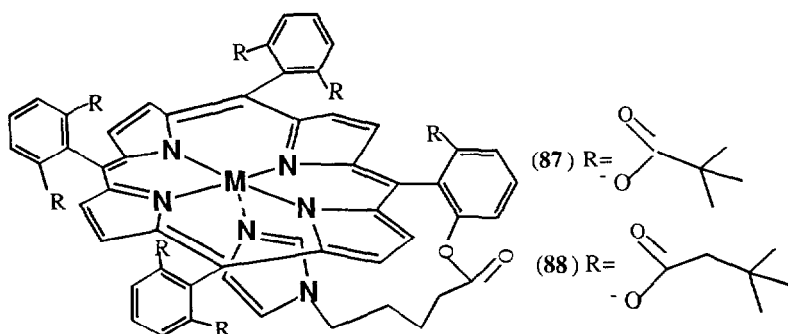
The "octopus"-porphyrins (89) and (90) have been synthesized and their Fe(II) and Fe(III)Br complexes prepared. Aggregates of the porphyrin complex Fe(90)Br dispersed in water together with 1-dodecyl-2- methylimidazole can be reduced to ascorbic acid. The resultant iron(II)porphyrin aggregates bind O$_2$ and CO reversibly [64].
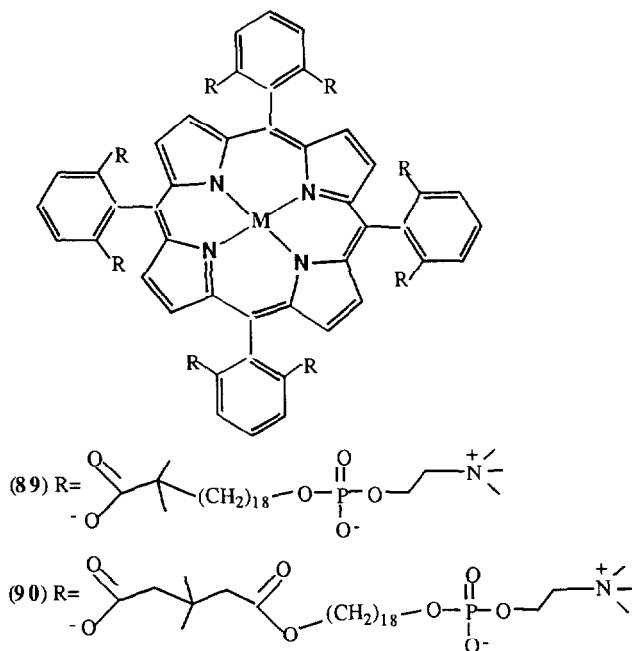
The lipid porphyrin derivatives (91), (92) and (93) form spherical unilamellar vesicles in water. Dodecylimidazole has been used as an axial ligand for the porphyrinatoiron(III) vesicles. The iron (III) complexes can be reduced by ascorbic acid. The resultant iron(II)porphyrin vesicles bind O_2 and CO reversibly [65].

R^1 = HNC(O)CMe$_2$(CH$_2$)$_{18}$OC(O)(CH$_2$)$_2$C(O)OCH$_2$CH(O(CH$_2$)$_{17}$Me)CH$_2$R^2
(91): M = Fe(II), R^2 = $^-$O$_3$PO(CH$_2$)$_2$NMe$_3$$^+$
(92): M = Fe(III)Br, R^2 = $^-$O$_3$PO(CH$_2$)$_2$NMe$_3$$^+$
(93): M = Fe(III)Br, R^2 = OH
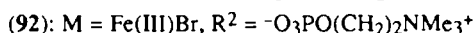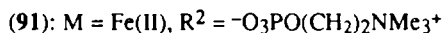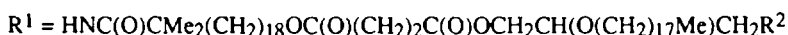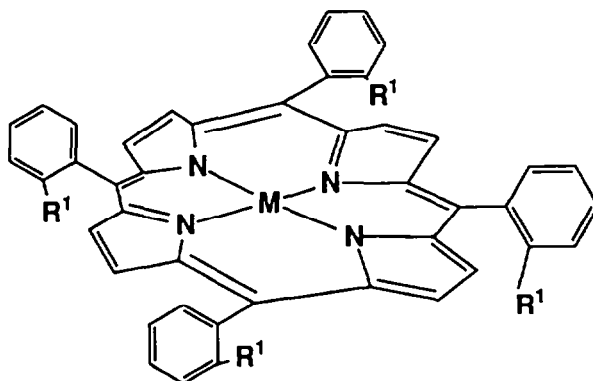
The oxidation of cyclohexane and cyclohexene by iodosylbezene, hydrogen peroxide, t-butyl hydroperoxide, and MCPBA, catalyzed by Fe(TDCPP)Cl (TDCCP = meso-tetrakis(2,6-dichlorophenyl)porphinato), Fe(TPP)Cl, Fe(TMP)Cl and Fe(cyclam)$^{2+}$, has been studied in the presence of labelled H_2^{18}O. Alkane hydroxylation and alkene epoxidation reactions led to incorporation of labelled oxygen into the oxygenated products whenever iodosylbenzene was used as an oxidant but only infrequently when other oxidants where used. The oxygen of the iodosylbenzene is exchanged with the water prior to the formation of reactive oxidants; the incorporation of labelled oxygen into products obtained from metal complex catalyzed oxygenation is not sufficient evidence that high valent metal oxo intermediates are involved in the mechanism [66].

The halogenated iron tetraarylporphyrins (94) and (95) (M = FeCl, X = Cl, Br) have been prepared and structurally characterized by X-ray crystallography. The porphyrins adopt saddle-shape conformations. Complex (94) was oxidized by m-chloroperoxybenzoic acid in CH_2Cl_2 to give the ESR-active species (94)$^{.+}$ (M = FeO, X = Cl). The ESR data for (94)$^{.+}$ (M = FeO, X = Cl) is typical for a quartet ground state of S_t= 3/2 and indicated that ferromagnetic coupling occurs between the low-spin Fe(IV) centre and the porphyrin π-radical cation. Comparison of the spectral properties of (94)$^{.+}$ (M = FeO, X = Cl) with those of (96)$^{.+}$ (M = FeO, X = H) indicate that they have similar electronic structures [67].

Resonance Raman spectroscopic evidence has been obtained for the oxygenated complex of cytochrome d terminal oxidase. An Fe-O$_2$ stretching vibration at 568 cm^{-1} was observed. The υ(Fe-

O_2) frequencies for cytochrome d terminal oxidase are very similar to those noted for other oxygen binding proteins such as hemoglobin, myoglobin and cytochrome c oxidase [68].
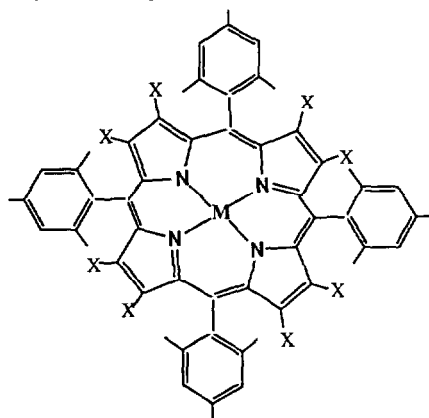
(94)-(96)

The axial ligation of ammonia, trifluoroethylamine (TFEA), and imidazole to water soluble and non-μ-oxo-dimer forming iron(III) porphyrin, [(97)Fe(III)(X)₂, X = OH⁻ or OH₂], in aqueous solution and the influence of such ligation on the rate of reaction of iron(III) porphyrin with t-BuOOH has been reported. Comparison of kinetic constants from this study with those of analogous water-ligated complexes suggests that the rate enhancement produced on mono ligation by the nitrogen bases. Ligation of two nitrogen donors to form (97)Fe(III)(Am)₂ inhibits the reaction suggesting that the hydroperoxide reduction by iron(III) occurs by axial ligation of hydroperoxide [69].
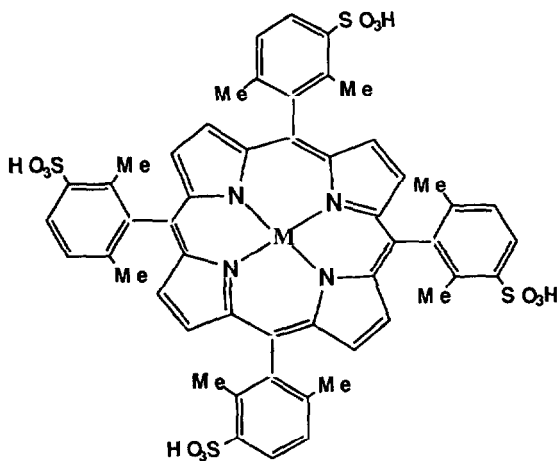
(97)

The direct observation of the "push effect" on heterolytic and homolytic O-O bond cleavage has been reported for a series of acylperoxoiron(III) porphyrins (98) having substituents at the

meso-positions of the porphyrin ring. The push effect on the heterolytic O-O bond cleavage was studied in methylene chloride at -80°C and found to be first order in [98]. Introduction of electron donating substituents (see below) at the *meso* positions facilitates the O-O bond cleavage. The homolytic bond cleavage study used the imidazole adduct of (98). Homolysis of the O-O bond is enhanced by imidazole ligation but the push effect is much less than that on heterolysis. A strong electron donor destabilizes the O-O bond by pushing electrons into the antibonding orbitals of peroxide and at the same time this encourages the polar transition state. These effects favour heterolysis of the O-O bond in (98) but the polar transition state upsets homolysis [70].

(98)
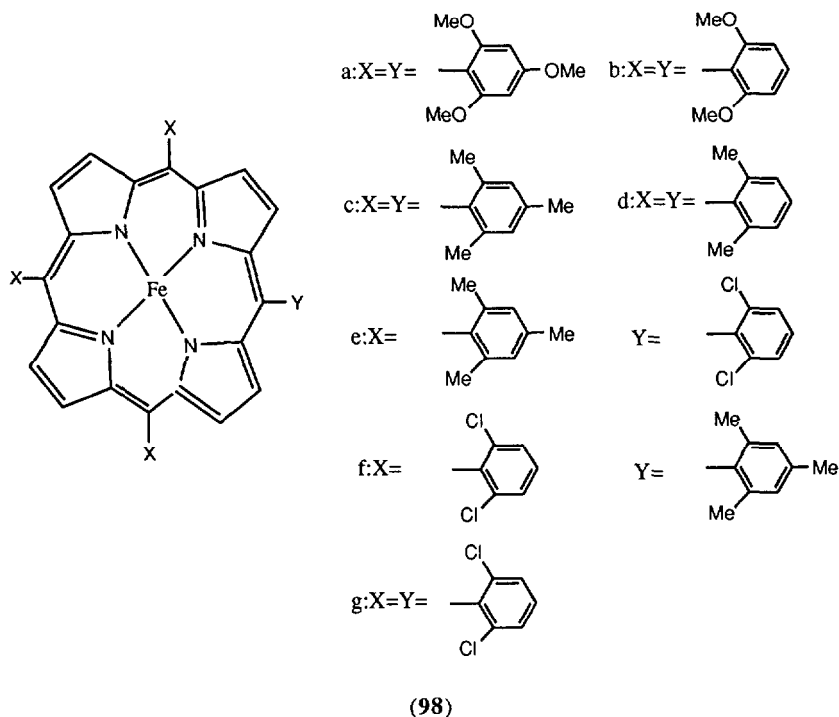
The effects of electron-withdrawing substituents bound to a porphyrin ring on the electronic structures and reactivities of oxoiron(IV) porphyrin π-cation radical complexes were studied using 2,7,12,17-tetramethyl-3,8,13,18-tetraaryl porphyrins and tetrakis-5,10,15,20-tetraarylporphyrins where aryl = mesityl, 2-chloro-6-methylphenyl, 2,6-dichlorophenyl and 2,4,6-trichlorophenyl. The electronic structures for the porphyrin radicals were investigated by low temperature UV-Visible absorption spectroscopy and proton NMR spectroscopy. The proton NMR spectrum for the (99) radicals show large downfield shifts of the pyrrole ß-methyl protons and small shifts of the *meso* protons which were attributed to the a_{1u} radical complexes. The type (100) radicals exhibited large downfield shifts of the *meso* proton signals and upfield shifts of the pyrrole ß-methyl proton signals which is consistent with an a_{2u} radical state. The reactivities of oxygen atoms of the porphyrin radicals were studied by competitive epoxidation of cyclohexene by two porphyrin radicals with

different radical orbital occupancies. The oxygen atom with the a_{1u} radical state was almost as reactive as that with the a_{2u} state. Results indicate reactivity of the oxygen atom of these porphyrin radicals depends more on its oxidation potential and is not affected by the orbital occupancy [71].

(99) (left)   (100) (right)
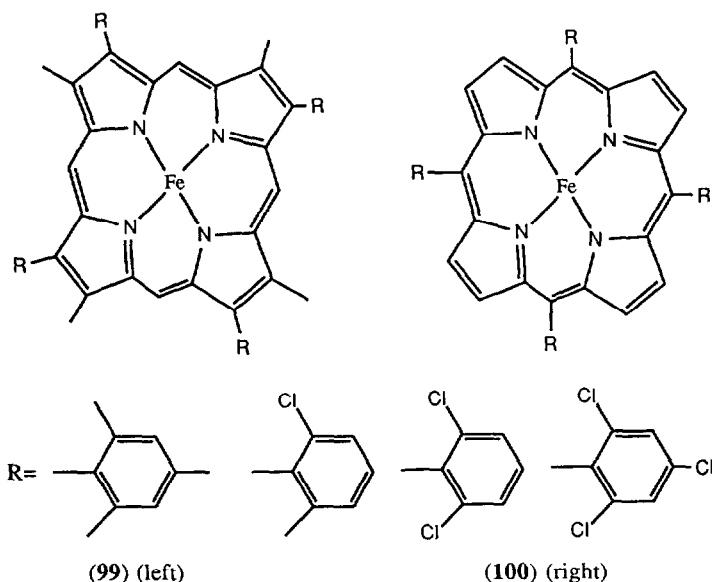
Kinetics and equilibria of binding of 1-methylimidazole, 1,2-dimethylimidazole, isonitriles and carbon monoxide to iron(II)tetraphenylporphyrin and iron(II)tetramesitylporphyrin containing various ligands in the sixth position have been determined. Those fifth and sixth ligand combinations which result in steric repulsion between the porphyrin and one of the ligands show much greater binding constants and slower dissociation rates with the iron(II)tetramesitylporphyrin than to iron(II)tetraphenylporphyrin. The large differences are attributed to a conformational effect in which phenyl groups with *ortho* substituents destabilize the domed form of the metalloporphyrin [72].

It has been demonstrated that axial ligation of an iron porphyrin and consequent modulation of its electrochemical properties can act to gate electron transfer in bilayer devices composed of a cationic silane polymer and an anionic pillared clay. The cationic polymer provides binding sites for Fe(III)(97)$^{3-}$ (101) anions. The axial ligation of (101) changes reversibly with solution pH and in weakly basic solutions electron transfer between the anions and an SnO_2 electrode is slow. Cyclic voltammetry and UV-VIS spectroscopy show that (101) contained within the silane film behaves as a pH-sensitive gate for electron transfer to and from the cations bound to the clay surface [73].

The coordination of CN$^-$ to α^4-tetrakis[o-N-methylisonicotinamido)phenyl]Fe(III)-porphyrin (102) and (103) towards O_2^- and CO_2^- radicals CN$^-$ binding to the porphyrins has been examined. It was found that in alkaline media formation of the dicyano complexes is complete at millimolar concentrations of CN$^-$ but the second reaction observed with 103 results from the reduction of the Fe(III) porphyrin by excess CN$^-$. The reaction is not observed with 102. The

superoxide anion reacts faster with (102) than (103) but the opposite is the case with respect to the rates of reaction with CO_2^-. The CO_2^- reduces (102) and (103) at diffusion-controlled rates with a steric factor contributing to a slightly smaller rate constant in the case of the picket fence porphyrin. Rates of reduction by O_2^- are less than diffusion-controlled with rate constants for the reactions of (102) and (103) following their $E_{1/2}$ values in accordance with the Marcus equation [74].


(102)   103)
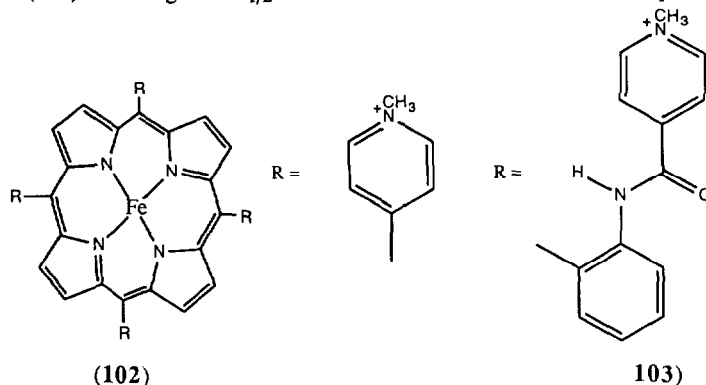
The reduction of fluorophenyl σ-bonded iron porphyrins in non-coordinating solvents was studied using electrochemical and spectrochemical methods. The investigated porphyrins are represented as $(P)Fe(C_6F_5)$ and $(P)Fe(C_6F_4H)$ where P^{2-} is the dianion of H_2OEP, H_2TPP, tetra-*m*-tolylporphyrin, tetra-*p*-tolylporphyrin, or tetrakis(*p*-trifluoromethyl)phenyl)porphyrin. Each σ-bonded compound undergoes up to seven different redox processes. The presence of the σ-bonded fluorophenyl ligand is responsible for the reduction of and being different from all previously investigated iron porphyrins. The first reduction of (P)FeR leads to (P)Fe(II) and R⁻, the latter which reacts with water in solution to give OH⁻ and RH. The OH⁻ displaces the axial fluorophenyl ligand and sets in motion a chain reaction which continues until all of the σ-bound porphyrins are converted to the monomeric (P)FeOH prior to the formation of the dimeric [(P)Fe]$_2$O on a longer time scale [75].

High-yield high turnover regiospecific hemin-catalyzed epoxidations using hydrogen peroxide or t-butyl hydroperoxide have been achieved. It has been reported that the decrease in epoxidation stereospecificity in the presence of hydroperoxides occurs after the rate limiting O-O bond cleavage. This loss of stereospecificity is not evidence for O-O bond homolysis in the first step of the mechanism. It was also found the oxene species ($>Fe^+=O$) prefers the oxidation of hydroperoxides to epoxidation and this preference decreases as the hemin is made more electronegative by substitution on the porphyrin [76].

8.5.2.3 Strapped porphyrin complexes

Using Soret-excited resonance Raman spectroscopy, the μ(Fe(II)-NO) and μ(Fe(III)-NO) stretching vibrations for several iron porphyrins [OEP, TPP, (104)-(107)] have been reported. The ν(Fe(II)-NO) and ν(Fe(III)-NO) stretching modes have been assigned at ~602 and ~524 cm^{-1},

respectively.   Comparing the ν(Fe(II)-NO) of iron porphyrins (~524 cm^{-1}) to those of hemoproteins (~554 cm^{-1}) shows the proteins' influence on the stretching frequency (~30 cm^{-1}) is significant. The effects of solvent and *trans* base on the Fe(II)-NO bond were also studied. The ν(Fe(II)-NO) stretching frequency was generally observed to increase for solvents of higher dipole moment. The Fe(II)-NO bond strength was determined to be independent of the electron-donating and stereochemical properties of the trans base. The Fe(II)-NO bond appears to be unique because Fe(II)-CO, Fe(II)-O$_2$, and Fe(II)-CN bond strengths are reported to be dramatically affected by the proximal ligand [77].
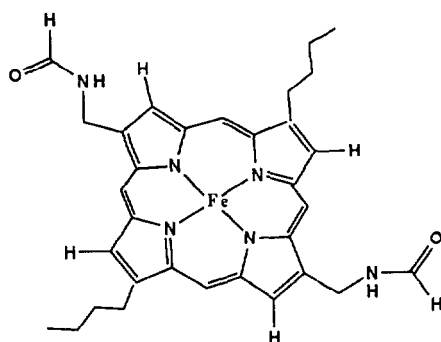
(104)
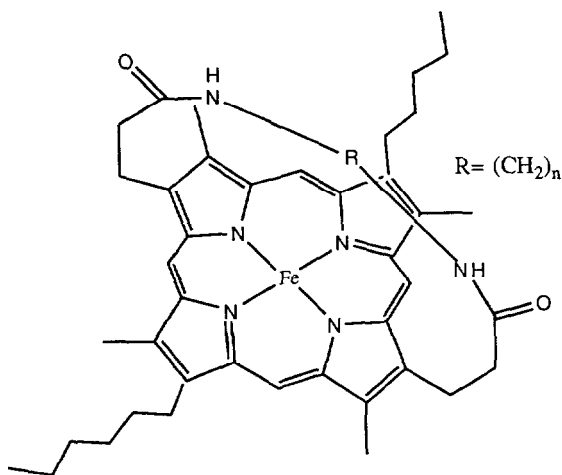
(105) (n = 5), (106) (n = 6), (107) (n = 7)

Spectroelectrochemical methods have been used to study the coordination chemistry of [Fe(III)(108)Cl] (109) and related complexes. The presence of 1-MeIm appears to generate the [Fe(III)(108)OH] complex (110); the hydroxide ion presumably being generated by reaction of the imidazole with trace amounts of water. The first reduction generates the species [Fe(II)(108)(1-MeIm)(dmso)] where the dmso molecule binds within the capping group. The dmso ligand is presumed to be coordinating through the sulfur atom. Reduction of (110) in the presence of 1-

MeIm in CH_2Cl_2 solution produces the five-coordinate species [Fe(II)(**108**)(1-MeIm)]; the Cl- ion is not replaced by the imidazole ligand until reduction has taken place [78, 79].
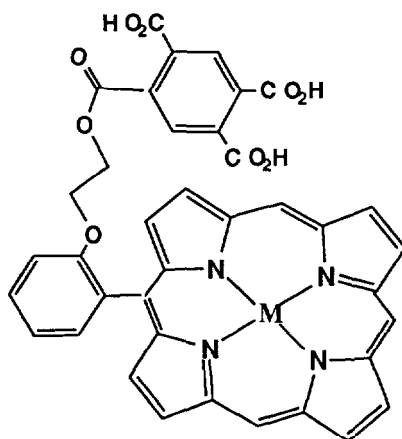
(108)
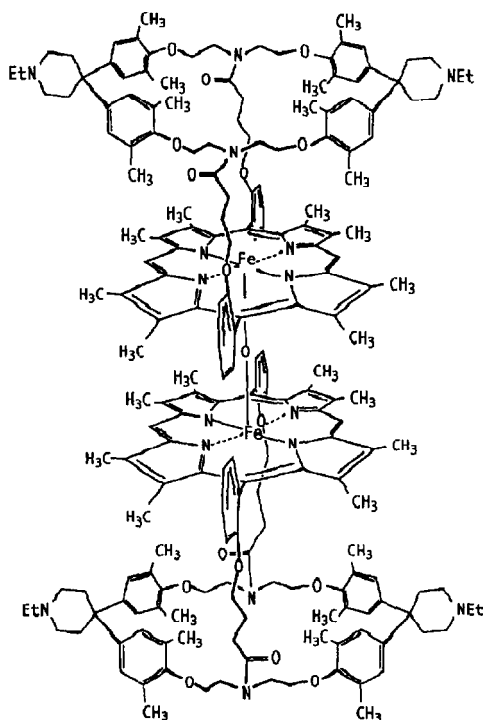
{Fe(108)}2

The iron porphyrin-cyclophane Fe(**108**)Br having a porphyrin attached by two straps to an apolar cyclophane binding site has been prepared. Treatment of **108** (M = FeBr) with base yielded

the corresponding μ-oxo dimer {Fe(108)}2 in which the two oxo-bridged porphyrin moieties are both capped by cyclophane binding sites. The μ-oxo dimer dissociates to the monomeric species under acidic conditions. Both the monomer and the dimer act as cytochrome P-450 mimics in protic solvents such as MeOH and CF_3CH_2OH. Using iodosylbenzene as O-transfer agent, (108) (M = FeBr) catalyzes the oxidation of acenaphthylene to acenaphthen-1-one [80].

8.5.2.4   Other porphyrin complexes

The kinetics of the reduction of Fe(III)(109) by p-cresol in chloroform and methanol have been determined. The rate law implies two parallel reaction pathways; one involves auto- or solvent-assisted reduction of the metalloporphyrin, the other involves the direct reaction between the metal complex and the reductant [81].

(109)

R=Me
R=H

(110)
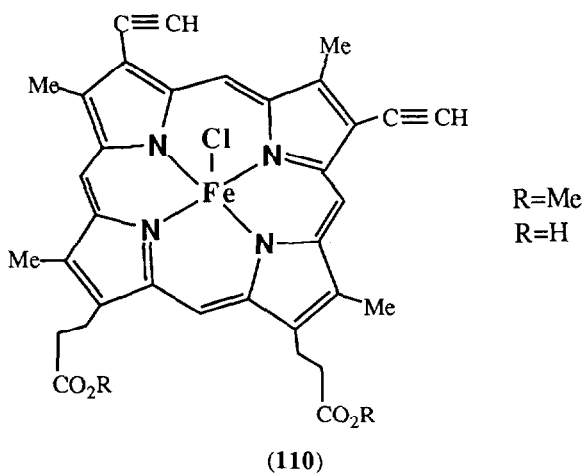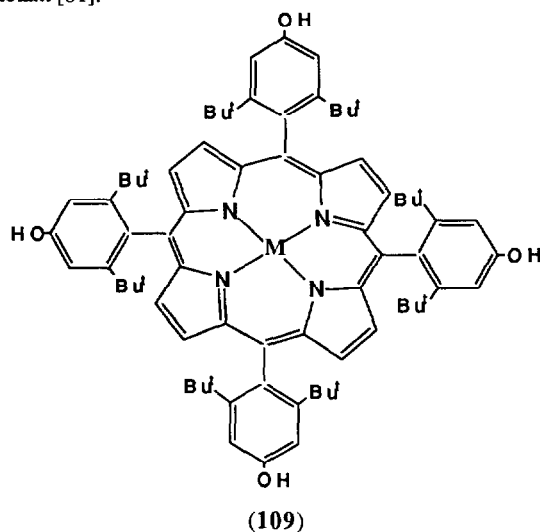
The diethynylporphyrin (**110**) has been synthesized. Reaction of (**110**) with iron(II) chloride affords [Fe(**110**)Cl] [82].

The quantum yields for photolysis of imidazole-iron(II)porphyrin-NO complexes in toluene, aqueous 1-methylimidazole, Nujol and glycerol have been reported. Polar solvents decrease NO quantum yields. The steric effects on NO photolysis were also investigated. The increasingly hindered porphyrins (mesoheme, anthracene-7,7,cyclophaneheme, adamantane-6,6-cyclophaneheme and pyridine-5,5-cyclophaneheme) all had similar quantum yields. The increased steric effects have relatively little influence on NO photolysis [83].

The first μ-nitrido dimer containing two different dianionic macrocyclic rings has been synthesized in the reaction of (TPP)Fe(III)N$_3$ and Fe(II)Pc. Mössbauer and EPR results suggest a low spin electronic configuration with one unpaired electron per (TPP)Fe-N-FePc dimer [84].

An analogue of the iron/copper bridged assembly in cytochrome c oxidase has been synthesized by the reaction of [Cu(Me$_6$tren)(OH$_2$)](ClO$_4$)$_2$ with lithium 2,6-di-*tert*-butyl-4-methylphenoxide and Fe(OEP)(OClO$_3$). The product, [(OEP)Fe-O-Cu(Me$_6$tren)](ClO$_4$) (**111**), has been characterized by X-ray crystallography and spectroscopic methods. The unprecedented Fe-O-Cu unit links a square pyramidal iron porphyrin to a trigonal-bipyramidal copper. The bond distances and +1 charge of the complex suggest the assignment of the oxygen atom as bridging oxo. Magnetic susceptibility measurements establish (**111**) as a tightly coupled S = 2 system and a silent EPR signal agrees [85]. Similarly, the oxo-bridged assembly [(OEP)Fe-O-Cu(Me$_6$tren)]$^+$ has been prepared by coupling the axially labile [Fe(OEP)-(OClO$_3$)] and the terminal hydroxo species [Cu(Me$_6$tren)(OH)]$^+$, generated *in situ*, in the presence of a suitable base. A high spin Fe(III) side product, possibly [Fe(OEP)-(OCH(Me)=CH$_2$)], is also produced.
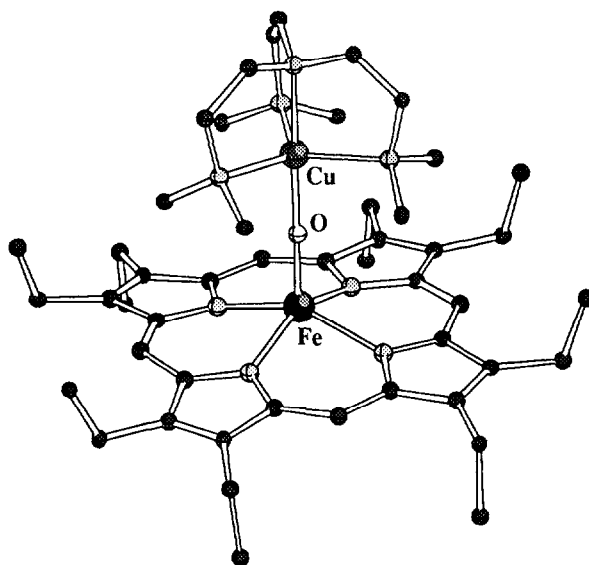
(**111**)

A similar Cu(II)-Fe(III) bridged species can be afford from the reaction of Fe(OEP)(OClO$_3$) with [Cu$_2$F$_2$(bnpy$_2$)$_2$](PF$_6$)$_2$ yielding [(OEP)Fe-F-Cu(bnpy$_2$)(OClO$_3$)](PF$_6$) (**112**) (bnpy = *N,N*-bis(2-pyridylethyl)benzylamine). Structural characterization revealed an asymmetric fluoride bridge linking a five coordinate high spin Fe(III) to a square pyramidal Cu(II) [86]. The same reaction in acetonitrile produces the complex [(OEP)Fe-F-Cu(bnpy$_2$)(MeCN)](PF$_6$)(ClO$_4$)·MeCN (**113**). The structures of the complexes are similar, both consisting of separate pyramidal halves, [Fe(OEP)]$^+$ and [Cu(bnpy$_2$)]$^{2+}$, linked by an unsupported fluoride bridge. Displacement of iron atoms from the porphyrin core centre and Fe-N bond lengths are typical of high spin five coordinate ferric porphyrins [87].
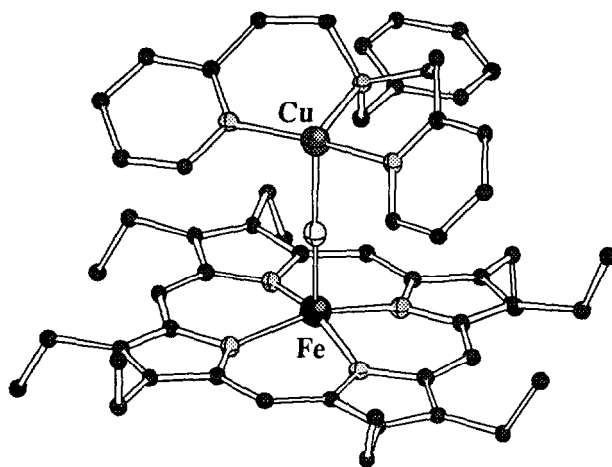
(**112**)

The reaction of Fe(III)TMP(meso-tetramesitylporphyrinato)-*N*-oxide with trifluoroacetic acid in toluene produces a dication of Fe(III)(TMP). The electronic structure of the complex is characterized to be ferric high spin with rhombic symmetry. The dication of Fe(III)(TMP) reacts with methanol to yield Fe(III)TMP N-methoxide. The dication is not thermally stable and is readily reduced to Fe(III)(TMP) π-cation radical even at −25°C in toluene [88].

Tetrathiometalate reduction of the iron(III) porphyrins to square planar iron(II) derivatives was studied. Little reduction was evident for WS$_4^{2-}$ below 260 K. At 273 K two species could be identified. The first was observed when (TPP)FeSO$_3$CF$_3$ was reacted with 0.25 equivalents of WS$_4^{2-}$. The pyrrole deuterium chemical shift of 73.9 ppm is consistent with a high spin iron(III) configuration and EPR signals agree. The axial EPR signal and the NMR chemical shift support (**114**) as a possible structure. When more than one half equivalent of WS$_4^{2-}$ was added to the iron porphyrin, a second derivative was obtained. This species has a pyrrole chemical shift at 85.8 ppm. The rhombic EPR for the this second species suggests a coordination type which is rare for iron porphyrins but common for other WS$_4^{2-}$ complexes; a didentate coordination geometry (**115**) is favored [89].

(114)   **(115)**
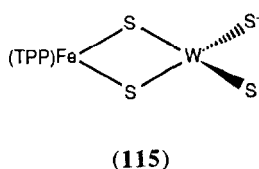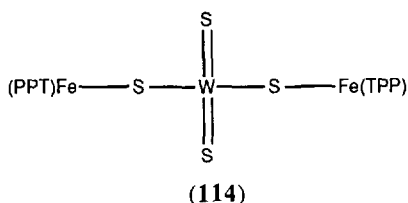
8.5.3 Complexes with chlorins

An extensive series of five- and six- coordinate (1-methylimidazole)-, (1-butylamine)-, and (pyridine) iron(II, III) chlorin complexes were characterized by magnetic circular dichroism (MCD) spectroscopy. Octaethylchlorin, mesochlorin and "methyl"chlorin (2,2,4-trimethyl-deuterchlorin) were studied. The results establish MCD spectral signatures for use in determining whether an iron chlorin containing protein contains either a histidine of a lysine axial ligand. The MCD spectra of iron chlorin complexes are most sensitive to the identity, number, and type of axial ligand along with oxidation and spin site, but insensitive to changes in the equatorial plane such as the site of pyrrole ring reduction [90].

8.5.4 Miscellaneous tetrapyrrole complexes

Two structures, A and B, have been proposed for the tetrapyrrolic macrocycle in verdohemochromes. Studies on {(116)Fe(III)Cl₂} suggest that both the Fe(II) and Fe(III) forms of verdohemes must have structure A. X-ray diffracion studies indicate the oxoporphyrin (C) acts like a porphyrin but the core size is smaller. The iron(III) complex is six-coordinate and high spin while the iron(II) is five coordinate and high spin [91].

A   B   C

(116)
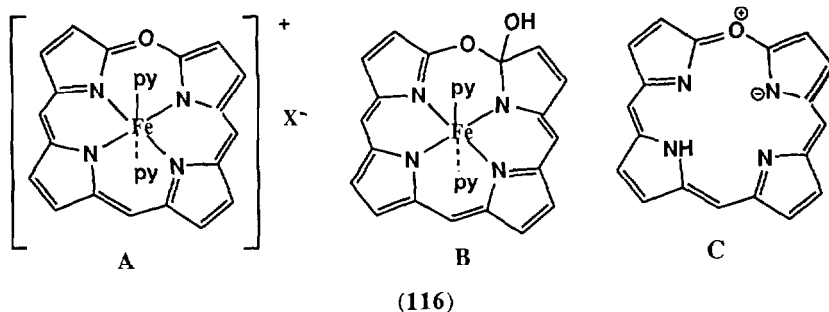
The reaction of the iron(III) octaethyloxophlorin dimer [Fe(III)(OEPO)]₂ with molecular bromine results in the formation of two new highly oxidized complexes, BrFe(III)(116·) **(117)** and Br₂Fe(III)(116Ox). Results from X-ray diffraction of **(117)** confirm the iron is five-coordinate with structural parameters consistent with the presence of high spin ($S = 5/2$) Fe(III). The magnetic moment of **(117)** is 4.9 μ_B suggesting strong antiferromagnetic coupling between the iron and

ligand spins. The complex $Br_2Fe(III)(OEPOx)$ has a magnetic moment of 5.7 μ_B and displays an EPR signal typical of an axially symmetric, high-spin Fe(III) complex wtih hyperfine splitting due to two axial ligands [92].
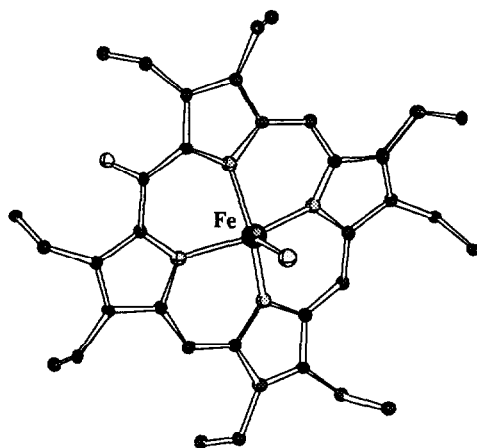
(117)

Treatment of {Fe(III)(116)}$_2$ with pyridine results in its cleavage to form {(py)$_2$Fe(III)(116)} ⇔ {(py)$_2$Fe(II)(116·)}. This cleavage was previously inferred from studies of the UV/vis spectra and has been confirmed by ^1H NMR studies. It is believed that - like the Mn(III) complex - the {(py)$_2$Fe(III)(116)} contains the ligand in the deprotonated form of the oxophlorin ligand corresponding to the tautomeric structure (116a) [93].
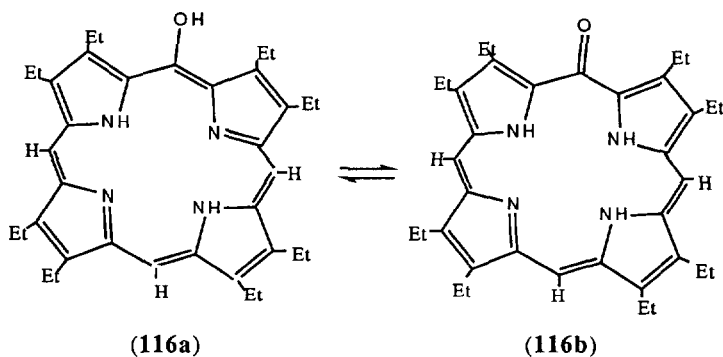
(116a)   (116b)

Low-spin (S = 1/2) six coordinate iron(III) complexes of (116) have been obtained by treating high-spin (S = 5/2) six coordinate (116)Fe(III)Cl$_2$ with strong-field ligands. The nucleophiles do not attack the oxoporphyrin ligand. The cyano complex (116)Fe(III)(CN)$_2$·1.6 CH$_2$Cl$_2$ has been isolated and characterized. The complex is centrosymmetric with the iron atom located at the centre of symmetry; hence, there is disorder in the location of the meso-oxygen atom. The Fe-N distances are 1.976 (9) and 1.955(9)Å. The magnetic moment is 2.4 μ_B at 20 °C in

solution, along with the EPR spectrum showing g = 2.4, 2.2, 2.18, confirms the low spin formulation. Addition of excess amounts of the strong field ligands results in the reduction of Fe(III) to Fe(II) [94].

Verdohemochrome was treated with ammonia and (118)Fe(III)Cl (119) was obtained [(118) = dianion of octaethylazaporphyrin]. The X-ray structure of (119) indicates that the azaporphyrin acts much like a porphyrin in forming a five coordinate iron complex with an axial chloride ligand. The iron atom is 0.49 Å above the N_4 plane. A dichloromethane molecule is hydrogen bonded to the *meso* nitrogen in the solid. This interaction plays a role in ordering the structure of the symmetrically substituted, core-modified porphyrin. Magnetic studies indicate it is a high spin complex. Complex (119) reacts with hydrogen chloride in dichloromethane to form high spin six-coordinate (H118)Fe(III)Cl₂. In dimethyl sulfoxide (119) reacts with silver nitrate to form high spin [(118)Fe(III)(dmso)₂]NO₃ [95].
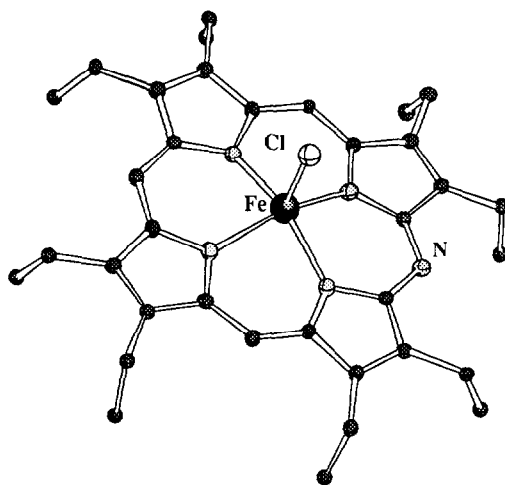
(119)

Further investigation of the structure of (OEP)Fe(III)Cl·CH₂Cl₂·N₂ was carried out due to doubts of the existence of the N_2 molecule. Re-examination of the structure and data suggest that the "two equal sized atoms separated by 1.21(2) Å" are not dinitrogen but disordered dichloromethane [96].

8.6   COMPLEXES WITH O-DONOR LIGANDS

8.6.1   Complexes with carboxylic acids and derivatives

The heats of formation of four aqueous Fe(III)-citrate complexes - FeL, FeL₂3-, FeHL⁺ and Fe(OH)L⁻ (L = citrate) have been determined by solution calorimetry [97].

The complexes [Fe(120)₃]·1.5H₂O (121), [Fe(122)₃]·2.5H₂O (123) and [Fe(124)₃].2H₂O (125) have been prepared. The complexes exhibit a band at *ca.* 320 nm which is

assigned to a ligand charge transfer transition and broad d-d absorptions at *ca.* 530 nm. Complex (**122**) has a magnetic moment at 6.06 μB, indicative of high-spin iron(III), while complexes (**120**) and (**124**) have lower values (3.43 and 4.10 μB, respectively) which may be due to antiferromagnetic behaviour. The cytotoxicity of these complexes has been investigated [98].

Pr^i; (**120**)

I ; (**122**)

Cl ; (**124**)
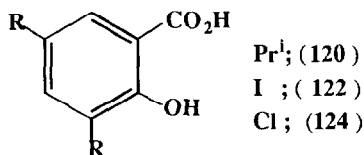
Three adamantanoid chelate tetranuclear iron(III) complexes Fe_4L_6 (Scheme 2) have been synthesized by the reaction of $FeCl_3$ with ligands (**126**), (**127**) (X = C_6H_4), and (**128**) (X = $C_{12}H_8$). Their identities have been determined by FAB mass spectrometry and, in the case of ligand (**127**), X-ray crystallography. The crystal structure of $Fe_4(127)_6$ reveals that the complex is achiral; the iron centres have the configuration $(\Delta,\Delta/\Lambda,\Lambda)$-*fac*. Cyclic voltammetry shows that the complex undergoes a chemically reversible four-electron reduction. No partially reduced intermediates could be observed [99].
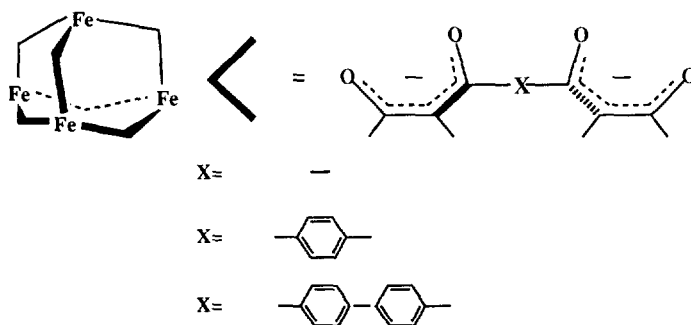
Scheme 2

The assembly of two types of ferrichrome analogs where tricarboxylates are anchors, amino acids (ala, leu, gly, pro, and ileu) are bridges and terminal hydroxamate groups are the iron binding sites has been reported. The type 1 analogues have only one methylene in the tricarboxylate chains while type 2 analogues have two methylenes. Both types of complexes assume the L-*cis* configuration when L-amino acids are used. In the iron complexes, the type 1 analogs have the amides positioned tangentially to the molecules cross section; whereas in the type 2 complexes the amides are oriented radially with the amide-NH pointing inward [100].

The application of loop-gap resonator technology to stopped-flow EPR has been used to measure rapid spin-trapping kinetics on a subsecond time scale. Hydroxyl radical production which is completed within 1 s of mixing Fe(II)-EDTA and H_2O_2 has been monitored. The initial rate of trapped hydroxyl radical was nearly dependent on both the initial Fe(II)-EDTA and initial H_2O_2 concentrations. The second order rate constant was 3.2×10^3 $M^{-1}s^{-1}$[101].

Type 1 - m=1

Type 2 - m=2
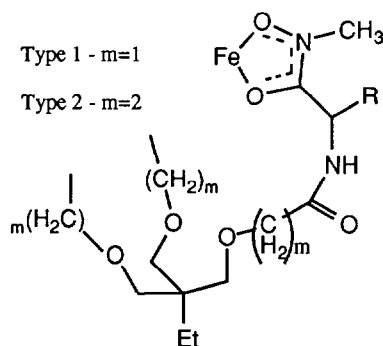
Scheme 3

Chiral analogues of enterobactin with hydrophilic or lipophilic properties have been reported. Both **(129)**-*R* and **(129)**-*S* bind ferric ions to give dark red complexes. The CD spectra of the ferric complexes were found to be mirror images. Similar to the ferric complex of enterobactin, the ferric complexes of **(129)**-*R* and **(129)**-*S* showed CD band in the ligand-to-metal charge transfer region (~540 nm) indicating that the ligand chirality induced a preference for Δ and Λ metal complexes. The assignment of Δ-*cis* was made to **(129)**-*S* and L-*cis* to **(129)**-*R* [102].

(129)
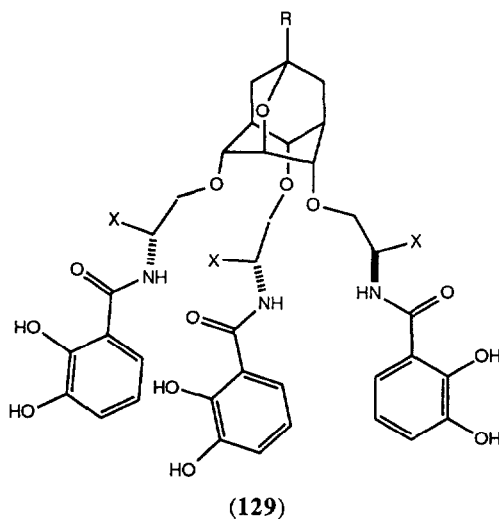
A series of synthetic tris(hydroxamates) **(130-133)** that bind iron(III) in a manner similar to that of the natural ferrioxamine have been prepared. Due to the presence of asymmetric carbons the synthetic binders differ from the natural compound in forming complexes of preferred chiral sense. The complexes' iron(III) release kinetics with CDTA (CDTA = cyclohexane-1,2-dinitrotetraacetate) were examined as indicators of their coordination properties. Iron(III) release was shown to occur by two rate limiting processes: a bimolecular ligand exchange step and a mononuclear step which measures the inertness of the complex under acidic conditions. Both

processes show a dependence on the nature of the amino acid. The bulkier the side chain and longer the chain length, the slower the dissociation and iron(III) exchange rates [103].
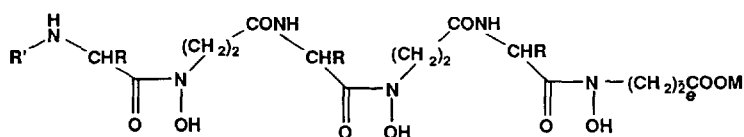
130 R= Me
131 R= ^{i}Bu
132 R= -CH$_2$NEt$_2$
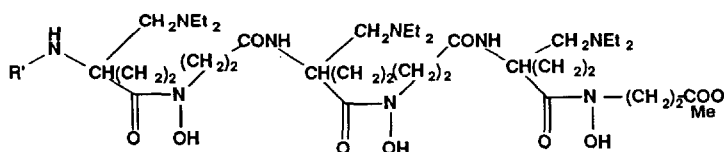
(133)

8.6.2   Complexes with other O-donor ligands

The aqueous complex equilibria of iron(II) and N-(phosphonomethyl)iminodiacetic acid (134), have been studied using glass electrode potentiometry. ML, MLH, ML$_2$ and ML$_2$H$_2$ species were detected. The postulated structure of the ML complex is shown in (134a) [104].
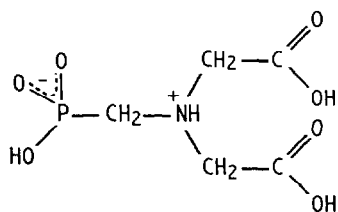
(134)
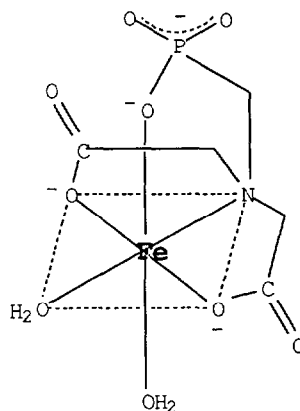
(134a)

The solubilities and derived transfer chemical potential trends for tris(hydroxamato)-iron(III) complexes in methanol-water and in tert-Butyl alcohol-water solvent mixtures have been determined. The ligands used were acethydroxamate (135), benzhydroxamate (136) and 4-methylphenylhydroxamate (137). The acethydroxamate complex is preferentially solvated by water, probably because of favoured hydration of the NHO$^-$ portion of the ligand. The lipophilic character of the benzyl/p-tolyl substituents of the other two complexes leads to preferential solvation of the alcohols [105].

R = Me (**135**), C₆H₅ (**136**), 4-MeC₆H₄ (**137**)

R = Me (**135**), C_6H_5 (**136**), 4-MeC$_6$H$_4$ (**137**)
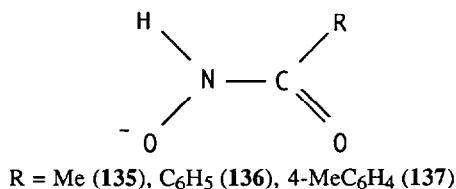
The structure of the dimeric complex di-μ-pyridoxinato-bis[aquadichloroiron(III)], [FeCl₂(μ-C₈H₁₀NO₃)(H₂O)]₂ (**138**), has been determined. The ligand binds through the phenolate oxygen and the O atoms of two deprotonated 4-hydroxymethyl groups which bridge the two iron atoms [106].

(**138**)
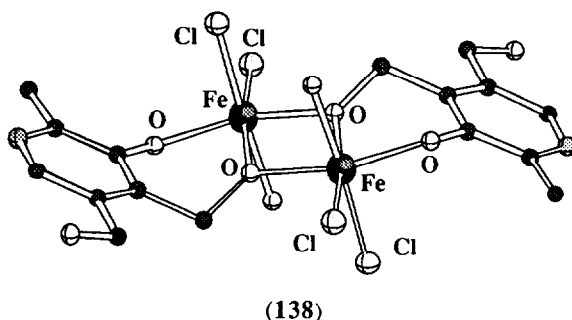
The complexes [FeI₂(OC(NMe₂)₂)₂] (**139**), [Fe₂I₄(OC(NMe₂)₂)₂] (**140**), and [FeI₃(OC(NMe₂)₂)] (**141**) have been prepared by reaction of FeI₂ or FeI₂/I₂ with tetramethylurea. Compunds (**139**) and (**141**) are isolated neutral complexes with a distorted tetrahedral coordination around Fe. It is proposed that (**140**) is an iodide-bridged dimer with a central Fe₂I₂ ring. The IR-spectra exhibit strong shifts of v_asC-N of tetramethylurea [107].

(**139**)   (**141**)
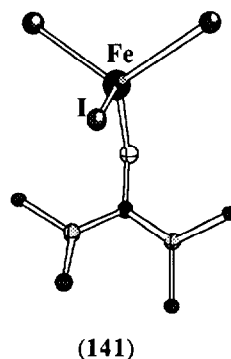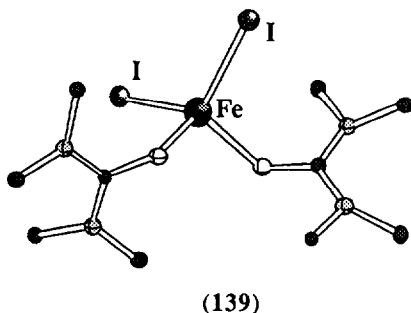
The formation of Fe(acac)²⁺, Fe(acac)₂⁺ and Fe(acac)₃ in MeCN has been studied by UV-VIS spectrophotometry. The speciation of the various complexes is dependent on the method of synthesis; for example, Fe(acac)²⁺ is formed quantitatively when Hacac is added to an MeCN solution of Fe(ClO₄)₃. When excess Hacac is added, only Fe(acac)²⁺ is obtained and no Fe(acac)₃ is observed. On the other hand, Fe(acac)₂⁺ was obtained by adding HClO₄ to an MeCN solution.

All $Fe(acac)^{2+}$, $Fe(acac)_2^+$ and $Fe(acac)_3$ were formed in the system of $Fe(ClO_4)_3$ with an addition of $Et_4N(acac)$. The solution resonance Raman spectra of all three complexes have been measured. The order of $v_{(Fe-O)}$ is $Fe(acac)^{2+}$ (474 cm^{-1}) > $Fe(acac)_2^+$ (462 cm^{-1}) > $Fe(acac)_3$ (451 cm^{-1}) and that of $n_{(C-O)}$ is $Fe(acac)^{2+}$ (1554 cm^{-1}) < $Fe(acac)_2^+$ (1578 cm^{-1}) < $Fe(acac)_3$ (1603 cm^{-1}). This indicates that the coordination strength of acac- to Fe becomes weaker, because the Lewis acidity of the metal decreases as the number of coordinated acac- molecules increases [108].

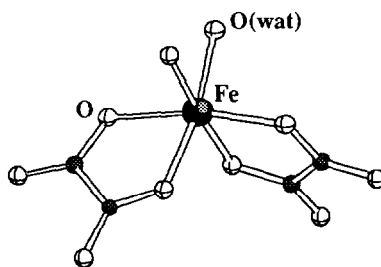The crystal and molecular structure as well as the magnetic properties of iron (II) crotonate trihydrate have been determined by X-ray crystallography and SQUID magnetometry. The crystal structure consists of infinite chains in which each metal atom is coordinated to two oxygens of one crotonate ring and one oxygen of a second crotonate ring. The crotonate dianion is able to transmit a weak antiferromagnetic coupling; J = –0.27 cm^{-1} [109].

Synthesis, X-ray structure and properties of the novel iron(III) complex of mixed k^3N- and k^3O-tripod ligands [n-Bu$_4$N][(HB(pz)$_3$Fe(P$_3$O$_9$)] (142) has been reported. The complex was synthesized by replacing the three coordinated chloride ions of [(HB(pz)$_3$)FeCl$_3$]$^-$ with P$_3$O$_9$$^{3-}$. The coordination geometry about the Fe is a distorted octahedra with a face occupied by three O atoms of P$_3$O$_9$$^{3-}$ and the opposite face occupied by three N atoms of the HB(pz)$_3$$^-$ ligand. Magnetic susceptibility of (142) measured in the solid state at room temperature is 5.6 µB suggesting a high spin complex which is consistent with the long Fe-N bond lengths [110].

(142)   (143)

The X-ray structures of [bpyH]$^+$[Fe(ox)$_2$(H$_2$O)$_2$]$^-$·H$_2$O (143) and the photoreaction product of (143), the three-dimensional polymeric compound [Fe(II)(bpy)$_3$]$_n^{2+}$[Fe(II)$_2$(ox)$_3$]$_n^{2n-}$ (144) have been determined. The [Fe(II)(ox)$_3$$_{/2}$]$^-$ units in (144) build a three-dimensional anionic network. The network can be described as a three-connected net consisting of 10-gons wherein the [Fe(bpy)$_3$]$^{2+}$ cations occupy the vacancies [111].
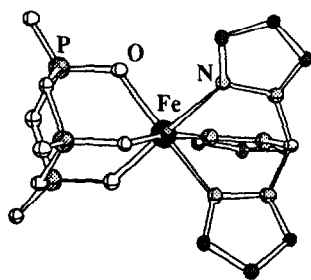
Correlations between optical charge transfer energies and electrochemical data for iron(II) catecholato complexes of the tetra-azamacrocycle, δ,l-5,7,7,12,14,14-hexamethyl-1,4,8,11-tetraazacyclotetradecane (145), [Fe(145)(di-^{t}BuCat)]$^+$ and [Fe(145)(Cl$_4$Cat)]$^+$, were studied. The comparisons suggest that the observed solvato chromism of the iron(II)-catecholato chromophores is due to the differences in solvation enthalpies of the two electronic isomers, [Fe(III)(145)(Cat)]$^+$ and [Fe(II)(145)(SQ)]$^+$, in their states of vibrational equilibrium [112]. Iron(III) complexes containing a single chelated catecholate dianion, according to the general formulas [Fe(L)Cat]Y

(L=SS-(145), cyclam; Cat = di-^{t}BuCat, Cl$_4$Cat; Y=ClO$_4$, PF$_6$) and [Fe(TACN)Cat]Cl have been synthesized. Magnetic measurements and EPR spectra indicate that all of these complexes are high-spin iron (III) derivatives. The tetraazamacrocycle derivatives of DTBCat are inert towards dioxygen while the triazamacrocycle one shows enhanced reactivity in polar solvents yielding quinone and extradiol cleavage reaction products. The different chemical behavior of these complexes supports the suggstion that the catechol cleavage reaction first requires the coordination of the dioxygen molecule to a coordinatively unsaturated iron(II) centre [113].

In order to investigate stabilization of trigonal prismatic geometries, the [Fe(III)(146)]$^{3-}$ complex has been synthesized. Two Fe(III) complexes of other members of this ligand family have also been characterized for comparative purposes: [Fe(147)]$^{3-}$ and [Fe(eta)$_3$]$^{3-}$ (eta = N,N'-diethylterephthalamide). Spectroscopic evidence suggests that π-bonding within the d-block metal complexes stabilizes the trigonal prismatic geometry [114].

(146) n = 1; (147) n = 2
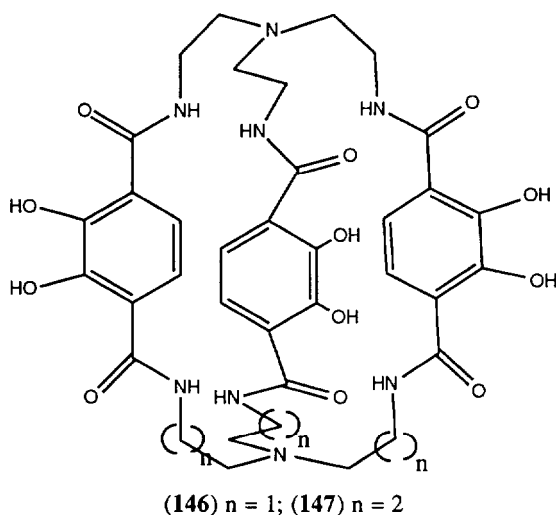
A series of Fe(III) tris(catecholate) complexes of chiral terephthalamide and catecholamide ligands have been studied in aqueous solution in respect to their stereoselective formation of the Δ or Λ coordination isomers. Steroselectivity is effected by non-bonded, weakly polar interactions between the aryl and methyl substituents of the chiral moities peripheral to the metal centre. With the symmetric didentate ligand N,N'-bis((S)-a-methylbenzyl)-2,3-dihydroxyterephthalamide (148), both the Fe(III) (149) and Ga(III) complexes exist purely in a Λ conformation in aqueous solution [115].

Kinetic studies of iron removal by three different types of ligands - catecholates, hydroxypyridonates and pyrophosphates - have been carried out in order to gain understanding of the mechanism by which iron is removed from transferrin by chelators. The relative rates of removal differ by up to two to three orders of magnitude. Although all anions promote iron removal by binding to the protein, pyrophosphate acts both as an ion mediator and a ferric ion chelator [116].
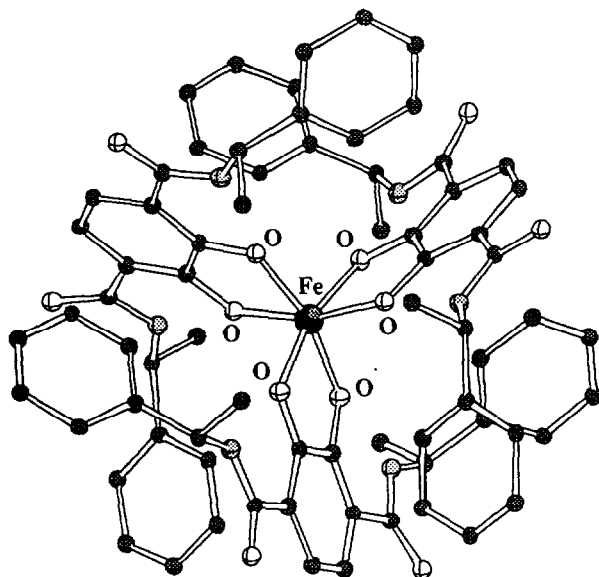
(149)

The kinetics of iron removal from lactoferrin to the catecholate ligand (150) are found to follow the same behavior as that of transferrin. However, the rate of iron removal from lactoferrin ($k_{max} = 6.5 \times 10^{-4}$ min^{-1}) is 100 times slower than from transferrin ($k_{max} = 6.2 \times 10^{-2}$min^{-1}) [117].
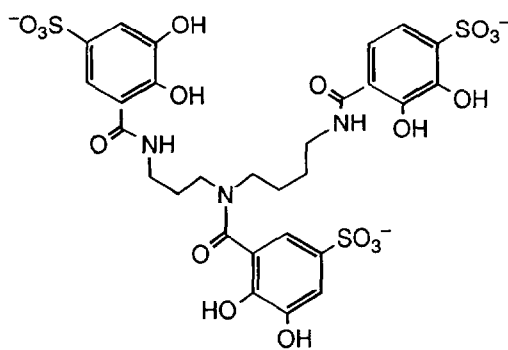
(150)

The hydroxylation of a phenoxo ferric complex to a catecholato complex with a peroxide (mCPBA) was reported as a plausible mimic for the peroxy oxidation by tyrosine hydroxylase. LFe(OC$_6$H$_4$-4-NO$_2$)$_2$ where L= HB(3,5-iPr$_2$pz)$_3$, was treated with mCPA in Et$_2$O and the 4-nitrophenol was formed and identified *in situ* by GC analysis. The same reaction using methanol as the solvent with LFe(OC$_6$H$_4$Cl)$_2$ and LFe(OC$_6$H$_4$-4Me)$_2$ gave 4-chlorocatechol and 4-methyl catechol, respectively. All attempts to spectroscopically detect the (acylperoxo)-(phenoxo)

intermediate in this reaction have failed, perhaps because this species undergoes an oxo-transfer reaction instantaneously [118].

In order to investigate the possiblity that chelation of Fe(III) by ferreascidin involves aromatic residues of the protein, spectrophotometric titrations of pyrocatechol and ferreascidin with Fe(III) were completed. Nitrilotriacetic acid was introduced in order to maintain solublity at pH 7.0. Formation of $[Fe(NTA)(pyrocatechol)]^{2-}$ is governed by a stability constant of $10^{32.5}$ M^{-2}. Corresponding studies of the interaction of iron(III) with the ascidia protein have provided evidence for the coordination of each ferric ion to one tyrosine and two DOPA residues. This interaction is characterized by a stability constant of 4×10^{17} M^{-1} [119].

The complex $[Cr(salen)(ox)Fe(taea)](BPh_4)$ (151) was synthesized and characterized in a study of oxalate-bridged heterodinuclear complexes. The effective magentic moment of the complex is 6.42 μ_B at 290 K which is slightly larger than the spin-only value of 6.24 μ_B for Cr(III)(S=3/2)-Fe(II)(S=4/2) based on the assumption of no magnetic interaction. The magnetic moment increases with decreasing temperature with a maximum of 6.70 μ_B at 6 K which is smaller than the spin-only value of 7.94 μ_B for S_T=7/2 [120].
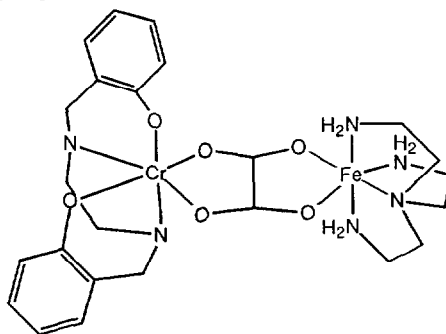
(151)

Using secondary ionization/charge stripping mass spectroscopy, the bond dissociation energies of the metal hydroxides of Fe have been obtained. The reaction for fragmentation of the doubly charged metal complex $FeOH^{2+}$ to produce M^+ + OH^+ is exothermic by 0.6 ± 0.5 eV. In the dication as in the monocation there is a large difference between early and mid to late transition metals in terms of bond dissociation. The dissociation to form M^{2+} and the corresponding neutral ligand is endothermic for all three metal complexes [121].

8.7   COMPLEXES WITH S–DONOR LIGANDS

The iron-peptide complexes Fe-(Z-cys-Pro-Leu-cys-Gly-NHCH$_2$C$_6$H$_4$-p-F)$_2$]$^{2-}$ (152), [Fe-(Z-cys-Pro-Leu-cys-Gly-NHCH$_2$CH$_2$C$_6$H$_4$-p-F)$_2$]$^{2-}$ (153) and [Fe-(Z-cys-Pro-Leu-cys-Gly-Gly-Phe-OMe)$_2$]$^{2-}$ (154) (Z=benzyloxocarbonyl, PCH$_2$OCO) have been synthesized. The absorption, CD, and ^{1}H NMR spectroscopic data indicate mononuclear Fe(II) complexes with chelate coordiantion of the four cysteine thiolate residues. In particular, the complex with a phenylalanine residue (154) exhibits absorption maxima at 312 (8240) and 332 nm (6750) and CD

transitions at 316 (-27.0) and 334 nm (16.1) in acetonitrile which are very similar to those of reduced rubredoxin in aqueous solution. The observation of isotropically shifted ^{19}F-NMR signals in both (152) and (153) indicates that there are π-π interactions between the aromatic ring and the sulfur of the cysteine residue [122]. Also, the coordination of the polypeptide ligands (Z-cys-pro-leu-cys-gly-X) to Fe decreases the T_1 relaxation times significantly. Variable-temperature ^{19}F NMR spectra indicate that the isotropic shifts are caused by the dipolar mechanism, *i.e.* through-space interactions between the aromatic group and Fe(II), for (153) and (155) (X=NH(C$_6$H$_4$F-*p*) while both contact (through backbone NH....S hydrogen bonding) and dipolar mechanisms are involved for 156 (X=NH(C$_6$H$_4$F-*m*) and 157 NHCH$_2$(C$_6$H$_4$F-*p*)[123].

n = 0 (155); 1 (157); 2 (153)
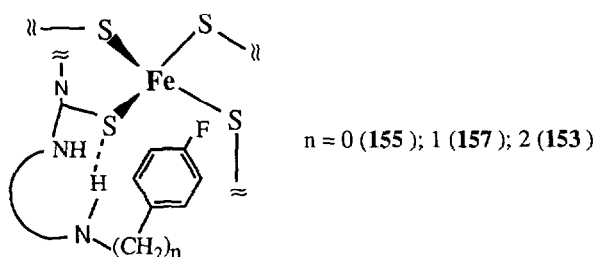
8.8   COMPLEXES WITH P-DONOR LIGANDS

The crystal structure of *trans*-[FeBr$_2$(dmpe)$_2$] has been determined. The Fe-P distances are indicative of low-spin Fe(II); they are similar to those in the analogous chloro complex but significantly shorter than those of [FeBr$_2$(dppen)$_2$] (dppen=1,2-*bis*(diphenylphosphino)ethylene) [124]. The addition of NaBPh$_4$ to alcoholic solutions of [FeCl$_2$(dmpe)$_2$] under nitrogen results in the formation of [FeCl(N$_2$)(dmpe)$_2$][BPh$_4$]. Reaction of the dinitrogen complex with acetonitrile affords [FeCl(CNMe)(dmpe)$_2$][BPh$_4$] [125]. Addition of 1,2-bis(2-propylphosphino)benzene to a suspension of FeCl$_2$ in benzene yields FeCl$_2$[1,2-(Me$_2$P)C$_6$H$_4$]$_2$. The ^{31}P NMR spectrum of FeCl$_2$[1,2-(Me$_2$P)C$_6$H$_4$]$_2$ shows that both the *cis* and *trans* isomers are present in solution. Reaction of the related complex FeCl$_2$[1,2-Me$_2$P)C$_6$H$_4$]$_2$ with NaBPh$_4$ in refluxing acetonitrile results in the formation of *trans*-[Fe(NCMe)$_2$(diphos)$_2$](BPh$_4$)$_2$; the structure of the cation has been determined by X-ray crystallography [126]. The dinitrogen complex [Fe(N$_2$)(depe)$_2$] (depe = 1,2-bis(diethylphosphino)ethane) has been prepared by reduction of [FeCl$_2$(depe)$_2$] with Na-naphthalene in thf under N$_2$ at room temperature. The crystal structure of the complex reveals a trigonal pyramidal coordination sphere around the iron with the dinitrogen ligand coordinated in an end-on fashion in one of the equatorial positions. The dinitrogen ligand is readily replaced by carbon monoxide [127]. In an attempt to prepare [Fe(NCMe)(dppm)]I$_2$, the complexes *trans*-[Fe(NCMe)$_2$(dppm)$_2$][FeI$_4$]·2H$_2$O (158) and [Fe(dppom)$_3$][I$_3$]$_2$ (dppom = Ph$_2$P(O)CH$_2$P(O)Ph$_2$) have been isolated and their crystal structures have been determined. It is likely that the earlier reported [Fe(NCMe)(dppm)]I$_2$ is, in fact, an impure sample of [Fe(NCMe)$_2$(dppm)]I$_2$[128].

(158)
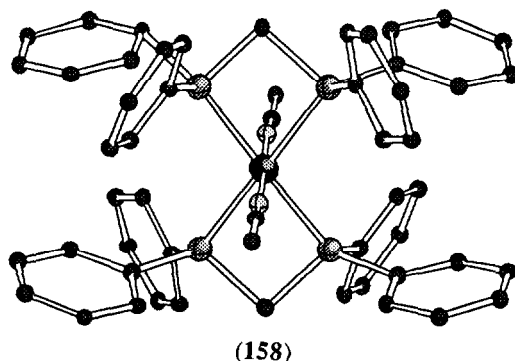
The complexes $Na_3[Fe(CN)_5\{P(OEt)_3\}]$ and $Na_2[Fe(CN)_5\{P(OEt)_3\}]$ have been synthesized and the photoaquation of the cyanide and triethylphosphite of the ferrous complex at acidic conditions has been studied. The photoaquation of the phosphite ligand was monitored by measuring the formation of $[Fe(CN)_5(Mepz)]^{2-}$ (Mepz = N-methylpyrazinium) via the intermediate $[Fe(CN)_5(H_2O)]^{3-}$. The quantum yields are $F_{CN} \approx 0.08$ and $F_{P(OEt)_3} \approx 0.13$ mol einstein^{-1} [129].

When mixed with $Fe(DPrPE)_2Cl_2$ (DPrPE = 1,2-bis(dipropylphosphinoethane), the unsymmetric ligands **159** and **160** displace DPrPE to give diamagnetic six-coordinate complexes of the type $Fe(PP_3)Cl_2$ [130].

(159)   (160)
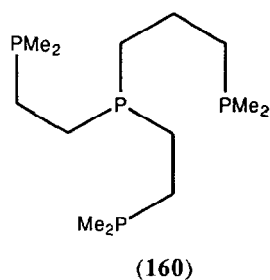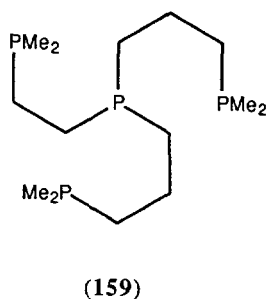
8.9   COMPLEXES WITH MIXED-DONOR LIGANDS

8.9.1   Complexes with mixed N,O-donor sets

The reactions of Fe(II) with the multidentate ligand, 7-[(3,5-dihalo-2-pyridyl)azo]-8-hydroxyquinoline-5-sulfonic acid (**161**) in aqueous solutions have been studied. By focusing on the coordination selectivity of chelate sites using polarographic and spectrophotometric methods. The Fe(II) ion selectively coordinates to the comparatively soft N,N,O-terdentate chelate site of the ligand [131]. The new tetradentate ligand (**162**), which contains both phenylazo and 8-quinolinol fragments, has been prepared. The ligand forms a 1:1 complex with Fe(II) in which the ligand coordinates in an N,O-didentate form through its 8-quinolinol fragment. The remaining coordination sites are filled by water [132].

(161) (X = Cl, Br)   (162)
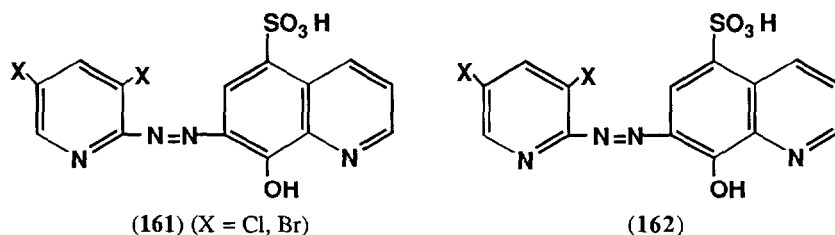
The phototransformation of Fe(III) nitrilotriacetate, Fe(NTA), under monochromatic excitation at different pH has been studied. Different photochemical behaviour was observed for different combinations of excitation wavelength and pH. In acidic medium, a redox process giving rise to Fe(II), HCHO and CO_2 always occurred but the stoichiometry of the photoproducts was bound to be dependent on the excitation wavelength. In neutral solution using a 365 nm excitation wavelength, a photosolvation with NTA release was observed while at 254 nm a subsequent redox process between OH and the hydrous ferric oxide could be detected [133].

The new ligand 1,3-pyrimidinyl-2,4,6-pyrimidinetrione has been synthesized and its Fe(III) complex (163) has been prepared. Elemental analysis indicates that a chloro-bridged dimer is formed. The low energy IR band due to the bipyrimidine ring is very weak. Bonds of 362 and 235 cm^{-1} are assigned to the terminal and bridging Fe-Cl stretches, respectively [134].

(163)
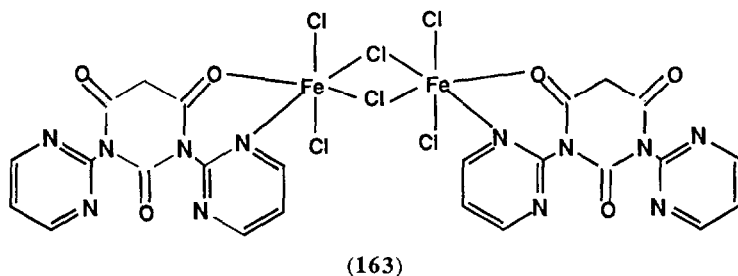
The complexes Fe(164)$_2$·H$_2$O, Fe(165)$_2$·3H$_2$O, Fe(165)$_3$, Fe(165)$_2$·3H$_2$O and Fe(166)$_2$phen·2H$_2$O have been prepared by direct electrochemical synthesis, i.e. the electrochemical oxidation of the metal in the presence of the appropriate ligand. There are no v(O-H) bands in the IR spectra, indicating that it is the monoanionic form of the ligand which coordinates to the metal. Various shifts in stretches for the different ligands indicate that they coordinate in their didentate forms [135].

(164)   (165)
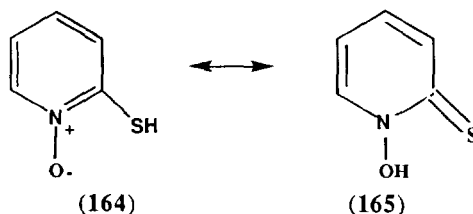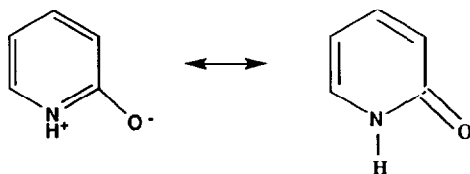
(166)

When the ligand 1,5-[*bis*(4-imindazolylmethyl)amino]-3-pentanol (167) is reacted with $Fe(NO_3)_3 \cdot 9H_2O$ and sodium acetate in acidic solution, the diferric complex $[Fe_2(OAc)_2(167)](ClO_4)_3 \cdot H_2O$ is formed. It can be electrochemically reduced to a mixed-valence species which is slowly reoxidized to the all-ferric complex upon exposure to open atmosphere. Magnetic measurements indicate antiferromagnetic coupling between the metal centre although variable temperature data could not be fitted to the isotropic Heisenberg model [136].
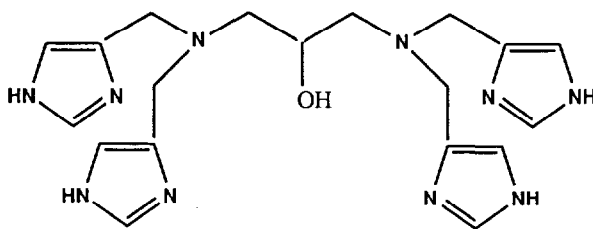
(167)

The ligand (168) has been prepared. Reaction of (168) with $Fe(ClO_4)_2 \cdot 6H_2O$ in the presence of sodium acetate in methanolic solution affords the complex $[Fe_2(168)(OAc)_2]ClO_4 \cdot H_2O$. The molecular structure of the iron complex has been determined by X-ray crystallography; the Fe-Fe distance is relatively large, *ca.* 3.53 Å. Mössbauer and magnetic measurements indicate that the complex contains antiferromagnetically coupled high-spin Fe(III) ions ($J \approx -6.0$ cm^{-1}) [137].

(168)
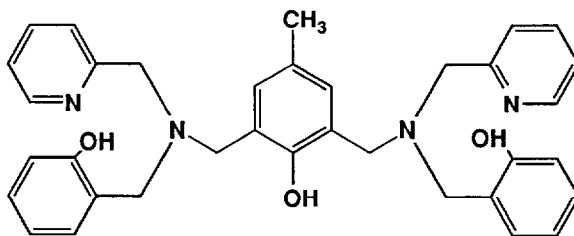
Three bis-(μ-halo) diferrous complexes, $[Fe_2(TLA)_2F_2](BF_4)_2$ (TLA = tris[(6-methyl-2-pyridyl)methyl]amine) (169) $[Fe_2(TMPzA)_2Cl_2](BPh_4)_2$ (TMPza = tris[(3,5-dimethyl-2-pyrazolyl)methyl]amine) (170) and $[Fe_2(TPA)_2Cl_2](BPh_4)_2$ (TPA = tris(2-pyridylmethyl)amine)

(171) have been synthesized. The Fe-Fe distances in the complexes are 3.20, 3.56 and 3.49 Å, respectively. The iron ions of the three complexes are ferromagnetically coupled ($J = 0.6$-5.0 cm^{-1}) and exhibit integer spin EPR signals in the vicinity of $g = 18$ [138].
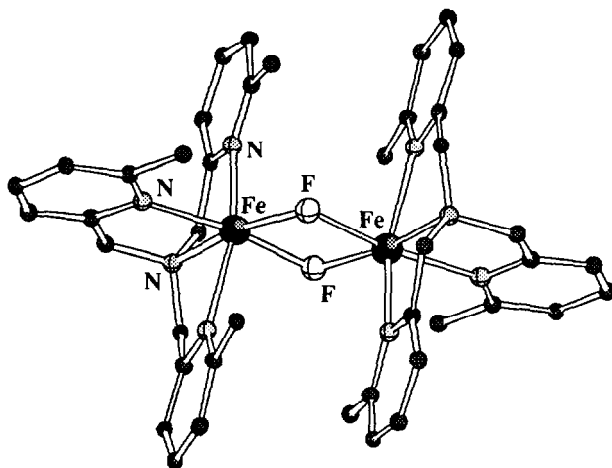
(169)
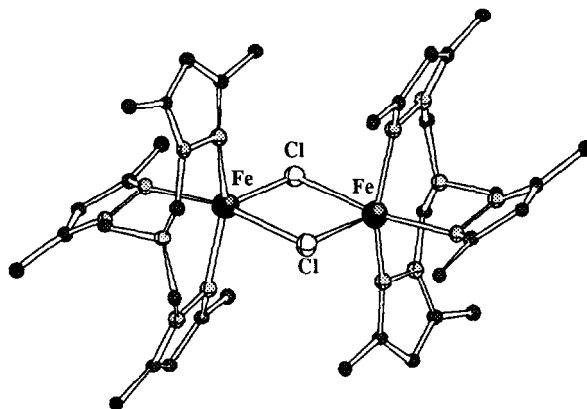
(170)

The polymeric complexes [Fe(172)L]ClO$_4$ [L = (173), (174), (175)] have been prepared and studied by X-ray crystallography, magnetic susceptibility measurements, EPR and Mössbauer spectroscopy. The crystal structure of the (175) complex reveals that it crystallizes in a zigzag-chain polymeric structure in which the iron atoms are equatorially coordinated by the N$_2$O$_2$-donor Schiff-base ligands and axially coordinated by the bridging 1,1'-tetramethylenediimidazole ligands. The variable-temperature magnetic susceptibility data indicate that the (173) complex is low spin (S = 1/2), the (174) complex exhibits a spin equilibrium (S = 5/2 ⇔ 1/2) and the (175) complex is essentially high spin although a spin equilibrium could be detected at low temperatures [139].
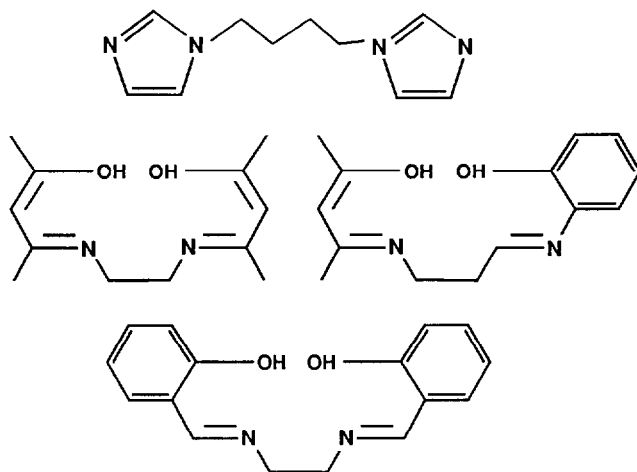
(172) (top), (173) (middle left), (174) (middle right), (175) (bottom)
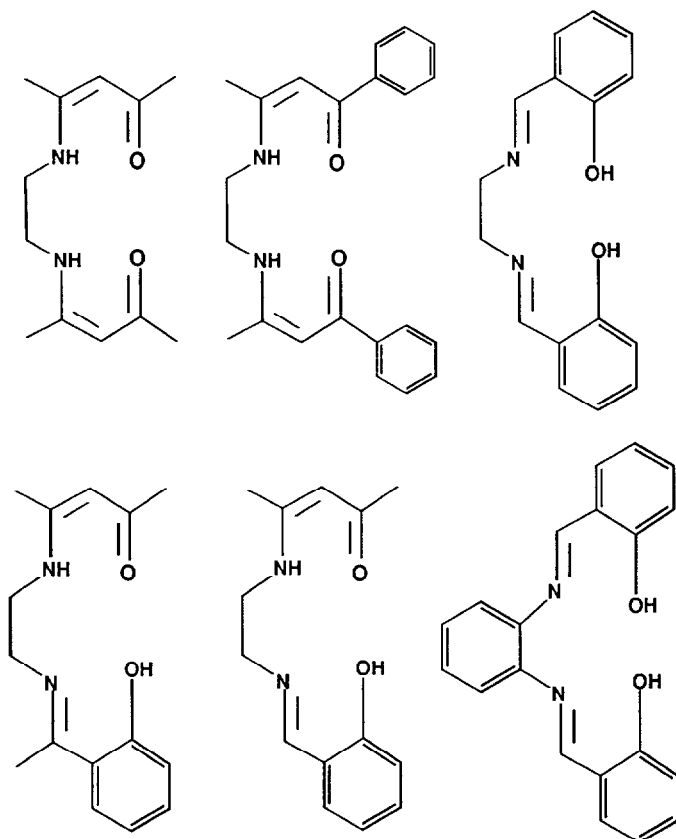
(176-178) (top)	(177-181) (bottom)

The electrochemical reduction of the Schiff-base complexes FeIII(L)Cl, where L is one of the Schiff bases (176-181), has been studied in aprotic solvents by cyclic voltammetry, coulometry and UV-visible spectroscopy. The reduction of FeIII(L)Cl into FeII(L)Cl occurs at a potential of *ca.* –0.5 V vs. SCE. An oxidation process attributable to oxidation of the Schiff base occurs around 1 V. If traces of oxygen (or residual water) are present, there is also a second reduction process at *ca.* –1 V which may be attributed to the reduction of the μ-oxo bridged Fe(III) dimers (L)Fe-O-Fe(L) [140].

The stability constants for ferric complexes of 1-hydroxy-2-pyridinone (182) have been determined by potentiometric titrations. The investigations have been carried out using 1:1, 1:2 and 1:3 (metal:ligand) solutions. Ferric hydroxides precipitate as the pH is increased. The stability constants (log β_n) are: Fe(1), 10.7; Fe(1)2, 9.5; Fe(1)3, 7.1 [141].

(182)
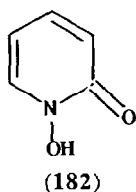
The dark green complex [FeCl2(183)]·H2O has been prepared. Infra-red spectroscopy indicates that the ligand is coordinating in its doubly protonated form; the structure of the complex is probably trigonal bipyramidal with the chloro ligands occupying axial positions. The magnetic moment of 5.46 μB and the Mössbauer spectrum of [FeCl2(183)]·H2O indicate that it is a high-spin iron (II) species. There is a change in the quadrupolar splitting going from low temperature to room temperature. This change may be due to thermal population of one or more of the four singly occupied 3d orbitals by the single electron originally lying in the lowest energy of an ^5A state. Reaction of anhydrous FeCl3 with (184) results in the formation of the brown complex [FeCl(184)(H2O)]. Magnetic measurements indicate that [FeCl(184)(H2O)] contains an high-spin Fe(III). The Mössbauer spectrum shows that there are two distinct iron sites that are antiferromagnetically coupled. It is suggested that [FeCl(184)(H2O)] has a dimeric structure [142].

(183) (R = H), (184) (R = Me)
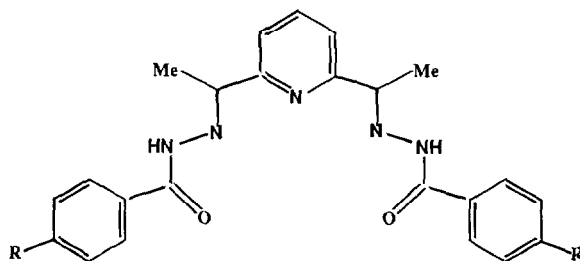
The ligands (**185-188**) have been reacted with Fe(OAc)$_2$ or FeCl$_3$ to form the mononuclear complexes Fe(**185**)(OH), Fe(**185**)(Cl).0.2LiCl·2H$_2$O, Fe(**186**)(OH), Fe(**186**)(OH), Fe(**187**)(OH)·MeOH, Fe(**186**)(OH)·1.5H$_2$O in which the metal coordinates in the inner N$_2$O$_2$ pocket. It is also possible to synthesize dinuclear complexes by the addition of two equivalents of iron. Mössbauer spectroscopy reveals that in all cases that of Fe$_2$(**188**)(OH)$_2$, the irons are oxidized to iron (III). Variable temperature magnetic susceptibility measurements show that there is antiferromagnetic coupling between the iron ions in the dinuclear complexes [143].

(**185**) R = -(CH$_2$)$_2$-
(**186**) R = -CMe$_2$CH$_2$-
(**187**) R = -CH$_2$CMe$_2$CH$_2$-
(**188**) R = -C$_6$H$_4$-

(**189**) R = H
(**190**) R = Me
(**191**) R = CH$_2$CO$_2$H
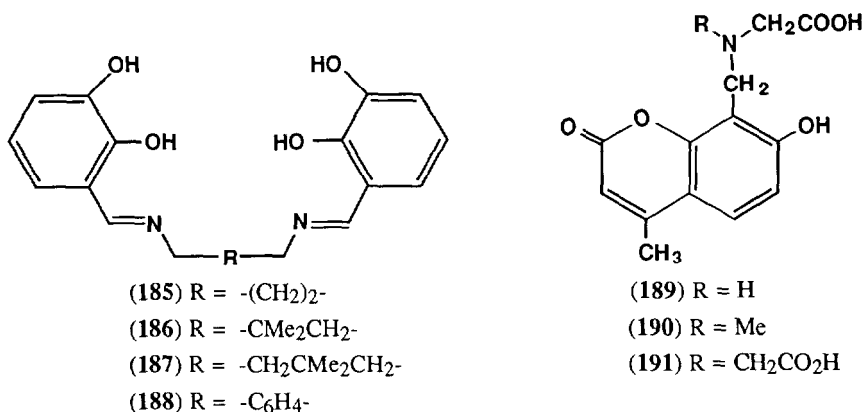
The ligands (**189-191**) form 1:1 complexes with iron(III). The stability constants (log β$_{11}$ mol^{-1} dm^{-3}) for [Fe(**189**)]$^+$ is 15.74±0.20, while those for [Fe(**190**)]$^+$ and [Fe(**191**)] are 15.69±0.20 and 18.67 ±0.20, respectively. Kinetic studies indicate that the reaction mechanism involves the initial (slow) coordination of the phenolato oxygen, followed by rapid donations of the amino nitrogen and carboxylato moiety to form mono (terdentato- and tetradentato-) iron (III) complexes (Scheme 4) [144].

[Fe(**189**)(H$_2$O)$_3$] (R = H)
[Fe(**190**)(H$_2$O)$_3$] (R = Me)

[Fe(**191**)(H$_2$O)$_2$]
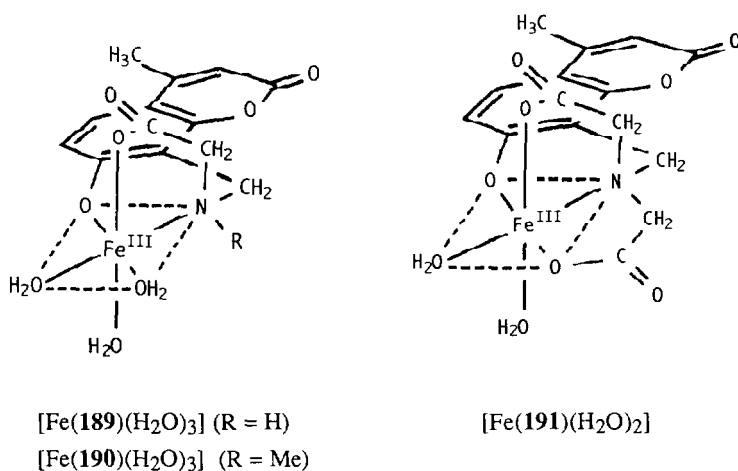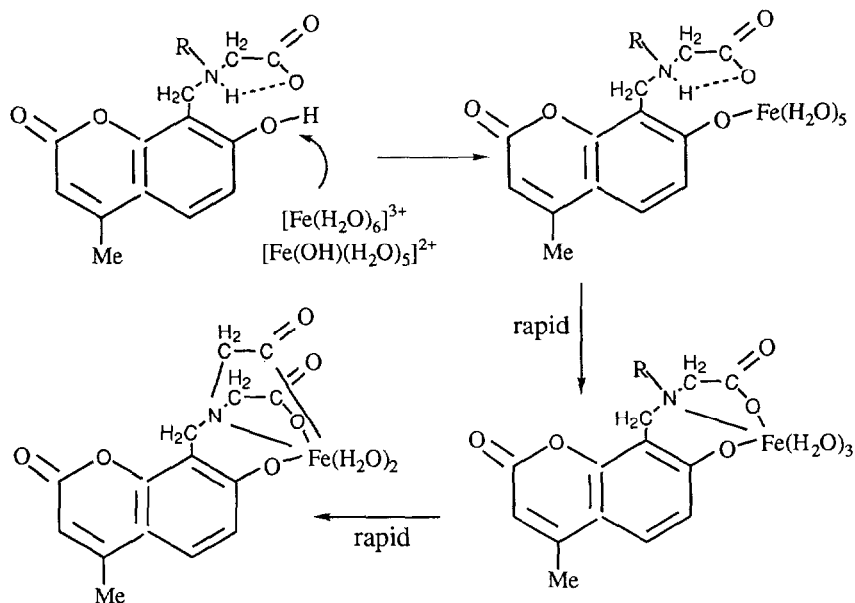
Scheme 4

The ligands (192) and (193) form stable complexes with iron(III), [Fe₂L₃] [L = (192), (193)]. Electrochemical measurements indicate that release of iron occurs upon reduction. The slope of E_{pc} in cyclic voltammetric experiments *vs* pH indicate that the Fe(II) complexes are protonated before dissociation: $Fe_2L_3 + H^+ + 2$ e- $\Leftrightarrow Fe_2HL_3^-$ [145, 146]. The kinetics of iron release from the dinuclear iron(III) complex $Fe_2(192)_3$ in the presence of edta has been studied by UV-VIS spectrophotometry. The release appears to take place in a two-step mechanism, one iron atom being released in each step. It is proposed that there are two conformers of the Fe_2L_3 complex. One conformation reacts directly with edta while the other reacts with an intermediate [147].

(192)   (193)
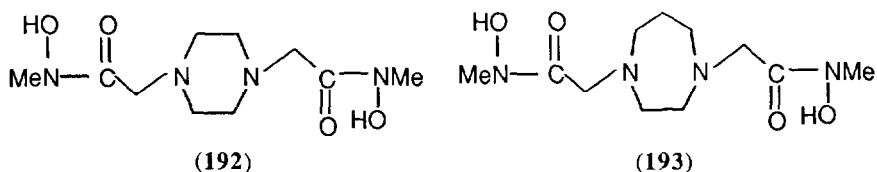
The synthesis and characterization of (194)iron(II)chloride, (195), is reported. The X-ray structure confirms a *pseudo*-octahedral structure with the chloride ligated *trans* to a nitrogen of the pentadentate ligand. The magnetic moment of (195) was found to be 4.92 µß indicating a high spin Fe(II) with four unpaired electrons [148].

(194)   (195)
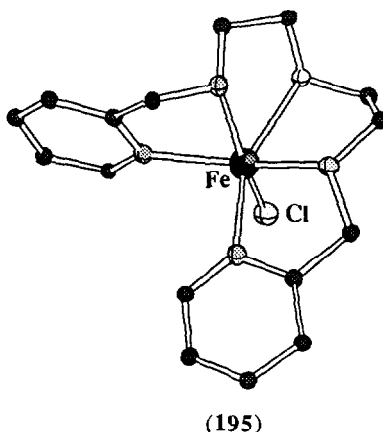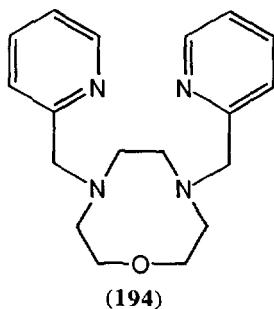
The absorption, low-temperature MCD and EPR spectra of the nitrosyl complexes [Fe(edta)(NO)], [Fe(196)(NO)] and [Fe(197)(NO)] have been obtained. The spectra of all three compounds are very similar. The EPR spectra are consistent with an S = 3/2 ground state spin system in which the lower m_s = ±1/2 Kramers doublet with $g_\perp \approx 4$ and $g_{||} \approx 2$ is observed. The variable-temperature MCD spectra indicate that there is thermal population of the upper m_s = 3/2 doublet. The spectra have been analyzed based on earlier calculations. The results lend some support to an earlier proposal that the S = 3/2 ground state results from the antiferromagnetic coupling of high-spin Fe(II) ion to NO⁻[149].

(196), R = -(CH$_2$)$_2$O(CH$_2$)$_2$O(CH$_2$)$_2$-
(197), R = -(CH$_2$)$_6$-
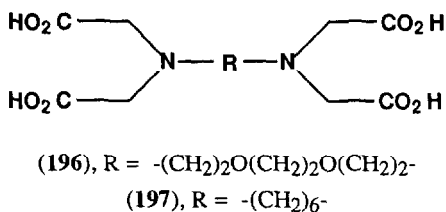
In order to understand how a solvate molecule in the crystal of a spin-crossover complex affects the transformation from low- to high-spin states, the series [Fe(198)$_2$]-(ClO$_4$)·S (199) where S = non-solvated C$_6$H$_6$, C$_6$H$_5$Cl, C$_6$H$_5$Br, o-C$_6$H$_4$Cl$_2$, or C$_6$H$_5$I were studied. In the series there are at least five different crystallographic phases but all have the same packing arrangements. In all cases there are stacks of Fe(III) cations surrounded by columns of ClO$_4$⁻ anions and S solvates molecules. It is clear that the solvate molecule affects intermolecular interactions both within the stacks of Fe(III) cations and between Fe(III) cations in neighbouring stacks. The space groups in which the complexes crystallize are dependent on temperature. When S = C$_6$H$_5$Cl and C$_6$H$_5$Br, the space group is P21/c at 296 K and P21/a at 158 K. The anions and cations remain in the same relative positions, however, half of the solvate molecules reorientate. Below ~50 K all six complexes are low-spin Fe(III) with μ_{eff} = 2.0 µB. As temperature is increased, all six exhibit spin-crossover transformations. The non-solvated complex exhibits the most gradual transformation and the

C_6H_5Cl is the most abrupt [150]. Variable temperature solid state ^2H NMR was used to examine C_6D_6, C_6D_5Cl and C_6D_5Br solvates in the series. Throughout the 147-295 K region, the solvate molecules were found to undergo rapid rotation about a local C_6 axis normal to the plane of the molecule. Of all the complexes only the C_6H_5Cl solvate exhibited a strong cooperativity in the spin-crossover transformation; in the other complexes cooperativity is very weak, if any [150].
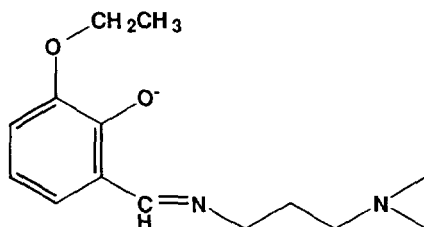
(198)
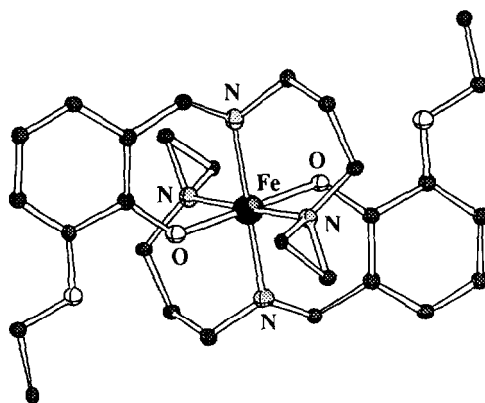
(199)

The reaction of $FeCl_2$ with (200) in tetrahydrofuran has been characterized by elemental microanalysis, NMR, IR and cycle voltammetry. The analogous copper complex [{$CuCl$}$_2$(μ-L)$_2$] has been characterized crystallographically showing that it is a dimeric oxygen bridged compound. In the iron complex two reduction waves were observed. The first potential is reversible and corresponds to mixed valence Fe(II)-Fe(III) species and the second is irreversible and is attributed to the formation of a Fe(II)Fe(III) dimer [151].
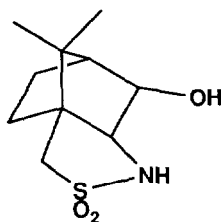
(200)

The high spin Fe(III) complexes of the hexadentate macrocyclic ligands 1,4,7-*tris*(3- or 5-tert-butyl-2-oxybenzyl)-1,4,7-triazacyclonane, which contain three *o,o*- (L_o^{3-}) or *o,p*- (L_p^{3-}) disubstituted phenolates, respectively, and which form a *pseudo*-octahedral environment have been photolyzed or chemically oxidized. It has been demonstrated that the species formed from Fe(III)L_p **(201)** or Fe(III)L_o **(202)** by ≈250 nm photolysis in chlorinated hydrocarbons or by reaction with one-electron oxidants (SO_4^-, $H_2PO_4^-$, or O_2^{-+}) in polar solvents is a radical cation with the unpaired spin located on one of the phenolate moieties of the macrocyclic ligand. The oxidation state of the metal centre (Fe(III)) is not changed. The oxidized molecules are thus systems in which the ligand carries the oxidation equivalent [152].
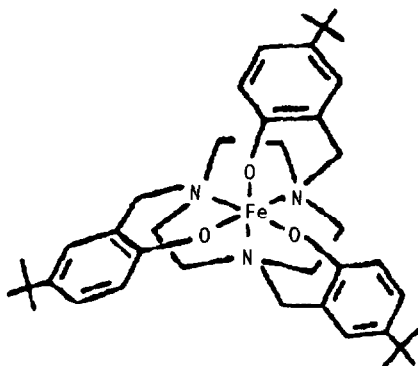
(201)

The Fe(III) complexes of the macrocyclic amino carboxylates **(203)** and **(204)** have been synthesized, characterized and evaluated for use as potential contrast agents for magnetic resonance imaging. X-ray crystallography reveals that four nitrogens and three oxygens are coordinated to the iron in both Na[Fe(203)]·5H₂O **(205)** and [Fe(204)]·3H₂O. None of the waters are coordinated to iron atoms and **(203)** has an uncoordinated carboxylate arm. Magnetic susceptibility and Mössbauer data confirm that both of the Fe(III) complexes are high spin (S = 5/2) [153].

The reactivities of two Fe(II) complexes, Fe(206)$^{2+}$ and Fe(207)$^{2+}$, with the superoxide anion have been investigated. Under non-aqueous conditions, both complexes react with superoxide giving *pseudo*-first-order rate constants, Fe(206)$^{2+}$: 350 ± 30 s^{-1} and Fe(207)$^{2+}$: 100 ± 10 s^{-1}. EPR spectroscopy indicates that the final product of Fe(206)$^{2+}$ with superoxide is an iron(III) complex while the Fe(207)$^{2+}$ product is EPR silent [154].

HOOC—⌐\N/⌐\N—R

HOOC—⌐\N/⌐\N—COOH

(203) (R=H), (204) (R=-CH₂CO₂H)

(205)

(206)

(207)
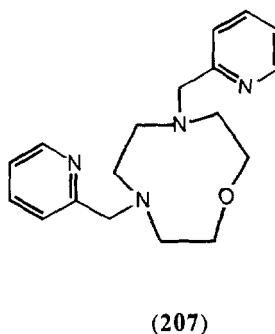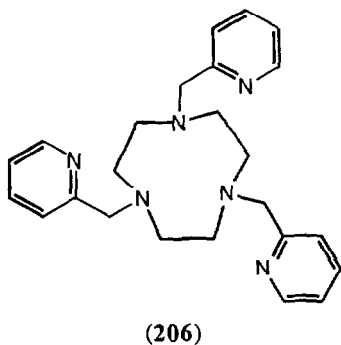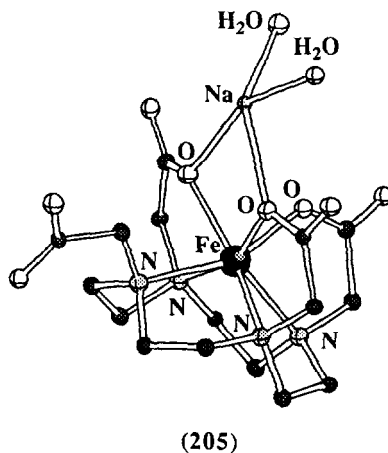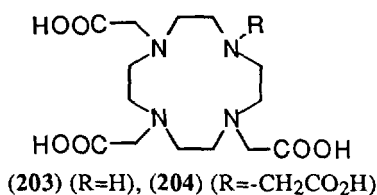
8.9.2   Complexes with mixed N,S-donor sets

Reflux of ligands (208), (209) or (210) with FeCl₃ in ethanol leads to cleavage of the S-But bonds and formation of the corresponding mononuclear iron(III) $N_2S^*_2S_2$ (S^* = thioether) complexes. Mössbauer spectroscopy, EPR and magnetic measurements confirm that these iron complexes are low-spin. The complex of ligand (209) exhibits a quasi-reversible Fe(III)/Fe(II) couple at $E_p = -1.66$ V while that of ligand (210) exhibits a quasi-reversible oxidation at 0.86 V [155].

The synthesis and characterization of (211) and its iron(III) complex (212) containing an N_3S_3 donor have been achieved. The ligand (213) also forms a stable iron(III) complex (214). The spectroscopic properties of (212) and (214) are compared to those reported for the iron-sulfur site in nitrile hydratase. Spectroscopy supports a high spin ferric ion in a pseudo-octahedral environment for (212). Cyclic voltammetry indicates that the trimercapto ligand (213) stabilizes the trivalent iron(III) more efficiently than the tris(thiophenolato) ligand (211) [156].
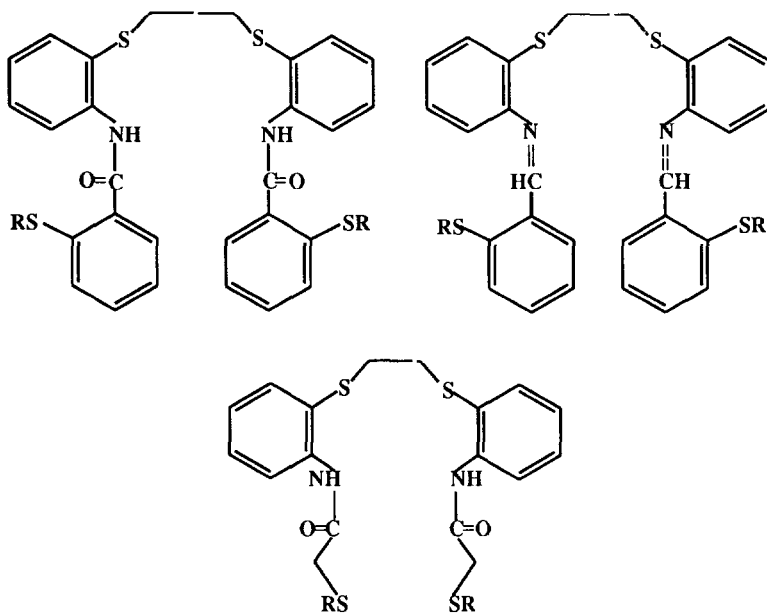
(208) (top left), (209) (top right), (210)
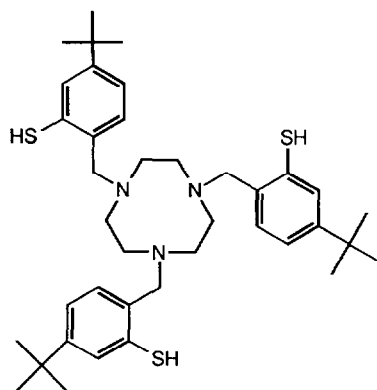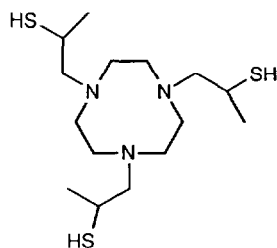
(211)   (213)
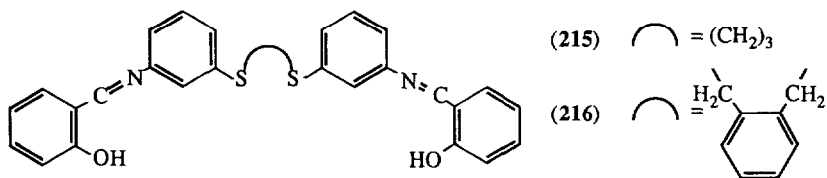
(215) $\cap$ = (CH$_2$)$_3$

(216) $\cap$ = H$_2$C—CH$_2$

8.9.3 Complexes with other mixed-donor ligands

Reaction of the hexadentate N,S,O-donor ligands (215) and (216) with anhydrous $FeCl_3$ results in the formation of [Fe(215)][FeCl$_4$] and [Fe(216)][FeCl$_4$], while the corresponding reaction with Fe(ClO$_4$)$_3$·6H$_2$O leads to the corresponding perchlorate salts. The iron (III) centres of the complex cations are low spin in the FeCl$_4^-$ salts and high spin in the ClO$_4^-$ salts [157].

8.10 IRON-OXO CLUSTERS

Garnet-red single crystals of K$_3$[FeO$_2$] have been obtained by heating a mixture of K$_6$[CdO$_4$] and CdO in closed Fe-cylinders at 450° during 40 days. The solid state structure consists of dumbbell-like [O-Fe-O]$^{3-}$ anions which are linked *via* potassium ions to form a three-dimensional network [158]. The kinetics of oxidation of alcohols by the ferrate ion under basic conditions have been studied. It is proposed that the mechanism involves a [2+2] addition of an Fe=O bond to the α-C-H of the alcohol to give an organometallic intermediate that subsequently decomposes by homolytic cleavage of the resulting C-Fe bond [159].

CaFe$_5$(PO$_4$)$_5$(OH)·H$_2$O and SrFe$_5$(PO$_4$)$_5$(OH)·H$_2$O have been synthesized hydrothermally and structurally characterized. The two compounds are isostructural. The complex framework consists of dimers of corner sharing and edge-sharing Fe(III)O$_6$ octahedra joined through Fe(II)O$_5$ trigonal bipyramids by corner- and edge-sharing and discrete Fe(III)O$_6$ octahedra. Mössbauer spectroscopy identifies one Fe(II) and four Fe(III) ions in the complexes [160]. A ferrous phosphate SrFe$_3$(P$_2$O$_7$)$_2$ has been hydrothermally synthesized and structurally characterized. The complex consists of zigzag infinite chains of FeO$_6$ octahedra sharing either trans of skew edges. The magnetic susceptibility of SrFe$_3$(P$_2$O$_7$)$_2$ indicates the complex is paramagnetic with an effective magnetic moment of 5.07 μ_B per Fe between 310 and 26 K. Below 26 K the magnetic susceptibility increases to a maximum at 6 K and then decreases rapidly. Mössbauer spectroscopy confirms the presence of Fe(II) [161].

8.10.1 Di- and tri-nuclear iron-oxo clusters

The structural features of the [Fe$_2$Cl$_6$O]$^{2-}$ have been re-examined. Eleven crystal structure determinations of salts containing [Fe$_2$Cl$_6$O]$^{2-}$ have been reported since 1978. Five of the salts were investigated by infrared and Raman spectroscopy and magnetic studies were carried out. Antiferromagnetic exchange coupling between the ferric ions was established in all cases. The coupling constant was found to be 112 ± 5 cm^{-1} irrespective of the structure of the [Fe$_2$Cl$_6$O]$^{2-}$ anion. The following conclusions have been made: i) the structure is dependent on the nature of the counter-cation. ii) a linear Fe-O-Fe unit has not been verified. iii) The Fe-O-Fe angles span from 146.5 to 170.8°. iii) Fe-O bond distances are identical within error (1.756 Å). iv) the geometry of Cl$_3$FeO is tetrahedral. v) the two corner sharing tetrahedra adopt different conformations depending on the nature of the counter-cation [162].

A ferrous complex of the ligand tris((benzimidazol2-yl)methyl)amine (ntb, **217**), [Fe(ntb)Cl$_2$](PF$_6$)$_{0.5}$Cl$_{0.5}$. In aqueous ethereal solution containing NEt$_4$Cl, this mononuclear complex dimerizes to form [Fe$_2$O(ntb)$_2$Cl$_2$](PF$_6$)$_2$ · 4 thf, whose crystal structure reveals that the Fe-O-Fe moiety is linear. When the same type of reaction is carried out using Fe(ClO$_4$)$_3$ · x H$_2$O as starting material, the acetate-bridged compound [Fe$_2$O(OAc)(ntb)$_2$](ClO$_4$)$_3$ is produced. The dinuclear complex may also be synthesized from the reaction of 1 with FeCl$_3$ · 6 H$_2$O in acetonitrile in the presence of KPF$_6$ and sodium acetate. Cyclic voltammetry of the iron-oxo dimer shows an electrochemically irreversible redox process which is postulated to be an Fe$_2$(III, III)/Fe$_2$(III, IV) couple. Magnetic measurements (Evans method) reveal antiferromagnetic coupling in both dinuclear compounds [163].

(217)   (218)
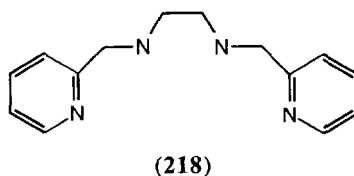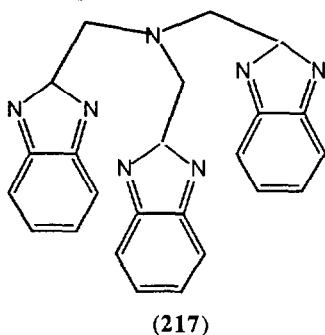
The monomeric complexes [(**218**)FeCl$_2$]X (X = ClO$_4^-$ (**219**), Cl$^-$ (**220**)) and the oxo-bridged dimeric complexes {[(**218**)(Cl)Fe]$_2$(μ-O)}(I$_3$)$_2$ (**221**), {[(**218**)Fe]$_2$(μ-O)(μ-OAc)}I$_3$.2H$_2$O (**222**) and {[(**218**)(Cl)Fe]$_2$(μ-O)(μ-CO$_3$)}I$_2$ (**222a**) have been synthesized and, in the case of (**219**), (**221**), (**222**) and (**222a**), characterized by X-ray crystallography. Complex (**221**) contains a linear Fe-O-Fe core with an Fe-Fe distance of *ca.* 3.60 Å while the bent cores of (**222**) and (**222a**) results in an Fe-Fe separation of 3.25 Å in both cases. All these oxo-bridged complexes exhibit relatively strong antiferromagnetic coupling between the ferric ions [(**221**), J≈-102.1 cm^{-1}; (**222**), J≈-118.2 cm^{-1}; (**222a**), J≈-113.6 cm^{-1}] [164].

(219)

(222a)
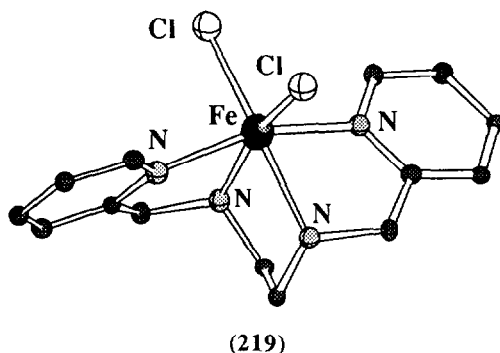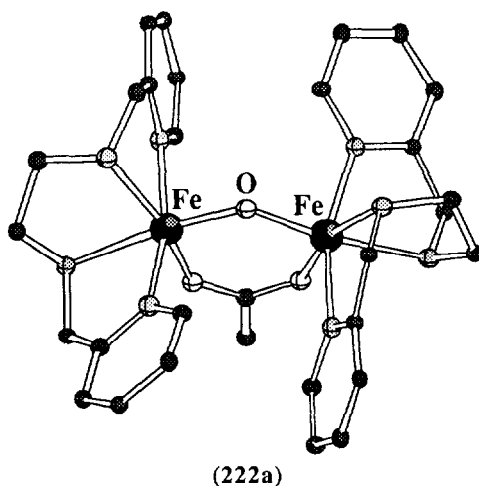
Using dinucleating ligands (223)-(225) that contain the 2-hydroxypropane backbone, diferrous complexes [Fe$_2$L(OCC$_6$H$_5$)]X$_2$ [L = (223)-(225)], which generate dioxygen species upon exposure to air have been characterized. These complexes differ from previously reported diferrous complexes in having accessible coordination sites which permit irreversible formation of dioxygen species. Both Fe(II) centres have trigonal bipyramidal geometries and NMR spectroscopic studies show that the remaining coordination sites are accessible to ligands such as dmso and Ph$_3$PO. The differing stabilities of the dioxygen species are reflected in differences of reactivity. The dioxygen adducts have tri-bridged (μ-1,2-peroxo)(μ-carboxylato)(μ-alkoxo) diferric cores. The (μ-1,2-peroxo) diiron structure is distinct from what is found for oxyhemerythrin which has a terminal hydroperoxide bound to one of the iron centres [165].
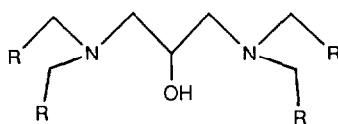
(223) (R = 2-benzimidazolylmethyl), (224) (R = 2-benzimidazolylethyl), (225) (R = Py)

The dinuclear complex [(Me$_3$TACN)Fe(μ-O)(μ-OAc)$_2$Fe(bpy)Cl]$^+$ (226) has been synthesized from the reaction of [(bpy)$_2$Fe$_4$O$_2$(Oac)$_7$][PF$_6$] with (Me$_3$TACN)FeCl$_3$ and 2,2'-bipyridine in acetonitrile. X-ray crystallography reveals that the complex is asymmetric; in addition to oxo- and acetate bridges, one iron atom is ligated by a Me$_3$TACN ligand in addition to oxo- and acetate bridges, one iron atom is ligated by a Me$_3$TACN ligand while the other is ligated by a bpy and a chloro ligand. The latter ligand may be replaced by water to form [(Me$_3$TACN)Fe(μ-O)(μ-OAc)$_2$Fe(bpy)(H$_2$O)]$^+$ (227). Complex (227) displays catalase activity by catalyzing the disproportionation of H$_2$O$_2$. Kinetic measurements show that the reaction follows zeroth-order kinetics from the start of the reaction until approximately 200-300 turnovers; the reaction is terminated by decomposition of complex (227). A proposed mechanism for the hydrogen peroxide

disproportionation is shown in Scheme 5. It is suggested that the binding of H_2O_2 or (HO_2^-) is the rate-determining step [166].

$[Fe_2(223)(OCC_6H_5)]X_2$

Scheme 5

The trinuclear carboxylate complex $[Fe_3(III)O(OBz)_6(OMe)_3]^+$ (228) has been synthesized. The Mössbauer spectrum of (228) shows a signal at $\delta = 0.31$ mm s^{-1} with $E_a \approx 0.35$

mm s^{-1}[167]. The reaction of FeCl(HB(3,5-iPr$_2$pz)$_3$) with Na(acac) produces Fe(acac)(HB(3,5-iPr$_2$pz)$_3$) whose reactivity is similar to Fe(OBz)(3,5-iPr$_2$pz)$_3$. Fe(acac)(HB(3,5-iPr$_2$pz)$_3$) reacts with dioxygen to produce a blue-green product, presumably a μ-peroxo adduct. This species is unstable and decomposes even at -78 °C. Greenish brown crystals of the oxidized product Fe$_3$O$_2$(μ-OAc)$_4$(HB(3,5-iPr$_2$pz)$_3$)$_2$ (229) were isolated from an acetonitrile solution of Fe(acac)(HB(3,5-iPr$_2$pz)$_3$) which was allowed to stand under aerobic conditions. The molecular structure of (229) was determined by X-ray crystallography. The IR spectrum shows the presence of a hydroxo group. The Mössbauer spectrum of (229) reveals high spin iron(III) states for all three iron atoms. From the spectroscopic data the formulation must be an all ferric compound with crystallographic disorder of the μ-oxo *bis*(μ-acetato) and μ-hydroxo *bis*(μ-acetato) bridges [168].

Electrospray mass spectrometric (ESMS) studies have been made on some representative examples of the trinuclear complexes [Fe$_3$O(RCOO)$_6$(H$_2$O)$_3$]$^+$ (R = H, Me, Et, ^{t}Bu) in methanol and pyridine/methanol solutions. The ES mass spectra of [Fe$_3$O(CH$_3$COO)$_6$(H$_2$O)$_3$]$^+$ show that the water molecules exchange completely with the solvent and for other iron derivatives, the core carboxylate ligands exchange completely with the acetate in the mobile phase used in the spectrometer [169].

Carbon-13 NMR spectroscopy was found to be useful for determining the number of inequivalent carboxylates bound to oxygen bridged diiron centres. Proton decoupled ^{13}C NMR spectra for the complexes [Fe$_2$O(OC^{13}CH$_3$)$_2$(HBpz$_3$)$_2$], [Fe$_2$O(OC^{13}CH)$_2$(HBpz$_3$)$_2$] and (Et$_4$N)[Fe$_4$O$_2$(OC^{13}CH$_3$)$_7$(HBpz$_3$)$_2$] were examined. Both the acetate and formate carbon resonances exhibit smaller linewidths (150 and 300 Hz) and isotropic shifts (13 and -29 ppm) compared to the methyl carbon resonance. For the {Fe$_4$O$_2$}$^{7+}$ species the ^{13}C resonances are shifted much further downfield. The large chemical shift difference of acetate bound in {Fe$_2$O} and in {Fe$_4$O$_2$}$^{7+}$ reflects the difference in magnetic moment of the tetranuclear species (μ$_{eff}$/Fe = 2.34 μ$_B$) compared to the more strongly coupled dinuclear species (μ$_{eff}$/Fe = 1.71 μ$_B$) [170].

The complex [Fe$_2$(TPA)$_2$O-(OAc)](ClO$_4$)$_3$ is an efficient catalyst for cyclohexane oxidation by TBHP (*tert*-butylperoxide) affording cyclohexanol, cyclohexanone, and (*tert*-butylperoxy)cyclohexane. The catalytic mechanism for TBHP utilization was explored by observing the effects of varying the tripodal ligands on the (μ-oxo)(μ-carboxylato)diferric catalysts and by varying the bridge on Fe$_2$O(TPA)$_2$. The cyclohexanol + cyclohexanone/(*tert*-butylperoxy)cyclohexane ratio increased as ligands became more electron donating (TPA < (230) < (231) < (217) < HB(pz)$_3$) and the reaction times also increased. The addition of dimethyl sulfide to the system suppresses cyclohexanol and cyclohexanone formation but does not affect (*tert*-butylperoxy)cyclohexane formation suggesting cyclohexanol and cyclohexanone must derive from an oxidant different from that responsible for (*tert*-butylperoxy)cyclohexane production [171].

(230)

(231)
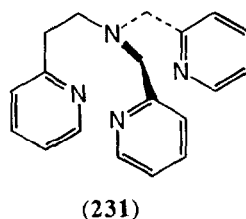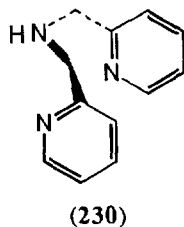
The thermodynamic and/or kinetic control of selective exchange reactions of the terminal over bridging carboxylate ligands of $Fe_2(H_2O)(CF_3CO_2)_4(tmen)_2$ (232) using a new set of rigid multifunctional phenol-containing ligands and bulky monocarboxylic acids has been reported. The reaction of (232) with (233) produces (234). A number of similar reactions are reported [172]. Fluorine-19 NMR studies reveal that analogues of ligand (233) replace the terminal rather than the bridging carboxylate ligands in complex (232) [173]. NMR analyses of $[Fe_2(OH)(O_2CR)_2(Me_3\text{-}TACN)_2]^+$ (235) and (232) have been reported confirming that the solid state structures are maintained in solution and provide spectroscopic distinction between a bridging hydroxide and a bridging water. The ^{19}F NMR spectra of (235) only show resonances of the bridging $CF_3CO_2^-$ ligand and $CF_3SO_3^-$ counterion. The ^{19}F NMR spectra of (232) each show two $CF_3CO_2^-$ resonances corresponding to bridging and terminal fluorine ligands [174].
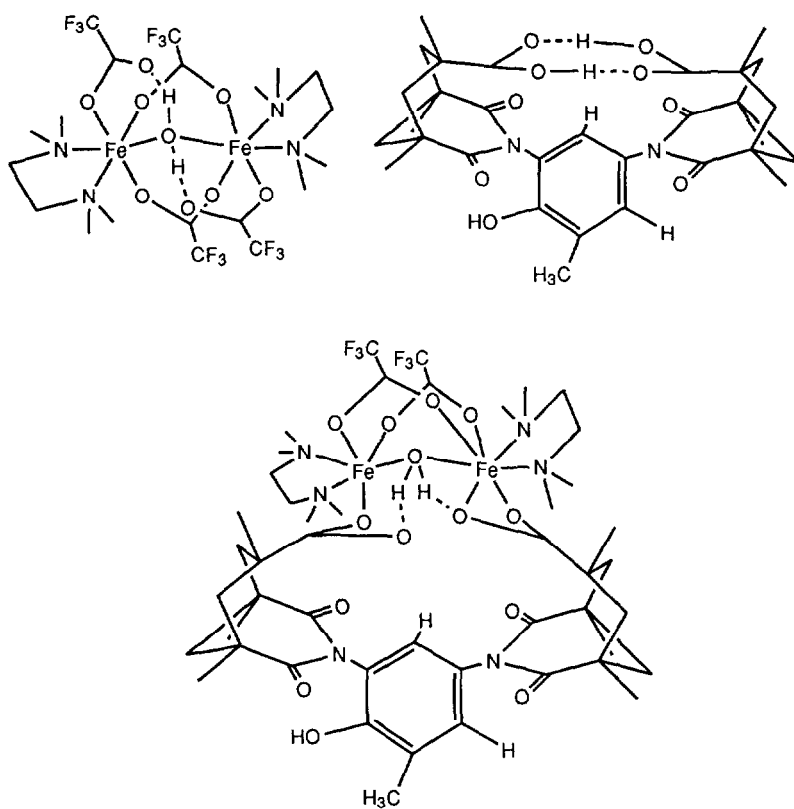
(232) (top left), (233) (top right), (234)

A series of Fe-O-Fe complexes, $Fe_2OL_4X_n(ClO_4)_m$, have been synthesized and characterized; they were designed for presenting one exchangeable coordination site (X = H_2O, Cl, CH_3CO_2, CF_3CO_2) per iron in order to allow oxidants and substrates to interact with the ferric ion. The coordination sphere of each iron is completed by two didentate nitrogen ligands (L = bpy, 4,4'-

dimethyl-2,2'-bipyridine, and phen). $Fe_2O(4,4'$-dimethyl-2,2'-bipyridine$)_4(CF_3CO_2)_2(ClO_4)_2$ (**236**) was characterized crystallographically. The complexes were found to catalyze the oxidation of cyclohexane, adamantane, toluene, benzyl alcohol and *trans*-stilbene by *tert*-butyl hydroperoxide. The complex $Fe_2O(bpy)_4(H_2O)_2(ClO_4)_4$ was the most effective catalyst [175].
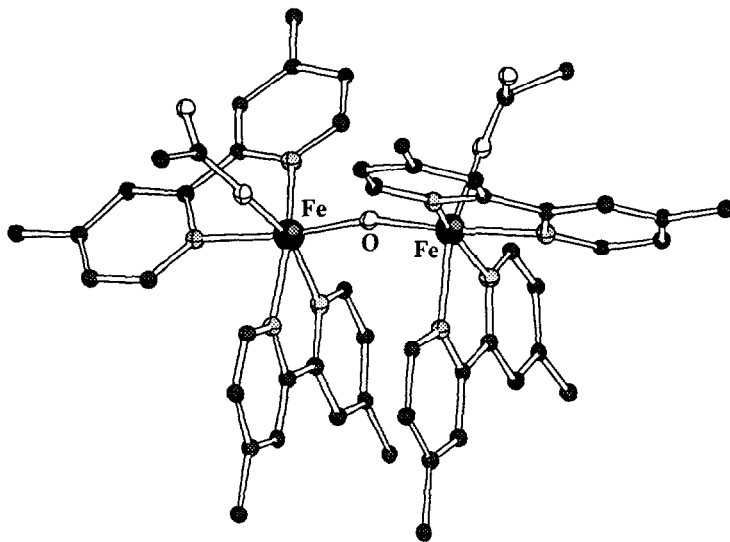
(**236**)
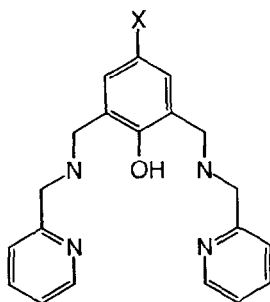
(**237**) (X = Me), (**241**) (X = Cl)

In order to gain insight into the integer-spin EPR signals found in the diferrous forms of diiron-oxo proteins, the following diiron complexes; $[Fe(II)_2(237)\{O_2P(OC_6H_5)_2\}_2]$ X where X = Cl (**238**), BF$_4$ (**239**), BPh$_4$ (**240**) and $[Fe(II)_2(241)\{O_2P(OC_6H_5)_2\}_2]BPh_4$ (**242**), were synthesized. Complexes (**238**)-(**240**) were prepared to incorporate a bridging anion with a larger bite and thus increase the Fe-O-Fe angle. Complex (**242**) was synthesized in order to determine the effects of charging basicity of the μ-peroxo group. Only the structure of (**238**) has been determined. Complexes (**238**)-(**240**) show EPR signals at g = 15 while (**242**) exhibits a low field EPR signal near g = 17 similar to that found for deoxyhemerythrin azide. This resonance originates

from a ground electronic state with integer spin indicating the metal centres are ferromagnetically coupled. The higher field signals of (238)-(240) arise from an excited state, thus the coupling interaction between the iron centres is found to be antiferromagnetic. The substitution of the carboxylic bridge to the phosphate bridge changes the metal-metal interaction from ferromagnetic to antiferromagnetic and it appears that the Fe-O-Fe angle plays an important role [176].
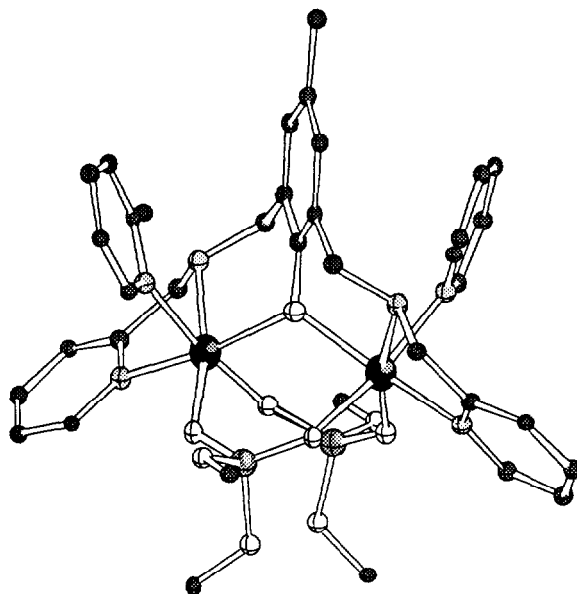
(238)

The new tripodal ligand 3-[*bis*(2-pyridyl-methyl)amino]propionic acid (243) has been synthesized. Reaction of (243) with $Fe(ClO_4)_3 \cdot 6H_2O$ and NEt_3 in methanol/water affords [{Fe(bpp)(H_2O)}$_2$O][ClO$_4$]$_2 \cdot 4H_2O$ (244). The water ligands of (244) may be substituted with (sodium) acetate to form the acetate-bridged complex [{Fe(bpp)}$_2$(MeCO$_2$)O][ClO$_4$]$_2 \cdot 5H_2O$ (245) or phosphates ($O_2P(OPh)_2$, $O_3P(OPh)$) to form the phosphate-bridged equivalents of (245). Variable-temperature magnetic susceptibility measurements on (244) (J = –114 cm^{-1}) and (245) (J = –110 cm^{-1}) show strong antiferromagnetic coupling between the two iron ions [177].
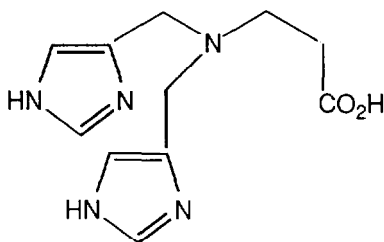
(243)

8.10.2   Heterometallic iron-oxo clusters

A series of new (μ-oxo)diiron(III) complexes of tris(2-pyridylmethyl)amine (TPA), [Fe$_2$O(TPA)$_2$(L)](ClO$_4$)$_2$, (L = sulfate, phosphate, arsenate, vanadate and molybdate) have been synthesized and characterized. The structure of the molybdate complex [Fe$_2$O(TPA)$_2$(MoO$_4$)](ClO$_4$)$_2$ (**246**) has been determined by X-ray crystallography. This complex has the largest Fe$\cdots$Fe separation (3.421Å) of all reported dibridge TPA complexes consistent with the large bite angle of MoO$_4{}^{2-}$. A linear correlation between the Raman ν_s(Fe-O-Fe) mode and the energy of the long-wavelength visible absorption band was seen thus providing a method in which UV-VIS can be used to estimate the Fe-O-Fe angle [178].
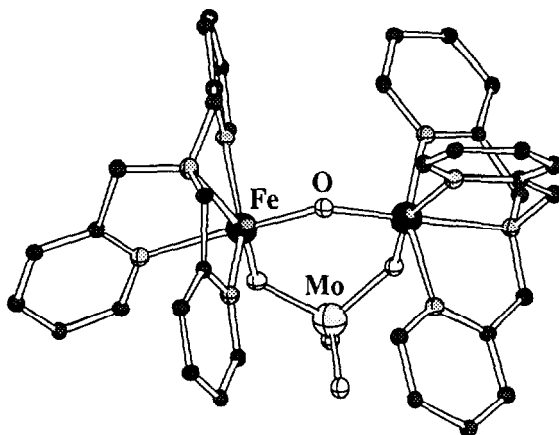
(246)

Inelastic incoherent neutron scattering (IINS) are reported for the complexes [Fe(III)$_2$MO(OOCMe)$_6$(py)$_3$](py) where M = Mn, Ni. The agreement in J values between IINS and bulk magnetic susceptibility studies is better for the Fe$_2$Mn than the Fe$_2$Ni complex. The J values for Fe$_2$Mn are temperature independent while the J values for Fe$_2$Ni are temperature dependent. The agreement between experiment and the Heisenberg-Dirac-Van Vleck spin-coupling model is excellent principally due to the fact that the Fe(III), Mn(II), and Ni(II) centres are orbitally non-degenerate [179].

8.10.3   Polynuclear iron-oxo clusters

The iron-oxo cluster M$_4$[Fe$_6$(μ_3-O)$_2$(μ_2-OH)$_6$(ida)$_6$]·nH$_2$O (I; M = Na, K; H$_2$ida = iminodiacetic acid) have been prepared by the reaction of FeCl$_3$ in H$_2$O with H$_2$ida and MOH. The cluster anion consists of 2 Fe$_3$(μ_3-O)(μ_2-OH) moieties which are connected by 4 OH bridges. The iron atoms are in octahedral environments with the ida$_2$-ligands bonding facially to each Fe atom. There are ten short Fe-Fe distances (<3.7 Å). The room-temperature magnetic moment of 4 μB/Fe atom indicates that antiferromagnetic coupling occurs. There is a sharp rise in magnetic

susceptibility at lower temperatures - it is postulated that this rise is due to inter-trimer ferromagnetic exchange [180].

The tetranuclear μ-oxo, μ-acetato complex $[Fe_4(\mu_3-O)_2(\mu-O_2CCH_3)_6Cl_2(3\text{-Mepy})_4]\cdot MeCN$ (247; 3-Mepy = 3-methylpyridine) has been synthesized and its structure determined by X-ray diffraction. Mössbauer spectroscopy indicates that there are two quadrupole splittings, one for each type of Fe(III) environment. The quadrupole splitting (QS) of 1.04 is assigned to the chloride bridged Fe-atoms, while the non-chloride-bonded Fe atoms have a splitting of 0.67 mm s^{-1} [181].

(247)
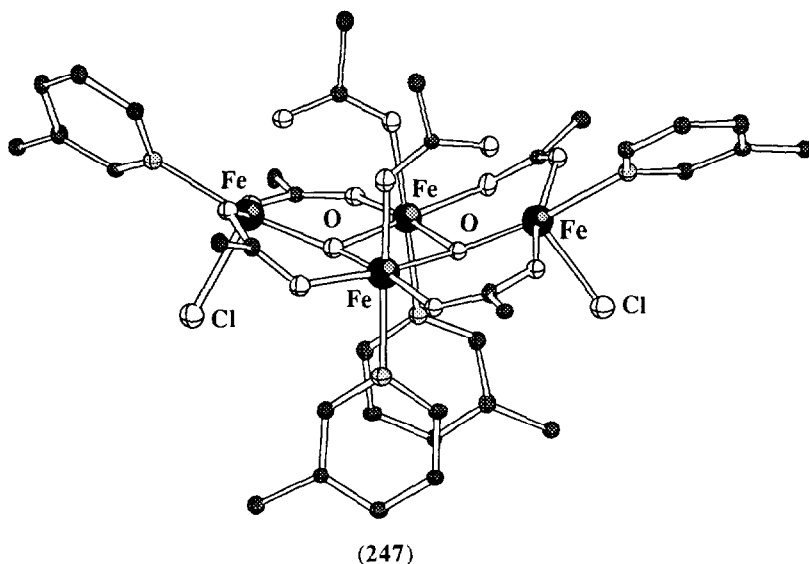
The magnetic properties of $\{[(TACN)_6Fe_8(\mu_3-O)_2(\mu_2-OH)_{12}]Br(H_2O)\}Br\cdot H_2O$, a molecule with eight iron(III) ions bridged by oxo and hydroxo groups, has been reported. The magnetic susceptibility and magnetization indicate that at low temperature spin levels with 8<S<10 are populated. Electron paramagnetic resonance confirms that levels of high spin multiplicity are populated at 4.2 K [182].

(248)
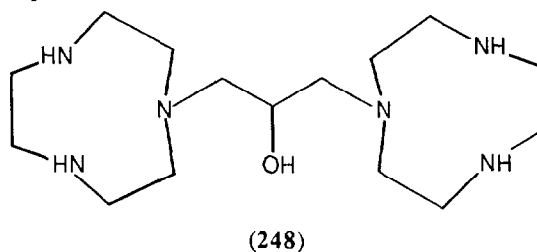
The synthesis and characterization of the new ligand (248), and the tetranuclear iron(III) complex (249) which it stabilizes have been reported. The structure of (249) contains a quadruply-charged tetranuclear iron(III) cation capped by two molecules of dtnp-OH which act as ditopic heptadentate ligands. The Fe$_4$O$_6$ core is composed of a tetrahedron of iron atoms bridged by six

oxygen atoms. The iron atoms are antiferromagnetically coupled with μ_{eff} = 1.81 μ_B/Fe at 300 K and 0.26 μ_B at 40 K. The same Fe(III) complex (249) can be synthesized *via* an Fe(II) source followed by air oxidation [183].
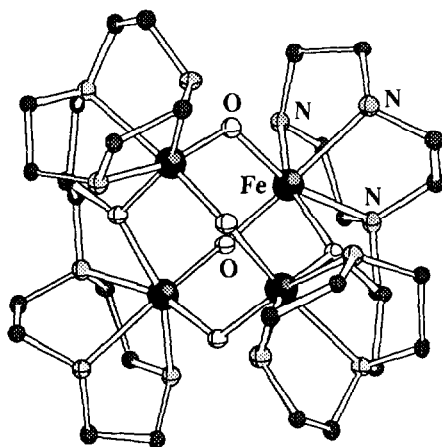
(249)
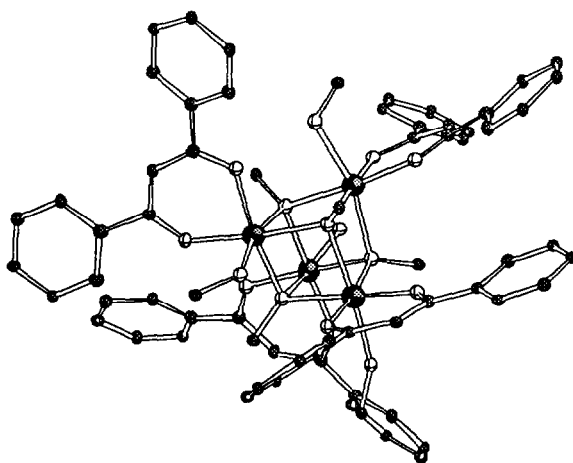
(251)

Three iron complexes with cubic $\{Fe_4(OR)_4\}^{n+}$ cores $[Fe(OMe)(MeOH)(DPM)]_4$ (250), $[Fe(OMe)(MeOH)(DBM)]_4$ (251), $[Fe(III)Fe(II)_3(OMe)_5(MeOH)_3(OBz)_4]$ (252), have been prepared and crystallized (HDPM = dipivaloylmethane, HDBM = dibenzoylmethane). A similar Mn complex has also been reported. The four iron ions and bridging alkoxide ligands are located at alternating vertices of a cube with either alcohol or alkoxide and ß-diketonate or benzoate ligands on the exterior of the core. The molecular symmetry for (250) and (251) is S_4 and is C_2 for (252). The cubes exhibit multiple electronic spectral features giving rise to intense red, blue, and green

colours of (250), (251), (252), respectively. Complexes (251) and (252) display a single quadrupole doublet in their high-temperature Mossbauer spectra with parameters characteristic of high spin iron(III). Magnetic studies suggest that the iron atoms in (250) are ferromagnetically exchange coupled with a coupling constant J = –1.88 cm^{-1}. In contrast, the iron atoms of (252) are antiferromagnetically exchange coupled [184].
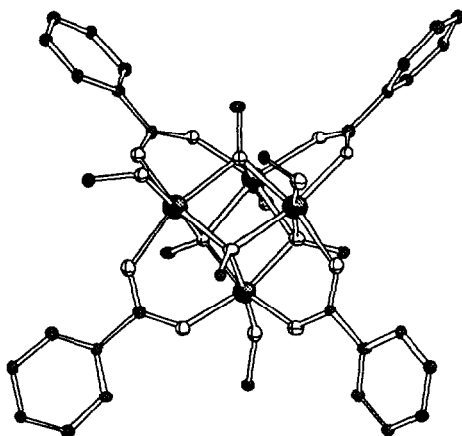
(252)

The synthesis and characterization of two new polyoxo hexanuclear Fe(III) complexes, [Fe$_6$(μ-OH)$_2$(μ_2-OH)$_2$(μ_2-O$_2$CH$_3$)$_{10}$(C$_7$H$_{11}$-O)$_2$]·4CH$_2$Cl$_2$ (253) and [Fe$_6$(μ_3-O)$_2$(C$_6$H$_6$NO)$_8$-Cl$_4$](ClO$_4$)$_2$·4MeCN (254) have been reported in conjunction with a study of spin frustration in hexanuclear ferric complexes. Complex (253) has six high spin Fe(III) ions and can be viewed as two trinuclear μ_3-oxo bridged subunits bridged by two μ_2-hydroxo and μ_2-acetato ligands. Complex (254) can be viewed as two asymmetric triangular Fe$_3$-μ_3-oxo subunits bridged together by alkoxo groups. For (253), the μ_{eff}/molecule was found to be 9.1 μ_B at 300 K and as the temperature decreases this value increases to a maximum of 10.55 μ_B at 30 K whereupon there is a decrease to 9.77 μ_B at 5 K. For (254), μ_{eff}/molecule was found to be 8.82 μ_B at 320 K. Unlike (253), the μ_{eff}/molecule of (254) decreases with decreasing temperature to 6.08 μ_B at 5.01 K. Fitting of variable-field magnetic data shows that (253) has an S$_t$ = 5 ground state. Since pairwise magnetic exchange interactions between high-spin Fe(III) ions are invariably antiferromagnetic, the S$_t$ = 5 ground state results from spin frustration. The spin frustration present in (254) is different than that in (253). Complex (254) has a ground state either with S$_t$ = 3 or a thermal average over several states where the average has an "effective" S$_t$ = 3 [185].

The trinuclear metal complexes [Fe$_3$O(O$_2$CCH$_3$)$_6$L$_3$]$^{n+}$ (L = water or pyridine; n = 0, 1) interact with chiral carboxylic acids, α-amino acids, amino alcohols, epihedrine isomers and polynucleic acids producing optically active substances exhibiting enhancing Cotton effects [186].

8.11   IRON-SULFUR, SELENIUM AND TELLURIUM CLUSTERS

8.11.1   Iron-sulfur cubanes

The new iron-sulfur cubane clusters $[Fe_4S_4(Ap)_4]^{2-}$ and $[Fe_4S_4(Cy)_x(Ap)_{4-x}]^{2-}$ (I; HAp = D-aspartic acid benzyl ester, HCy = L-cysteine Et ester hydrochloride; x = 1, 2, 3) have been prepared and characterized by ^{1}H NMR spectroscopy. The temperature dependence of the isotropically shifted ^{1}H NMR signals of the a-CH and b-CH$_2$ protons was used to distinguish between the bound amino acids. Reaction of $[Fe_4S_4(SBu^t)_4]^{2-}$ with the (tridentate) peptides GCGGCGGCGamide (9-mer-CysH3) (G = glycyl, C = cysteinyl) and GSGGSGGGSGamide (9-mer-SerH3) (S = serinyl) resulted in the formation of site-differentiated $[Fe_4S_4(9-mer-Cys)(SCMe_3)]^{2-}$ and $[Fe_4S_4(9-mer-Ser)(SCMe_3)]^{2-}$. Exchange of the remaining coordinated thiolate enabled substitution of other amino acids (Cys, Asp, Tyr) at the differentiated site [187].

The nucleophilic sulfur atoms of the disulfur ligands in $Fe_4S_6(C_5H_4R)_4$ (R = H, Me) easily undergo electrophilic addition of an alkyl group to produce the cluster compounds $[Fe_4(\mu_3-S)((\mu_3-S_2)-CH_2-(\mu_3-S_2))-(C_5H_4R)_4]^{2+}(FeCl_4)^{2-}$. The X-ray structure of the latter for R = Me shows that a CH$_2$ bridge is present between the sulfur atoms of each of the disulfido ligands. The structure of this new iron-sulfur cluster differs from the parent compound in that only the S-S distances increase from 2.04 to 2.19Å [170].

The cubane cluster $[Fe_4S_4(SAd)_4]^{2-}$ (Sad = adamantanethiolate) exhibits two stable redox couples in dry dmf, $[Fe_4S_4(SAd)_4]^{2-/3-}$ and $[Fe_4S_4(SAd)_4]^{-/2-}$. The oxidized form, $[Fe_4S_4(SAd)_4]^-$, is a model for the oxidized form of high-potential iron proteins. It is susceptible to hydrolysis, but attack by water may be suppressed by the addition of free adamantanethiol in H$_2$O/dmf or solubilization in aqueous poly[(2-dimethylamino)hexanamide] (PDAH) [188].

The kinetics of the acid-catalyzed substitution of the first thiolate ligand of $[Fe_4S_4(SR)_4]^{n-}$ (R = Ph, n = 2,3; R = Et, Bu^t, n = 2) in MeCN has been studied by stopped-flow spectrophotometry. The acid used was $[NHEt_3]^+$ and the thiolate nucleophiles were used as their tetraethylammonium salts. The substitutions are dissociative and the rate of substitution is not rate-limited by protonation. The mechanism is consistent with that shown in Scheme 6. The lability of the protonated clusters falls in the sequence $[Fe_4S_4(SEt)_4]^{2-} > [Fe_4S_4(SBu^t)_4]^{2-} \approx [Fe_4S_4(SPh)_4]^{3-} > [Fe_4S_4(SPh)_4]^{2-}$ while for the unprotonated clusters, the sequence is $[Fe_4S_4(SPh)_4]^{2-} = [Fe_4S_4(SPh)_4]^{3-} >> [Fe_4S_4(SR)_4]^{2-}$ (R = alkyl). The fact that other ligands may function as competitive inhibitors has been used to monitor the transient binding of the potential ligands Cl$^-$, Br$^-$, N$_3^-$, CN$^-$, N$_2$O, CO, C$_2$H$_2$, PhCCH, C$_2$H$_4$, N$_2$ and H$_2$ to $[Fe_4S_4(SR)_4]^{2-}$ (R = Et, Ph). Transient coordination to $[Fe_4S_4(SEt)_4]^{2-}$ is observed for Cl$^-$, Br$^-$, N$_3^-$, CN$^-$, N$_2$O and CO but no coordination could be observed for $[Fe_4S_4(SPh)_4]^{2-}$ [189].

The stepwise ligand substitution on 4Fe-4S clusters in dmso using NaCp or LiFlu (Flu = fluorenide) has been monitored by NMR and UV-VIS spectroscopies. Addition of NaCp (or LiFlu) results in the release of an equimolar amount of PhS- to form a reactive intermediate which is postulated to be $[Fe_4S_4(SPh)_3(Cp)]^{2-}$ or $[[Fe_4S_4(SPh)_3]_2O]^{4-}$. Reaction of $(Et_4N)_2[Fe_4S_4(SPh)_4]$ with NaCp or LiFlu, MeI, and RSH (R = Et, Me$_3$C) in thf gave $[Fe_4S_4(SPh)_{4-x}(SR)_x]^{2-}$ (R = Bu^t, x = 1; R = Et, x = 1, 2, 4) [190].

$Fe_3Fe\text{-}SR^{2-}$

$$L \updownarrow\ K_L$$

$$[NHEt_3]^+$$

$Fe_3Fe\text{-}SR^{2-} \underset{K_1}{\rightleftharpoons} Fe_3Fe\text{-}SR^- \xrightarrow[slow]{k_2} Fe_3Fe^- \xrightarrow[fast]{R'S^-} Fe_3Fe\text{-}SR'^{\,2-}$$

$$K_3 \updownarrow\ R'S^-$$

$Fe_3Fe\text{-}SR'^{\,2-}$
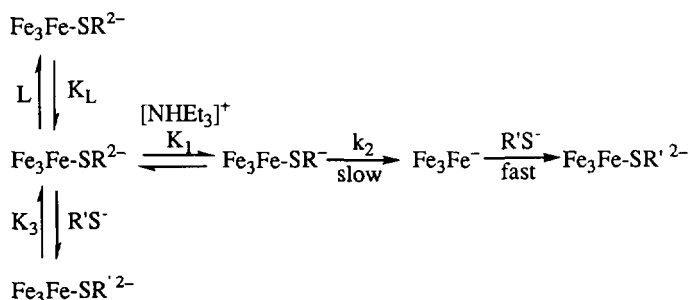
Scheme 6

The equilibria and kinetics of the reversible binding of 1-hydroxy-ethane-2-thiolate at oxidized and reduced forms of the transformed [4Fe-4S] cluster in Fd III are reported. Under fast scan conditions, the thiolate-ligated species appears as a trapped redox couple with $E^{\circ\prime} = -585$ mV, whereas at slow scan rates the equilibrium is established at all times and the reduction potential of the couple depends on the thiolate concentration. An associative mechanism is proposed involving nucleophilic attack by the thiolate at the labile Fe subsite [191].

The iron-ligated cysteines of oxidized HiPIP II from *Ectothiorhodospira halophila* have been assigned by ^{1}H NOE, NOESY and TOCSY NMR measurements. As in the *Chromatium vinosum* and *Rhodocyclus gelatinosus* systems, the cluster can be described as two iron(III) and two mixed valence ions, but in the *Ectothiorhodospira halophila* system the two pairs are oriented in a different way within the protein frame. The overall reduction potential of the Fe-S cluster of these proteins is retained rather than the oxidation numbers inside the cluster itself. It seems that the overall redox potential is determined by the hydrogen bonds and by the electrostatic potential of each protein atom [192].

The substitution of selenium for sulfur in the [4Fe-4S] core of the high potential iron protein (HiPIP) from *Chromatium vinosum* and HiPIP II from *Ectothiorhodospiza halophila* did not produce significant changes in the electronic structure of the core. EPR spectra showed only a small increase in anisotropy and average g-values. The lack of significant change from the Se substitution suggests that the valence distributions in various HiPIPs are structural properties imposed by the protein matrices and not properties of the cubanes [193].

A spin density analysis which emphasizes the significance of the local terms of the spin Hamiltonian description of exchange-coupled systems has been developed. The method is based on theoretical determination of local spin densities and their calibration to appropriate monomeric complexes. When this analysis is applied to the spin densities calculated for $[Fe_2S_2(SH_4)]^{2-}$ and $[Fe_2S_2(SH_4)]^{3-}$, it appears that local spin densities differ from those calculated for the $[Fe(SCH_3)_4]^-$ and $[Fe(SCH_3)_4]^{2-}$ monomers. The spin densities on the iron atoms are smaller in the dinuclear systems. The results are fully consistent with the spectroscopic characteristics of these centres in proteins [194]. Using an effective-Hamiltonian approach, the electronic properties of mixed valent iron-sulfur clusters have been analyzed taking into account the effects of double exchange, vibronic coupling, and antiferromagnetic exchange. The basic mechanism behind partial electron delocalization in trinuclear clusters due to double exchange and vibronic coupling is

illustrated using the simple d^1-d^1-d^2 mixed valence cluster with one excess electron and S=1/2 paramagnetic core spins. This model is extended to the electronic configuration d^5-d^5-d^6 which is characteristic for $[Fe_3S_4]^0$ clusters. Magnetic hyperfine parameters of *FdII* are also analyzed within the model [195].

The hyperfine tensors of the protons of CH_2 groups in a paramagnetic $[Fe_4S_4]^{3+}$ species called "centre IV", created by gamma irradiation in single crystals of the synthetic model compound $\{N(C_2D_5)\}_2[Fe_4S_4(SCH_2C_6D_5)_4]$, have been measured by ENDOR spectroscopy. From the anisotropic analysis of the tensors, it is found that the paramagnetic centre is close to the $|7/2,3,1/2\rangle$ state, the first number representing the spin state of the mixed-valence pair, the second the spin state of the ferric pair and the third the resulting spin of the cluster [196].

The iron-sulfur clusters $[Fe_4S_4X_4]^{2-}$ (X = Cl, SPh, SCH_2Ph, SEt, SBu^t), $[Fe_2S_2Cl_4]^{2-}$ and $[Fe_6S_6Cl_6]^{3-}$ have been coordinated to polypyrrole alkylammonium)-modified electrodes. The incorporation of the clusters in the polymer films was established by cyclic voltammetry and reflectance FTIR spectroscopy. The existence of the electroreduced $[Fe_4S_4(SPh)_4]^{2-}$ cluster was confirmed by low-temperature EPR spectroscopy [197].

The reaction of $(Bu_4N)_2[Fe_4S_4(255)(SEt)]$ with H_2S in CH_2Cl_2 produces a hydrosulfide cluster $[Fe_4S_4(255)SH]^{2-}$ (256) and an μ-sulfido double cubane species $[\{Fe_4S_4(255)\}_2S]^{4-}$. When (256) is reacted with Fe(III) porphyrins, Fe_4S_4-sulfide heme assemblies are produced. Various Fe(III)(OEP) complexes were reacted with (256) and all produced the identical product $[Fe_4S_4(LS_3)-S-Fe(OEP)]^{2-}$ (257). The isotropic shifts suggest that (257) is a sulfide-bridged assembly in which the five-coordinate high spin Fe(III) and the cluster are electronically coupled as there is increased unpaired spin density in the Fe_4S_4 component [198].
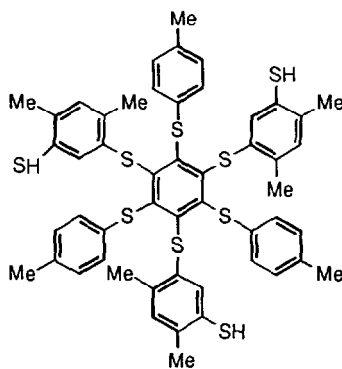
(255)

The iron-tellurium clusters $[Fe_4Te_4(SPr^i)_4]^{2-/3-}$ have been synthesized and structurally characterized by X-ray crystallography. The reduced cluster has significantly longer Fe-Fe and Fe-S bonds [199].
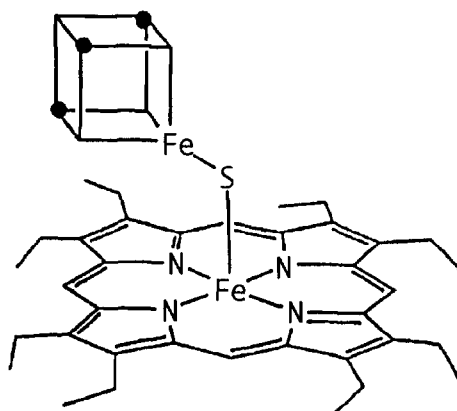
(256)

8.11.2   Heterometallic iron-sulfur clusters

Reaction of the basket cluster [Fe$_6$S$_6$(PMePh$_2$)$_4$I$_2$] with two equivalents of [RuI$_2$(MeCN)$_4$] affords the new cluster [(MeCN)$_4$(Ph$_2$MePS)Ru-Fe$_8$S$_6$I$_8$-Ru(SPMePh$_2$)(MeCN)$_4$] whose structure has been determined by X-ray crystallography. The cluster consists of a [Fe$_8$S$_6$I$_8$]$^{4-}$ unit which bridges two [Ru(SPMePh$_2$)(MeCN)$_4$]$^{2+}$ units via μ$_5$-sulfides [200].

The first example of MoFe$_3$S$_4$ cubane clusters with carboxylate ligands coordinated to the Mo atom have been synthesized and characterized. The reaction of [MoFe$_3$S$_4$Cl$_3$(Cl$_4$cat)(L)]$^{2-}$ (258) (where L = CH$_3$CN, dmf, dmso) with anhydrous oxalic acid affords a μ-oxalate-bridged double cubane, {[MoFe$_3$S$_4$Cl$_4$]$_2$(μ-C$_2$O$_4$)}$^{4-}$ (259). The reaction of (259) with one equivalent of (Et$_4$N)$_2$(C$_2$O$_4$) in CH$_3$CN affords the single cubane (Et$_4$N)$_3$[MoFe$_3$S$_4$Cl$_4$(μ-C$_2$O$_4$)] (260). Cluster (259) is EPR active indicating that the C$_2$O$_4^{2-}$ bridge does not permit strong electronic coupling between the cubane subunits. Reactions of (258) with citric acid, R-citramalic acid and citrate have afforded clusters whose analytical and spectroscopic data suggest that they are analogous to (259) and (260) [201].

The Fe K-edge EXAFS has been investigated for reduced and oxidized Mo-Fe and V-Fe protein samples from *Azotobacter Vinelandii*. For the dithionite-reduced Mo-Fe protein, the EXAFS is dominated by Fe-S and Fe-Fe interactions at 2.32 and 2.64 Å. An Fe-Mo interaction is apparent at 2.71Å. A longer Fe-Fe interaction at 3.8 and an Fe-S distance at 4.3 Å are also observed. A similar pattern is observed for the V-Fe reduced protein. In both the Mo-Fe and V-Fe proteins, the first coordination sphere Fe-S distances contract slightly upon thionine oxidation [202].

(259)
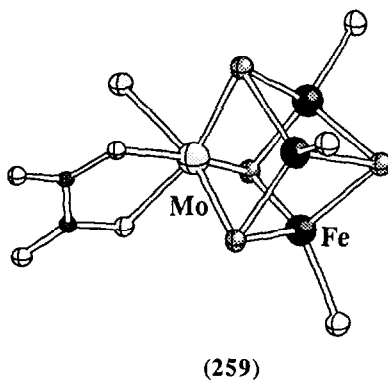
The uncharged clusters $MFe_4S_6(PEt_3)_4Cl$ (M = V, Mo) have been synthesized and characterized by ^1H NMR, mass spectrometry, and x-ray crystallography. The $MoFe_4S_6(PEt_3)_4Cl$ (261) and $VFe_4S_6(PEt_3)_4Cl$ (262) complexes are isostructural and present a new type of cluster architecture where a cuboidal Fe_4S_3 fragment is bridged by three μ_2-S atoms to a $MPEt_3$ unit whose M-P bond is coincident with an imposed C_3 axis. The Mo and Fe EXAFS spectra of (261) have been measured and analyzed by the GNXAS method; first coordination shell distances were determined with high accuracy. The clusters $MFe_4S_6(PEt_3)_4Cl$ (M = Mo, V) contain a subunit of 10 atoms $(Fe_4S_4(\mu_2$-$S)_3)$ with a core bond connectivity and spatial disposition analogous to the Kim-Rees FeMo cofactor model [203].
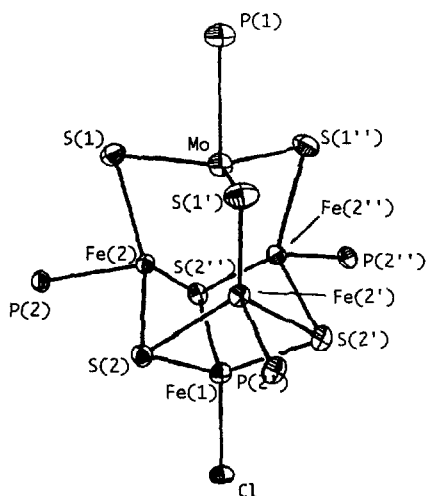
The metal-sulfur-phosphorus framework of (261)

The mixed-metal clusters $[(VFe_3S_4(SEt)_3)_2(\mu$-$SEt)_3]^{3-}$ (263), $[(NbFe_3S_4(SEt)_3)_2(\mu$-$SEt)_3]^{3-}$ and $[(NbFe_3S_4(SEt)_3)_2(\mu$-$SEt)_3]^{5-}$ have been synthesized. A structure determination of 263 reveals that the cluster anion has an imposed D_{3h} symmetry and the V···V distance is 3.601 Å. These clusters, together with those previously reported, form a set $[M_2Fe_6S_8(SEt)_9]^{3-}$ whose

members (M = V, Nb, Mo, W, Re) possess the same charge, identical ligands and congruent structures. Redox potentials for the reversible couples $[M_2Fe_6S_8(SEt)_9]^{3-/4-}$ and $[M_2Fe_6S_8(SEt)_9]^{4-/5-}$ decrease in the order M = V > Nb > Mo > W > Re and parallel the trend in ^{57}Fe isomer shifts - M = V < Nb ≈ Mo < W ≈ Re [204].

Reduction of hydrazine to ammonia was observed when the single cubanes $[(Cl_4cat)MoFe_3S_4Cl_3(CH_3CN)]^{2-}$ (**264**) and $[(citr)MoFe_3S_4Cl_3]^{3-}$ were used as catalysts. Only low concentrations of ammonia were observed when $\{[(Cl_4cat)MoFe_3S_4Cl_3]_2(N_2H_4)\}^{4-}$ was used and $[(Cl_4cat)MoFe_3S_4Cl_2]_2-(\mu-N_2H_4)(\mu-S)]^{4-}$ did not promote the reduction. EPR spectra of reaction solutions are identical to those obtained from solutions of the pure catalyst prior to catalysis and show the $MoFe_3S_4$ core retains integrity. Absence of NH_3 production in attempts using $[(Cl_4cat)MoFe_3S_4Cl_2]_2-(\mu-N_2H_4)(\mu-S)\}^{4-}$ indicate that the hydrazine molecule is activated by coordination to one $MoFe_3S_4$ cubane. Stoichiometric and catalytic reductions of the terminally coordinated phenylhydrazine in $[(Cl_4cat)MoFe_3S_4Cl_3(PhN_2H_3)]^{2-}$ (**265**), which result in the formation of ammonia and aniline, have also been carried out [205].
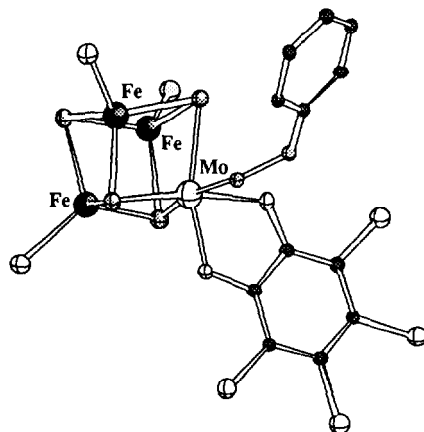
(265)
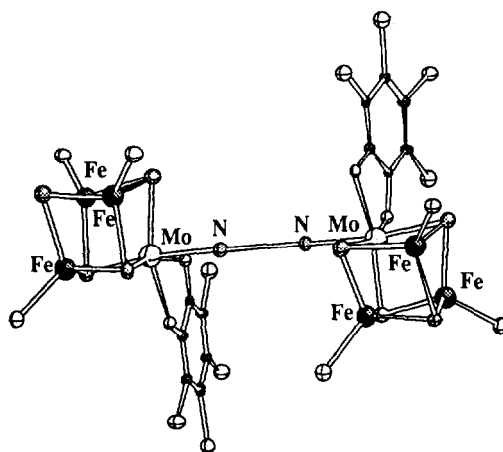
(266)

It was found that the reaction of (264) with anhydrous hydrazine or pyrazine produces the singly bridged double cubanes $(Et_4N)_4[(Cl_4cat)MoFe_3S_4Cl_3]_2(\mu$-L) L = N_2H_4 (266) or $C_4H_4N_2$ (267). The synthesis of (266) can also be achieved by the chemical oxidation of $(Et_4N)_4[(Cl_4cat)MoFe_3S_4Cl_2]_2(\mu$-S)($\mu$-$N_2H_4$) with two equivalents of $Fe(Cp)_2(PF_6)$. The X-ray structures of both complexes are reported. The intramolecular Mo-Mo distance in (266) is 5.41Å. In (267) the pyrazine ring is nearly orthogonal to the Mo-Fe-S-S plane in one of the two subunits and the intramolecular Mo-Mo distance is 7.46 Å [206].

The oxidative degradation of the $MoFe_3S_4$ structural units in the doubly-bridged double cubane $[(MoFe_3S_4Cl_2(Cl_4Cat)]_2(\mu_2$-S)($\mu_2$-$NH_2OH)]^{4-}$ leads to the formation of the hetero-dinuclear thiomolybdate complexes $[(Cl_4Cat)$-Mo(O)(μ-S)$_2FeCl_2]^{2-}$ (268) and $[(S)Mo(O)(\mu$-S)$_2FeCl_2]^-$ (269) are observed. The structure of (268) has been determined and a predominant feature is the $Fe(\mu$-S)$_2Mo$ rhombic unit which is common for Fe-MoS_4 complexes. Unlike the Fe-MoS_4 complexes, the formal oxidation state of the Fe is very close to +3, thus fixing the Mo oxidation state at +5. The second degradation product is a double salt of $(Et_4N)_2FeCl_4$ and (269) [207].
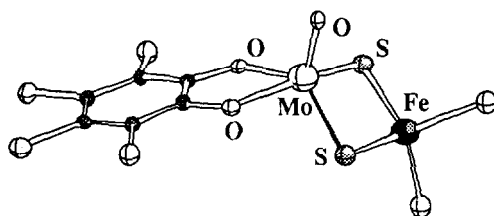
(268)

Incubation of Fe_3S_4 ferredoxin from *Pyrococcus furiosus* with Zn^{2+} or Ni^{2+} yields the mixed-metal clusters $[ZnFe_3S_4]^+$ and $[NiFe_3S_4]^+$. These clusters along with $[Fe_3S_4]^0$ and $[NiFe_3S_4]^+$ complexed with CN^- were analyzed by Mössbauer spectroscopy. In $[Fe_3S_4]^0$, two sites form a delocalized $Fe^{3+}\cdot Fe^{2+}$ pair while the third site has a localized Fe^{3+} valence state. Upon incorporation of a divalent heterometal, the Fe_3S_4 fragment can accommodate one additional electron leading to a localized Fe^{2+} site in the $[ZnFe_3S_4]^+$ (cluster spin S = 5/2) ferredoxin. In contrast, the S = 3/2 states of Ni and its CN^- complex lack a localized Fe^{2+} site. The three Fe sites display the same quadrupole splittings and isomer shifts. Isomer shift data suggest a shift of d-electron density from the Fe_3S_4 core fragment to the Ni site [208].

8.11.3 Other iron-sulfur clusters

Laser (1064 nm) ablation of FeS and $KFeS_2$ yields 45 gaseous $[Fe_xS_y]^-$ ions detected and characterized by FTICR mass spectrometry and these ions are distributed in two distinct regions of the x/y composition map. Series 1 is a linear progression of triplets of ions with the composition of $[Fe_nS_{n-1}]^-$, and $[Fe_nS_n]^-$, and $[Fe_nS_{n+1}]^-$ for n = 3-10 while ions in series 2 contain an additional S_5, $[Fe_nS_{n+5}]^-$ and $[Fe_nS_{n+6}]^-$ for n = 1-7. Ions in series 1 are probably globular clusters while

series 2 ions contain an additional chelating polysulfide ligand or could contain a structural principle of extended chains of ribbons of linked tetrahedra [209].

It is reported that the reduction of $Fe_2(NO)_4(\mu\text{-SR})_2$ (R = Me, Et, But) by MBR_3H (M = Li, Na or K; R = Et or ^sBu) affords different products dependent on the amount of reducing equivalents used. It is proposed that the product formed when one equivalent is used is $[HFe_2(NO)_4(\mu\text{-SR})_2]^-$ while the use of two equivalents leads to the formation of $[Fe_2(NO)_4(\mu\text{-SR})_2]^{2-}$ [210].

Reaction of $[Fe_4S_4(NO)_4]$ with four equivalents of triphenylphosphine in refluxing dichloromethane results in the formation of the cuboidal cluster $[Fe_4S_3(NO)_4(PPh_3)_3]$ **(270)** and one equivalent of triphenylphosphine sulfide. Cluster **(270)** may be oxidized by $NOPF_6$ or I_2. The distances between the three basal Fe atoms decrease by 7-19 pm upon oxidation. Reaction of **(270)** with excess triphenylphosphine results in the formation of $[Fe_6S_6(NO)_6]^-$ **(271)**. Cluster **(271)** exhibits four sequential reversible reductions in the interval –0.7 to –1.7 V as well as a quasi-reversible oxidation step near 0 V.

It has been shown that the magnitude of the M-S-M angle in polynuclear complexes with thiolate bridges can be modulated by ligand nucleophilicities. The synthesis and characterization of a homoleptic iron complex with 2-propanethiolate ligands $[Fe_2(SC_3H_7)_6]^{2-}$ **(272)** and a compound with tetrahedral MS_4 coordination and three thiolate bridges, $[Fe_2(SC_4H_9)_5]^-$ **(273)** were reported. The structure of **(272)** consists of two FeS_4 tetrahedra which share a common edge and is closely related with the analogous ethanethiolate complex. When the isopropyl residues are replaced by t-butyl groups, the two FeS_4 tetrahedra share a common face resulting in three thiolate bridges [211].

A variable temperature proton NMR spectroscopic investigation of the electronic structure of the trinuclear iron cluster of the oxidized *Desulforvibrio gigas* Ferredoxin II is reported. On the basis of nuclear Overhauser effect and relaxation measurements, the two most downfield-shifted signals are assigned to a pair of ß-CH_2 protons of one of the cysteinyl residues coordinated to the [3Fe-4S] cluster. These two most downfield shifted signals show Curie type temperature dependence while all others show anti-Curie temperature dependence. Using a Heisenberg-Dirac-Van Vleck spin coupling model, it is found that the observed different types of temperature dependence can be explained by the presence of different exchange coupling interactions between the three iron sites. The ß-CH_2 protons of the cysteine ligated to one iron site show Curie behaviour while protons of cysteines bound to the other two iron sites show anti-Curie behaviour [212].

(273)   (275)
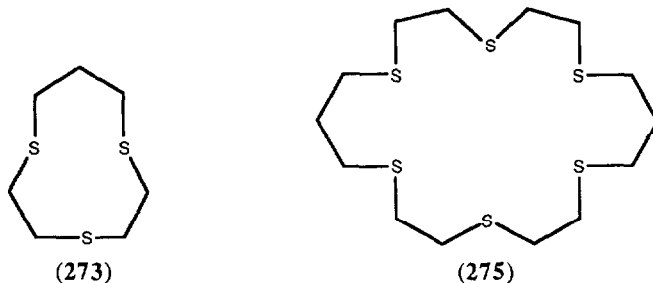
The structures of a *meso* stereoisomer of $[Fe(273)_2](ClO_4)_2$ **(274)** and of $[Fe(275)](ClO_4)_2$ **(276)** have been reported. The iron(II) complexes are low spin and the ligands

function as strong-field ligands. In the *meso*-(274) complex the iron ion is located at a crystallographic inversion centre and the two six membered chelate rings are in an *anti* or *trans* relationship, not a *gauche* relationship as in a previously reported stereoisomer. The (275) ligand complexes with iron(II) to form exclusively the *cis* facial diastereoisomer. The synthesis, and characterization by ^{13}C NMR spectroscopy, of a third iron(II) complex with the ligand 18-crown-6 are also reported [213].

(274)   (276)
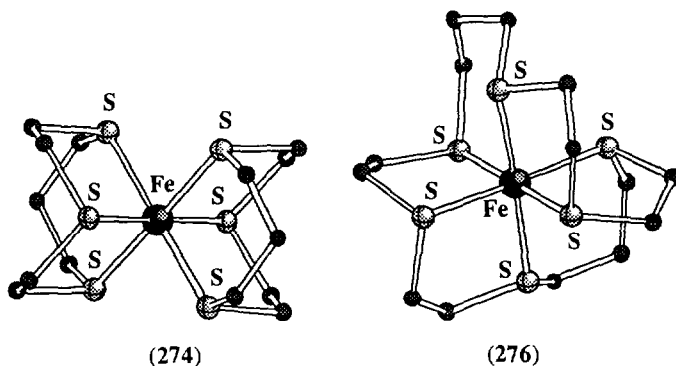
The metathesis reaction of $FeCl_2(dmpe)_2$ with $[(thf)_2LiTeSi(SiMe_3)_3]_2$ yields $Fe[TeSi(SiMe_3)_3]Cl(dmpe)_2$ (277). The tellurolysis $Fe[N(SiMe_3)_2]_2$ with $HTeSi(SiMe_3)_3$ in the presence of a Lewis base (dmpe) yields $Fe[TeSi(SiMe_3)_3]_2(dmpe)_2$ (278). In (278), the iron is coordinated by two *trans* tellurolates and two dmpe ligands. The Fe-Te bond length is 2.723Å. In the related structure of (277), the Fe-Te bond is shorter (2.682Å) than found in the *bis*-tellurolate but longer than previously reported Fe-Te bond lengths (2.536-2.646Å) [214].

(277)
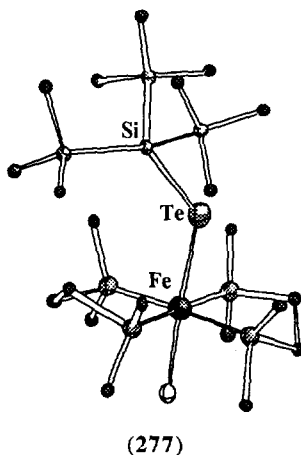
REFERENCES

1.   A. Hills, D. L. Hughes, M. Jimenez-Tenorio, G. J. Leigh and A. T. Rowley, *J. Chem. Soc., Dalton Trans.*, 20 (1993) 3041.
2.   U. Calov, R. Seydel, K. H. Jost, R. Hedel and G. Reck, *Z. Anorg. Allg. Chem.*, 619 (1993) 1939.

3. G. Decap, R. Retoux and Y. Calage, *Z. Anorg. Allg. Chem.*, 619 (1993) 1850.
4. I. Fábián and R. van Eldik, *Inorg. Chem.*, 32 (1993) 3339.
5. T. Hirao, M. Higuchi, I. Ikeda, Y. Ohshiro, *J. Chem. Soc., Chem. Commun.*, (1993) 194.
6. R. C. Dunbar *et al.*, *J. Am. Chem. Soc.*, 115 (1993) 12477.
7. T. Koerner and H. Sabrowsky, *Z. Anorg. Allg. Chem.*, 619 (1993) 1231.
8. D. A. Foucher, D. H. Macartney, L. J. Warrack and J. P. Wilson, *Inorg. Chem.*, 32 (1993) 3425.
9. M. E. Shortreed, S. R. Wylie and D. H. Macartney, *Inorg. Chem.*, 32 (1993) 1824.
10. R. S. Wylie and D. H. Macartney, *Inorg. Chem.*, 32 (1993) 1830.
11. S. Dasgupta, E. Vallazza and R. Schmid, *J. Chem. Soc., Dalton Trans.*, 15 (1993) 2387.
12. K. Ozutsumi, E. Hasegawa, M. Kurihara and T. Kawashima, *Polyhedron*, 12 (1993) 2185.
13. S. Alshehri, J. Burgess and C. D. Hubbard, *Transition Met. Chem. (London)*, 18 (1993) 228.
14. P. Bonhote, M. Ferigo, E. H. Stoeckli and W. Marty, *Acta Crystallogr., Sect. C: Cryst. Struct. Commun.*, 49 (1993) 2102.
15. F. Armand, H. Sakuragi and K. Tokumaru, *New J. Chem.*, 17 (1993) 351.
16. M. Ray, R. Mukherjee, J. F. Richardson and R. M. Buchanan, *J. Chem. Soc., Dalton Trans.*, 16 (1993) 2451.
17. J. K. McCusker, H. Toftlund, A. L. Rheingold and D. N. Hendrickson, *J. Am. Chem. Soc.*, 115 (1993) 1797.
18. J. K. McCusker *et al.*, *J. Am. Chem. Soc.*, 115 (1993) 298.
19. M. V. Twigg, *Transition Met. Chem. (London)*, 18 (1993) 175.
20. Y. Zang, T. E. Elgran, Y. Dong and L. Que Jr., *J. Am. Chem. Soc.*, 115 (1993) 811.
21. K. Sriramam, B. S. R. Sarma, K. Kalidas, J. Sreelakshmi and C. Ramakrishna, *Transition Met. Chem. (London)*, 18 (1993) 231.
22. T. Granier, B. Gallois, J. Gaultier, J.-A. Real and J. Zarembowitch, *Inorg. Chem.*, 32 (1993) 5305.
23. S. Christie, S. Subramanian, L. Wang and M. Zaworotko, *Inorg. Chem.*, 32 (1993) 5415.
24. G. J. Long, F. Grandjean and S. Trofimenko, *Inorg. Chem.*, 32 (1993) 1055.
25. J. J. McGarvey, H. Toftlund, A. H. R. Al-Olbaidi, K. P. Taylor and S. E. J. Bell, *Inorg. Chem.*, 32 (1993) 2469.
26. A. Gulino, E. Ciliberto, S. Di Bella and I. Fragalà, *Inorg. Chem.*, 32 (1993) 3759.
27. C. G. Bochet, C. Piguet and A. F. Williams, *Helv. Chim. Acta*, 76 (1993) 372.
28. S. Mahapatra and R. N. Mukherjee, *Polyhedron*, 12 (1993) 1603.
29. E. Andres, G. De Munno, M. Julve, J. A. Real and F. Lloret, *J. Chem. Soc., Dalton Trans.*, 14 (1993) 2169.
30. R. J. Guajardo, S. E. Hudson, S. J. Brown and P. K. Mascharak, *J. Am. Chem. Soc.*, 115 (1993) 7971.
31. C. M. Mikulski, Y. Nujoma, R. J. Luckenbill and N. M. Karayannis, *Transition Met. Chem. (London)*, 18 (1993) 118.
32. J. Kröber, E. Codjovi, O. Kahn, F. Grolière and C. Jay, *J. Am. Chem. Soc.*, 115 (1993) 9810.
33. K. K. M. Yusuff and A. R. Karthikeyan, *Transition Met. Chem. (London)*, 18 (1993) 435.
34. P. Chaudhuri *et al.*, *Inorg. Chim. Acta*, 212 (1993) 241.
35. K. L. Bieda, A. L. Kranitz and J. J. Grzybowski, *Inorg. Chem.*, 32 (1993) 4209.
36. J. J. Grzybowski *et al.*, *Inorg. Chem.*, 32 (1993) 5266.
37. V. Manivannan, S. Dutta, P. Basu and A. Chakravorty, *Inorg. Chem.*, 32 (1993) 4807.
38. V. E. Zavodnik, V. K. Belsky, Y. Z. Voloshin and O. A. Varzatskii, *J. Coord. Chem.*, 28 (1993) 97.
39. D. V. Stynes, D. B. Leznoff and D. G. A. Harshani de Silva, *Inorg. Chem.*, 32 (1993) 3989.
40. G. A. Impey and D. V. Stynes, *J. Am. Chem. Soc.*, 115 (1993) 7868.
41. S. Subramanian and M. J. Zaworotko, *Can. J. Chem.*, 71 (1993) 433.
42. N. M. Levy, E. Stadler, A. S. Mangrich, M. A. C. Melo and V. Drago, *Transition Met. Chem. (London)*, 18 (1993) 613.
43. R. J. Motekaitis, W. B. Utley and A. E. Martell, *Inorg. Chim. Acta*, 212 (1993) 15.
44. D. Hanke *et al.*, *Inorg. Chem.*, 32 (1993) 4300.
45. K. L. Kostka *et al.*, *J. Am. Chem. Soc.*, 115 (1993) 6746.
46. N. F. Curtis and D. C. Weatherburn, *Inorg. Chem.*, 32 (1993) 5838.
47. R. D. Bach, M.-D. Su, J. L. Andrés and H. B. Schlegel, *J. Am. Chem. Soc.*, 115 (1993) 8763.
48. J. V. B. Oriedo and D. H. Russell, *J. Am. Chem. Soc.*, 115 (1993) 8376.
49. A. Sauer-Masarwa, N. Herron, C. M. Fendrick and D. H. Busch, *Inorg. Chem.*, 32 (1993) 1086.

50. L. D. Dickerson, M. A. Sauer, N. Herron, C. M. Fendrick and D. H. Busch, *J. Am. Chem. Soc.*, 115 (1993) 3623.
51. M. Masarwa, M. A. Sauer, N. Ye and D. H. Busch, *J. Coord. Chem.*, 28 (1993) 355.
52. T. Nyokong, *J. Chem. Soc., Dalton Trans.*, 23 (1993) 3601.
53. H. Grennberg and J. E. Bäckvall, *Acta Chem. Scand.*, 47 (1993) 506.
54. M. Hoshino, K. Ozawa, H. Seki and P. C. Ford, *J. Am. Chem. Soc.*, 155 (1993) 9568.
55. S. Tollari, D. Vergani, S. Banfi and F. Porta, *J. Chem. Soc., Chem. Commun.*, 5 (1993) 442.
56. M. F. Isaac *et al.*, *Inorg. Chem.*, 32 (1993) 4030.
57. T. Yoshimura, H. Kamada, H. Toi, S. Inaba and H. Ogoshi, *Inorg. Chim. Acta*, 208 (1993) 9.
58. K. Woo and D. A. Sweigart, *Inorg. Chem.*, 32 (1993) 4979.
59. A. L. Balch, G. L. Latos, B. C. Noll and S. L. Phillips, *Inorg. Chem.*, 32 (1993) 1124.
60. T. Ogura *et al.*, *J. Am. Chem. Soc.*, 115 (1993) 8527.
61. T. Higuchi, K. Shimada, N. Maruyama and M. Hirobe, *J. Am. Chem. Soc.*, 115 (1993) 7551.
62. G. G. Haraldsson, J. E. Baldwin, J. G. Jones and J. Debernardis, *Polyhedron*, 12 (1993) 2453.
63. E. Tsuchida, T. Komatsu, K. Arai and H. Nishide, *J. Chem. Soc., Dalton Trans.*, (1993).
64. T. Komatsu, K. Nakao, H. Nishide and E. Tsuchida, *J. Chem. Soc., Chem. Commun.* (1993).
65. E. Tsuchida, T. Komatsu, K. Arai and H. Nishide, *J. Chem. Soc., Chem Commun.*, (1993) 730.
66. W. Nam and J. S. Valentine, *J. Am. Chem. Soc.*, 115 (1993) 1772.
67. P. Ochsenbein *et al.*, *Angew. Chem.*, 105 (1993) 1504.
68. M. A. Kahlow, T. M. Loehr, T. M. Zuberi and R. B. Gennis, *J. Am. Chem. Soc.*, 115 (1993) 5845.
69. M. J. Beck, E. Gopinath and T. C. Bruice, *J. Am. Chem. Soc.*, 115 (1993) 21.
70. K. Yamaguchi, Y. Watanabe and I. Morishima, *J. Am. Chem. Soc.*, 115 (1993) 4059.
71. H. Fujii, *J. Am. Chem. Soc.*, 115 (1993) 4641.
72. C. F. Portela, D. Magde and T. G. Traylor, *Inorg. Chem.*, 32 (1993) 1313.
73. D. Rong and T. E. Mallouk, *Inorg. Chem.*, 32 (1993) 1454.
74. V. B. McLaughlin, M. Faraggi and D. L. Leussing, *Inorg. Chem.*, 32 (1993) 941.
75. K. M. Kadish *et al.*, *Inorg. Chem.*, 32 (1993) 4179.
76. T. G. Traylor, T. Tsuchiya, Y. S. Byun and C. Kim, *J. Am. Chem. Soc.*, 115 (1993) 2775.
77. L. A. Lipscomb, B.-S. Lee and N.-T. Yu, *Inorg. Chem.*, 32 (1993) 281.
78. J. H. Cameron and S. C. Turner, *J. Chem. Soc., Dalton Trans.*, 13 (1993) 1941.
79. J. H. Cameron and S. C. Turner, *Polyhedron*, 12 (1993) 1675.
80. D. R. Benson, R. Valentekovich, S. W. Tam and F. Diederich, *Helv. Chim. Acta*, 76 (1993) 2034.
81. N. N. Daeid and K. B. Nolan, *Inorg. Chim. Acta*, 211 (1993) 55.
82. X. Jiang and K. M. Smith, *J. Chem. Soc., Chem. Commun.*, 13 (1993) 1054.
83. T. G. Traylor *et al.*, *J. Am. Chem. Soc.*, 115 (1993) 4808.
84. C. Ercolani, S. Hewage, R. Heucher and G. Rossi, *Inorg. Chem.*, 32 (1993) 2975.
85. S. C. Lee and R. H. Holm, *J. Am. Chem. Soc.*, 115 (1993) 5833.
86. S. C. Lee and R. H. Holm, *J. Am. Chem. Soc.*, 115 (1993) 11789.
87. S. C. Lee and R. H. Holm, *Inorg. Chem.*, 32 (1993) 4745.
88. H. Tsurumaki, Y. Watanabe and I. Morishima, *J. Am. Chem. Soc.*, 115 (1993) 11784.
89. Y. O. Kim, B. Song and H. M. Goff, *Inorg. Chem.*, 32 (1993) 1304.
90. A. M. Huff, C. K. Chang, D. K. Cooper, K. M. Smith and J. H. Dawson, *Inorg. Chem.*, 32 (1993) 1460.
91. A. L. Balch *et al.*, *J. Am. Chem. Soc.*, 115 (1993) 1422.
92. A. L. Balch, L. Latos-Grazynski, B. C. Noll, L. Szterenberg and E. P. Zovinka, *J. Am. Chem. Soc.*, 115 (1993) 11846.
93. A. L. Balch, B. C. Noll, S. M. Reid and E. P. Zovinka, *Inorg. Chem.*, 32 (1993) 2610.
94. A. L. Balch, B. C. Noll and N. Safari, *Inorg. Chem.*, 32 (1993) 2901.
95. A. L. Balch, M. M. Olmstead and N. Safari, *Inorg. Chem.*, 32 (1993) 291.
96. R. E. Marsh, M. M. Olmstead, W. P. Schaefer and V. Schomaker, *Inorg. Chem.*, 32 (1993) 4658.
97. Q. Chen, X. Zhang, C. H. Wu and L. G. Hepler, *Can. J. Chem.*, 71 (1993) 937.
98. J. D. Ranford, P. J. Sadler and D. A. Tocher, *J. Chem. Soc., Dalton Trans.*, 22 (1993) 3393.
99. R. W. Saalfrank, B. Hoerner, D. Stalke and J. Salbeck, *Angew. Chem.*, 105 (1993) 1223.
100. I. Dayan, J. Libman, Y. Agi and A. Shanzer, *Inorg. Chem.*, 32 (1993) 1467.
101. J. Jiang, J. F. Bank and C. P. Scholes, *J. Am. Chem. Soc.*, 115 (1993) 4742.
102. B. Tse and Y. Kishi, *J. Am. Chem. Soc.*, 115 (1993) 7892.
103. P. Yakirevitch, N. Rochel, A. M. Albrect-Gary, J. Libman and A. Shanzer, *Inorg. Chem.*, 32 (1993) 1779.

104. M. A. Dhansay and P. W. Linder, *J. Coord. Chem.,* 28 (1993) 133.
105. J. Burgess and M. S. Patel, *J. Coord. Chem.,* 29 (1993) 65.
106. V. K. Sabirov, K. M. A. Porai and Y. T. Struchkov, *Acta Crystallogr. Sect. C,* 49 (1993) 1611.
107. S. Pohl, U. Opitz, W. Saak and D. Haase, *Z. Anorg. Allg. Chem.,* 619 (1993) 608.
108. M. Handa, H. Miyamoto, T. Suzuki, K. Sawada and Y. Yukawa, *Inorg. Chim. Acta,* 203 (1993) 61.
109. A. Cornia, A. C. Fabretti, A. Giusti, F. Ferraro and D. Gatteschi, *Inorg. Chim. Acta,* 212 (1993) 87.
110. K. N. Han, D. Whang, H. J. Lee, Y. Do and K. Kim, *Inorg. Chem.,* 32 (1993) 2597.
111. S. Decurtins, H. W. Schmalle, P. Schneuwly and H. R. Oswald, *Inorg. Chem.,* 32 (1993) 1888.
112. A. Dei, *Inorg. Chem.,* 32 (1993) 5730.
113. A. Dei, D. Gatteschi and L. Pardi, *Inorg. Chem.,* 32 (1993) 1389.
114. T. B. Karpishin, T. D. P. Stack and K. N. Raymond, *J. Am. Chem. Soc.,* 115 (1993) 182.
115. T. B. Karpishin, T. D. P. Stack and K. N. Raymond, *J. Am. Chem. Soc.,* 115 (1993) 6115.
116. N. S. A. Kretchmar, A. Craig and K. N. Raymond, *J. Am. Chem. Soc.,* 115 (1993) 6758.
117. T. D. Y. Chung and K. N. Raymond, *J. Am. Chem. Soc.,* 115 (1993) 6765.
118. N. Kitajima, M. Ito, H. Fukui, Y. Morooka, *J. Am. Chem. Soc.,* 115 (1993) 9335.
119. S. W. Taylor, C. J. Hawkins and D. J. Winzor, *Inorg. Chem.,* 32 (1993) 422.
120. M. Ohba, H. Tamaki, N. Matsumoto and H. Okawa, *Inorg. Chem.,* 32 (1993) 5385.
121. S. McCullough-Catalano and C. B. Lebrilla, *J. Am. Chem. Soc.,* 115 (1993) 1441.
122. W. Y. Sun, N. Ueyama and A. Nakamura, *Inorg. Chem.,* 32 (1993) 1095.
123. W. Y. Sun, N. Ueyama and A. Nakamura, *J. Chem. Soc., Dalton Trans.,* (1993) 1871.
124. L. D. Field, T. W. Hambley and B. C. K. Yau, *Acta Crystallogr., Sect. C: Cryst. Struct. Commun.,* C49-2 (1993) 224.
125. D. L. Hughes, G. J. Leigh, M. Jimenez-Tenorio and A. T. Rowley, *J. Chem. Soc., Dalton Trans.,* (1993) 75.
126. C. Redshaw, G. Wilkinson, B. B. Hussain and M. B. Hursthouse, *Polyhedron,* 12 (1993) 363.
127. S. Komiya *et al., J. Chem. Soc., Chem Commun.,* (1993) 787.
128. J. E. Barclay, D. J. Evans, D. L. Hughes and G. J. Leigh, *J. Chem. Soc., Dalton Trans.,* (1993) 69.
129. L. C. G. Vasconcellos *et al., Inorg. Chim. Acta,* 214 (1993) 23.
130. N. Bampos, L. D. Field, B. A. Messerle and R. J. Smernik, *Inorg. Chem.,* 32 (1993) 4084.
131. H. U. Huang, F. Kai, T. Shoda and M. Nakamura, *J. Coord. Chem.,* 28 (1993) 155.
132. H. U. Huang *et al., J. Coord. Chem.,* 30 (1993) 131.
133. S. L. Andrianirinaharivelo, J. F. Pilichowski and M. Bolte, *Transition Met. Chem. (London),* 18 (1993) 37.
134. K. S. Siddiqi, N. Nishat, A. Jabeen and S. A. A. Zaidi, *Transition Met. Chem. (London),* 18 (1993) 591.
135. J. Sanmartin, M. R. Bermejo, V. J. A. Garcia, J. Romero and A. Sousa, *Transition Metal Chem. (London),* 18 (1993) 528.
136. M. Kodera *et al., Inorg. Chim. Acta,* 214 (1993) 97.
137. A. Neves *et al., Inorg. Chim. Acta,* 214 (1993) 5.
138. Y. Zang, H. G. Jang, Y. M. Chiou, M. P. Hendrich and L. Que, Jr., *Inorg. Chim. Acta,* 213 (1993) 41.
139. M. Fukuya *et al., J. Chem. Soc., Dalton Trans.,* 22 (1993) 3277.
140. B. Carre *et al., Polyhedron,* 12 (1993) 641.
141. Y. J. Li and A. E. Martell, *Inorg. Chim. Acta,* 214 (1993) 103.
142. A. S. M. Al-Shihri, J. R. Dilworth, S. D. Howe, J. Silver and R. M. Thompson, *Polyhedron,* 12 (1993) 2297.
143. P. Guerriero, S. Tamburini, P. A. Vigato, U. Russo and C. Benelli, *Inorg. Chim. Acta,* 213 (1993) 279.
144. H. Yoshida, T. Ozawa, K. Jitsukawa and H. Einaga, *Polyhedron,* 12 (1993) 1319.
145. M. A. Santos, M. A. Esteves, M. Candida, T. Vaz, M. L. S. S. Goncalves, *J. Chem. Soc., Dalton Trans.,* (1993) 927.
146. M. A. Santos, M. A. Esteves, M. Candida, T. Vaz, M. L. S. S. Goncalves, *Inorg. Chim. Acta,* 214 (1993) 47.
147. M. A. Santos, M. A. Esteves, J. M. G. Martinho, *J. Chem. Soc., Dalton Trans.,* 20 (1993) 3123.
148. W. S. Szulbinski, P. R. Warburton, D. H. Busch and N. W. Alcock, *Inorg. Chem.,* 32 (1993) 297.
149. J. A. Farrar, R. Grinter, D. L. Pountney and A. J. Thomson, *J. Chem. Soc., Dalton Trans.,* 18 (1993) 2703.

150. A. J. Conti, R. K. Chadha, K. M. Sena, A. L. Rheingold and D. N. Hendrickson, *Inorg. Chem.*, 32 (1993) 2670.
151. M. F. N. N. Carvalho, et al., *Inorg. Chem.*, 32 (1993) 5160.
152. J. Hockertz, S. Steenken, K. Wieghardt and P. Hildebrandt, *J. Am. Chem. Soc.*, 115 (1993) 11222.
153. C. A. Chang, et al., *Inorg. Chem.*, 32 (1993) 3501.
154. W. S. Szulbinski, P. R. Warburton and D. H. Busch, *Inorg. Chem.*, 32 (1993) 5368.
155. R. Shukla, P. K. Bharadwaj and U. C. Johri, *Polyhedron*, 12 (1993) 1553.
156. T. Beissel et al., *Inorg. Chem.*, 32 (1993) 124.
157. S. Pal and S. N. Poddar, *Polyhedron*, 12 (1993) 2465.
158. H. Jin et al., *J. Am. Chem. Soc.*, 115 (1993) 5290.
159. F. Bernhardt and R. Hoppe, *Z. Anorg. Allg. Chem.*, 619 (1993) 969.
160. D. G. Lee and H. Gai, *Can. J. Chem.*, 71 (1993) 1394.
161. E. Dvoncova and K. H. Lii, *Inorg. Chem.*, 32 (1993) 4368.
162. K. H. Lii, P. F. Shih and T. M. Chen, *Inorg. Chem.*, 32 (1993) 4373.
163. G. Haselhorst, K. Wieghardt, S. Keller and B. Schrader, *Inorg. Chem.*, 32 (1993) 0020-1669.
164. R. M. Buchanan, R. J. O'Brien, J. F. Richardson and J. M. Latour, *Inorg. Chim. Acta*, 214 (1993) 33.
165. N. Arulsamy, D. J. Hodgson and J. Glerup, *Inorg. Chim. Acta*, 209 (1993) 61.
166. Y. Dong et al., *J. Am. Chem. Soc.*, 115 (1993) 1851.
167. B. Mauerer, J. Crane, J. Schuler, K. Wieghardt and B. Nuber, *Angew. Chem. Int. Ed. Engl.*, 32 (1993) 289.
168. D. Fu, G. Wand, W. Tang and K. Yu, *Polyhedron*, 12 (1993) 2459.
169. N. Kitajima et al., *Inorg. Chem.*, 32 (1993) 3583.
170. A. van der Bergen, R. Colton, M. Percy and B. O. West, *Inorg. Chem.*,32 (1993) 3408.
171. R. H. Beer and S. J. Lippard, *Inorg. Chem.*, 32 (1993) 1030.
172. R. A. Leising, J. Kim, M. A. Perez and L. Que, Jr., *J. Am. Chem. Soc.*, 115 (1993) 9524.
173. K. S. Hagen, R. Lachicotte and A. Kitaygorodskiy, *J. Am. Chem. Soc.*, 115 (1993) 12617.
174. K. S. Hagen, R. Lachicotte, A. Kitaygorodskiy and A. Elbouadili, *Angew. Chem.*, 105 (1993) 1404.
175. R. Lachicotte, A. Kitaygorodskiy and K. S. Hagen, *J. Am. Chem. Soc.*, 115 (1993) 8883.
176. S. Menage et al., *Inorg. Chem.*, 32 (1993) 4766.
177. H. G. Jang, M. P. Hendrich and L. Que, Jr., *Inorg. Chem.*, 32 (1993) 911.
178. A. Hazell, K. B. Jensen, C. J. McKenzie and H. Toftlund, *J. Chem. Soc., Dalton Trans.*, (1993).
179. R. C. Holz et al., *Inorg. Chem.*, 32 (1993) 5844.
179. R. P. White et al., *J. Am. Chem. Soc.*, 115 (1993) 7778.
180. C. J. Harding, R. K. Henderson and A. K. Powell, *Angew. Chem., Int. Ed. Engl.*, 32 (1993) 570
181. L. Wu, M. Pressprich, P. Coppens and M. J. DeMarco, *Acta Crystallogr., Sect. C*, C49 (1993) 1255.
182. C. Delfs et al., *Inorg. Chem.*, 32 (1993) 3099.
183. J. L. Sessler et al., *Inorg. Chem.*, 32 (1993) 4277.
184. K. L. Taft et al., *J. Am. Chem. Soc.*, 115 (1993) 11753.
185. C. A. Christmas et al., *J. Am. Chem. Soc.*, 115 (1993) 12483.
186. H. Ahmad, G. Snatzke and Atta-ur-Rahman, *J. Am. Chem. Soc.*, 115 (1993) 12533.
187. D. J. Evans, *Inorg. Chim. Acta*, 203 (1993) 253.
188. H. Kambayashi, H. Nagao, K. Tanaka, M. Nakamoto and S. M. Peng, *Inorg. Chim. Acta*, 209 (1993) 143.
189. R. A. Henderson and K. E. Oglieve, *J. Chem. Soc., Dalton Trans.*, (1993) 1467.
190. T. Tomohiro, M. Kodaka, H. Y. Okuno, *Inorg. Chim. Acta*, 204 (1993) 1.
191. J. N. Butt et al., *J. Am. Chem. Soc.*, 115 (1993) 1413.
192. L. Banci et al., *J. Am. Chem. Soc.*, 115 (1993) 3431.
193. I. Bertini, S. Ciurli, A. Dikiy and C. Luchinat, *J. Am. Chem. Soc.*, 115 (1993) 12020.
194. P. Bertrand, *Inorg. Chem.*, 32 (1993) 741.
195. S. A. Borshch, E. L. Bominaar, G. Blondin and J. J. Girerd, *J. Am. Chem. Soc.*, 115 (1993) 5155.
196. J. M. Mouesca, G. Rius and B. Lamotte, *J. Am. Chem. Soc.*, 115 (1993) 4714.
197. C. J. Pickett, K. S. Ryder and J. C. Moutet, *J. Chem. Soc., Dalton Trans.*, 24 (1993) 3695.
198. L. Cai, J. A. Weigel and R. H. Holm, *J. Am. Chem. Soc.*, 115 (1993) 9289.
199. H. O. Stephan, C. Chen, G. Henkel, K. Griesar and W. Haase, *J. Chem. Soc., Chem. Commun.*, 10 (1993) 886.

200. S. Pohl, W. Barklage, W. Saak and U. Opitz, *J. Chem. Soc., Chem. Commun.*, 16 (1993) 1251.
201. D. Coucouvanis, K. D. Demadis, C. G. Kim, R. W. Dunham, J. W. Kampf, *J. Am. Chem. Soc.*, 115 (1993) 3344.
202. J. Chen *et al.*, *J. Am. Chem. Soc.*, 115 (1993) 5509.
203. E. Nordlander *et al.*, *J. Am. Chem. Soc.*, 115 (1993) 5549.
204. W. Cen, S. C. Lee, J. Li, F. M. MacDonnell and R. H. Holm, *J. Am. Chem. Soc.*, 115 (1993) 9515.
205. D. Coucouvanis *et al.*, *J. Am. Chem. Soc.*, 115 (1993) 12193.
206. P. E. Mosier, C. G. Kim and D. Coucouvanis, *Inorg. Chem.*, 32 (1993) 2620.
207. D. Coucouvanis, S. Al-Ahmed, C. G. Kim, P. E. Mosier and J. W. Kampf, *Inorg. Chem.*, 32 (1993) 1533.
208. K. K. P. Srivastava *et al.*, *Inorg. Chem.*, 32 (1993) 927.
209. J. El Nakat, K. J. Fisher, I. G. Dance and G. D. Willett, *Inorg. Chem.*, 32 (1993) 1931.
210. C. N. Chau and A. Wojcicki, *Polyhedron*, 12 (1993) 1261.
211. G. Henkel and C. Chen, *Inorg. Chem.*, 32 (1993) 1064.
212. A. L. Macedo, I. Moura, J. J. G. Moura, J. Le Gall and B. H. Huynh, *Inorg. Chem.*, 32 (1993) 1101.
213. G. J. Grant, S. M. Isaac, W. N. Setzer and D. G. VanDerves, *Inorg. Chem.*, 32 (1993) 4284.
214. D. E. Gindelberger and J. Arnold, *Inorg. Chem.*, 32 (1993) 5813.